DEVELOPMENT OF AN IMAGE-GUIDED ENDOSCOPIC ROBOT FOR COMPUTER-ASSISTED SURGERY

VERA SA-ING

**A THESIS SUBMITTED IN PARTIAL FULFILLMENT
OF THE REQUIREMENTS FOR
THE DEGREE OF MASTER OF ENGINEERING
(BIOMEDICAL ENGINEERING)
FACULTY OF GRADUATE STUDIES
MAHIDOL UNIVERSITY
2011**

COPYRIGHT OF MAHIDOL UNIVERSITY

Thesis
entitled

DEVELOPMENT OF AN IMAGE-GUIDED ENDOSCOPIC ROBOT FOR COMPUTER-ASSISTED SURGERY

……...
Mr. Vera Sa-ing
Candidate

……...
Assist. Prof. Jackrit Suthakorn,
Ph.D., (Robotics)
Major advisor

……...
Lect. Saowapak Thongvigitmanee,
Ph.D., (Electrical Engineering)
Co-advisor

……...
Prof. Chumpon Wilasrusmee,
M.D. (First Class Honor)
Co-advisor

……...
Prof. Banchong Mahaisavariya,
M.D., Dip Thai Board of Orthopedics
Dean
Faculty of Graduate Studies
Mahidol University

……...
Assist. Prof. Jackrit Suthakorn,
Ph.D., (Robotics)
Program Director
Master of Engineering Program in
Biomedical Engineering
Faculty of Graduate Studies

Thesis
entitled

DEVELOPMENT OF AN IMAGE-GUIDED ENDOSCOPIC ROBOT FOR COMPUTER-ASSISTED SURGERY

was submitted to the Faculty of Graduate Studies, Mahidol University
for the degree of Master of Engineering (Biomedical Engineering)
on
March 23, 2011

……...
Mr. Vera Sa-ing
Candidate

……...
Lect. Songpol Ongwattanakul,
Ph. D. (Electrical and Computer Engineering)
Chair

……...
Lect. Jartuwat Rajruangrabin,
Ph.D., (Electrical Engineering)
Member

……...
Assist. Prof. Jackrit Suthakorn,
Ph.D., (Robotics)
Member

……...
Prof. Chumpon Wilasrusmee,
M.D. (First Class Honor)
Member

……...
Lect. Saowapak Thongvigitmanee,
Ph.D., (Electrical Engineering)
Member

……...
Prof. Banchong Mahaisavariya,
M.D., Dip Thai Board of Orthopedics
Dean
Faculty of Graduate Studies
Mahidol University

……...
Assist. Prof. Rawin Raviwongse, Ph.D.
Dean
Faculty of Engineering
Mahidol University

ACKNOWLEDGEMENTS

Firstly, I would like to express my profound thank my major advisor, Assist. Prof. Dr. Jackrit Suthakorn, who always supports, teaches and pushes me to keep working all these years. I gratefully thank you my co-advisor, Dr. Saowapak Thongvigitmanee, for her suggestion throughout my master study and teach excellent image processing classes. She always helps me to make the all parts of my thesis, moreover, she spend more times for assistance all my works in my thesis. Without her, I would not have the successful research experience. To me, Dr. Saowapak Thongvigitmanee is more than a co-advisor; she is also a source of inspiration and wisdom in my life. I would like to thank you my co-advisor, Prof. Chumpon Wilasrusmee, for giving the good experience for the real surgery. This surgery is the much information in my thesis.

I would also like to thank my committee members, Assist. Prof. Dr. Jackrit Suthakorn, Dr. Saowapak Thongvigitmanee, Prof. Chumpon Wilasrusmee, Dr. Songpol Ongwattanakul, and Dr. Jartuwat Rajruangrabin for their participations in this work. My dissertation will consume some of their valuable time. I really do appreciate their efforts.

Furthermore, I would like to acknowledge the Thailand Graduate Institute of Science and Technology (TGIST) and National Electronics and Computer Technology Center (NECTEC) of National Science and Technology Development Agency (NSTDA), Thailand, for the good supporting in education and research they offered me. I would like to thank the Center for Biomedical and Robotics Technology (BART LAB), Mahihol University, Thailand, for the supporting in the facility.

Important thing to thank you, I would like to thank my parents and my family for their supporting, understanding, and willpower for my hard work all these years.

Vera Sa-ing

DEVELOPMENT OF AN IMAGE-GUIDED ENDOSCOPIC ROBOT FOR COMPUTER-ASSISTED SURGERY

VERA SA-ING 5038134 EGBE/M

M.Eng. (BIOMEDICAL ENGINEERING)

THESIS ADVISORY COMMITTEE: JACKRIT SUTHAKORN, Ph.D. (ROBOTICS), SAOWAPAK THONGVIGITMANEE, Ph.D. (ELECTRICAL ENGINEERING), CHUMPON WILASRUSMEE, M.D. (FIRST CLASS HONOR)

ABSTRACT

Laparoscopic surgery is a type of minimally invasive surgery (MIS) that is performed with several laparoscopic tools as well as a laparoscope equipped with a CCD camera. Since the working space for controlling a laparoscope in the operating room is usually limited, the camera operator is required to be highly skilled in controlling the laparoscope, and he/she may become fatigued after a long period of operation. Thus, our motivation was aimed at resolving the camera operator problem.

In this research, we developed a new minimally invasive robotics surgery system (MIRS), which consisted of a new design for the laparoscopic-holder assisting robot and a new algorithm for image-tracking the tip of the laparoscopic instrument. The laparoscopic-holder assisting robot consists of three parts: the passive base part, the bending laparoscope part, and the external manipulator part. For the object tracking part, we developed a new image-tracking algorithm named the "Adaptive Mean-Shift Kalman Tracking." This algorithm is based on the mean-shift algorithm combined with the Kalman filter for tracking the laparoscopic instrument in laparoscopic surgery. Moreover, the target boundary of the object of interest is automatically adjusted in the algorithm to increase the tracking performance. In this research, we tested the operationalized techniques with different scenarios from simulated videos, real surgical videos, and real-time experiments in a phantom box. The experimental results show there is a high potential for the proposed MIRS system to be suitable for tracking the tip of the laparoscopic instrument in real laparoscopic surgery.

KEY WORDS: LAPAROSCOPIC SURGERY /OBJECT TRACKING /
LAPAROSCOPIC ROBOT /
MEAN-SHIFT ALGORITHM / KALMAN FILTER

103 pages

การพัฒนาหุ่นยนต์เอนโดสโคปช่วยการผ่าตัดควบคุมด้วยผลการประมวลภาพ
DEVELOPMENT OF AN IMAGE-GUIDED ENDOSCOPIC ROBOT FOR COMPUTER-ASSISTED SURGERY

วีระ สอิ้ง 5038134 EGBE/M

วศ.ม. (วิศวกรรมชีวการแพทย์)

คณะกรรมการที่ปรึกษาวิทยานิพนธ์: จักรกฤษณ์ สุทธากรณ์, Ph.D. (ROBOTICS),เสาวภาคย์ ธงวิจิตรมณี, Ph.D. (ELECTRICAL ENGINEERING), เรือโท นายแพทย์ จุมพล วิลาศรัศมี, M.D. (FIRST CLASS HONOR)

บทคัดย่อ

การผ่าตัดแบบลาปาโลสโคปิกเป็นการผ่าตัดแบบแผลเล็ก ที่ทำการผ่าตัดกับเครื่องมือที่มีขนาดเล็ก ประกอบด้วยกล้องเอนโดสโคปและเครื่องมือต่างๆ งานวิจัยนี้มุ้งแก้ไขปัญหาที่เกิดจากผู้ควบคุมกล้องเอนโดสโคป เนื่องจากพื้นที่ใช้ในการควบคุมกล้องเอนโดสโคปมีอย่างจำกัด ทำให้ผู้ควบคุมกล้องเอนโดสโคปต้องมีความชำนาญอย่างมากในการควบคุมกล้อง นอกจากนี้ความเหนื่อยล้าของผู้ควบคุมกล้องเอนโดสโคปจากการผ่าตัดเวลานาน มีผลทำให้การควบคุมกล้องเอนโดสโคปเกิดการผิดผลาดได้

ดังนั้นงานวิจัยนี้จะทำการพัฒนาระบบการผ่าตัดแผลเล็กที่ใช้หุ่นยนต์ โดยแบ่งการวิจัยออกเป็น 2 ส่วนใหญ่ๆ คือ การออกแบบและพัฒนาหุ่นยนต์ใหม่ที่ช่วยในการถือและควบคุมกล้องเอนโดสโคป และการพัฒนาอัลกอริทึมใหม่ที่ใช้ในการติดตามเครื่องมือในการผ่าตัด ระบบใหม่นี้จะช่วยแก้ปัญหาที่เกิดจากผู้ควบคุมกล้องเอนโดสโคป โดยหุ่นยนต์ใหม่ที่ช่วยถือและควบคุมกล้องเอนโดสโคปจะมีการออกแบบเป็น 3 ส่วน ประกอบด้วย ส่วนที่หนึ่งใช้ยึดติดกับเตียงคนไข้ ส่วนที่สองใช้ในการควบคุมกล้องเอนโดสโคปในการเข้าออกช่องท้องของคนไข้ และส่วนสุดท้ายใช้ในการเคลื่อนที่ภายนอกเพื่อควบคุมกล้องให้เคลื่อนที่ในรูปแบบกรวย ในส่วนของอัลกอรทึมที่ใช้ในการติดตามวัตถุ ผู้วิจัยได้พัฒนาอัลกอริทึมใหม่ชื่อ Adaptive Mean-Shift Kalman Tracking ซึ่งใช้หลักการของอัลกอริทึม Mean-Shift ร่วมกับ Kalman filter พร้อมทั้งทำการปรับขนาดของบริเวณที่ใช้ในการติดตามวัตถุแบบอัตโนมัติเพื่อให้การติดตามมีความแม่นยำมากขึ้น ในกรณีที่วัตถุถูกบดบังด้วยวัตุอื่นหรือหายไปจากบริเวณที่กำหนดไว้ ในการวิจัยนี้มีการทดสอบการทำงานของหุ่นยนต์และอัลกอลิทึมใหม่ในหลายๆ กรณี ประกอบไปด้วย การทดสอบในวีดีโอที่จัดทำขึ้นเอง การทดสอบในวีดีโอระหว่างการผ่าตัดจริง และการทดสอบแบบ real time จากผลการทดลองทั้งหมดทำให้สรุปได้ว่าระบบการผ่าตัดแบบใหม่นี้สามารถนำไปใช้ในการถือกล้องเอนโดสโคปและติดตามเครื่องมือผ่าตัดได้จริงในการผ่าตัด

103 หน้า

CONTENTS

CONTENTS (cont.)

LIST OF TABLES

LIST OF FIGURES

LIST OF FIGURES (cont.)

LIST OF FIGURES (cont.)

CHAPTER I
INTRODUCTION

1.1 BACKGROUND

1.1.1 Minimally Invasive Surgery

Minimally invasive surgery (MIS) is new technology of surgery that performs surgery though small incisions called “ports.” This surgery uses a special set of surgical instruments to reduce the size of incisions, and to access a target organ during surgery. With the traditional “open surgery” as shown in Figure 1.1[1], trauma usually exists at the incision site, thus causing a lot of pain and inconvenience after the operation. MIS surgery causes less traumas, bleeding, infection, pain, and scarring. Operative time may be longer, but hospitalization and patient recovery times are shorter. However, MIS is technically more difficult for a surgeon than traditional open surgery. The surgeon must be trained extensively to become familiar with advanced instruments for MIS. For example, with skilled surgeon, the endoscope operator may become fatigued after holding endoscope for a long period of time. This may produce the human error. However, surgeons who have more experience can perform faster surgery and smaller incision, thus reducing the operation time, the patient recovery time, the pain and any risk that may occur.

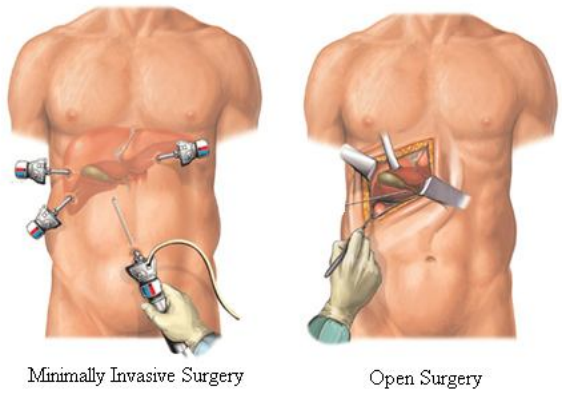

Figure 1.1 MIS and Open Surgery

Typical MIS involves laparoscopic surgery which is minimally invasive surgery within the abdominal cavity. During this surgery, the internal abdomen is insufflated with CO_2 and cannulas, which is essential metal tubes, through small incisions about 1-2cm wide to provide entry ports for laparoscopic surgical instruments. The overview of laparoscopic surgery is shown in Figure 1.2. In addition, this figure depicts the main instruments including a laparoscope instrument, which is a camera, for viewing the surgical site, and a surgical instrument. These instruments differ from the conventional instruments. For example, the working end of the instrument is longer by approximately 30 cm.

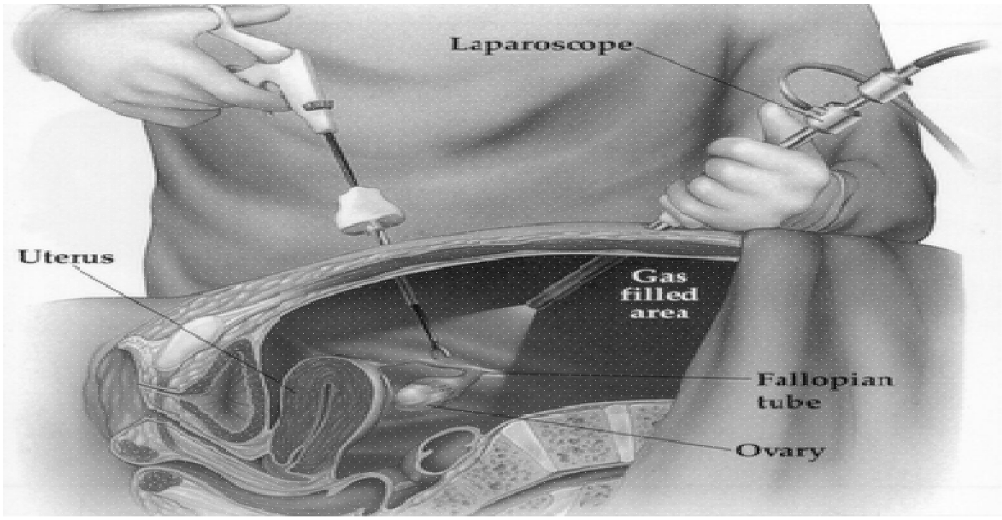

Figure 1.2 Laparoscopic Surgery

The surgical instruments used in laparoscopic surgery. The surgeon inserted inside the patient's abdomen enters by the cannula, as shown in Figure 1.3. These instruments have many motions, such as sliding in and out, rotating about their axes, and pivoting about the centers of rotation in the abdominal wall. The surgeon monitors the procedure through a television monitor which displays the abdominal worksite image provided by a special instrument called "laparoscopic camera or laparoscope," as shown in Figure 1.4.

Figure 1.3 Blunt trocar with cannula and Hassan's adapter [2]

Figure 1.4 Laparoscope and laparoscopic image

Although MIS technology has many advantages compared to open surgery, it still has the following drawbacks:

1. Visualization of the surgical site is reduced. The operation site is viewed on a video monitor which is a two dimensional image and placed somewhere in the operating room. Therefore, the surgeon must learn the appropriate geometric transformations to properly correlate hand motions to the tool tip motions.
2. The surgeon's ability to orient the instrument tip is reduced. The motions of the instruments are restricted by the small incision point; therefore, the surgeon may not approach particular internal organs or tissues and control the force on the instruments to manipulate them. As a result, the suturing becomes particularly difficult.

3. The surgeon's ability to feel the instruments interaction at tissue is reduced. The mechanical advantage designed into MIS instruments reduces the ability to feel grasping or cutting forces at the handle.

Since the expansion of minimally invasive medical practice remains limited by the lack of dexterity that surgeons can operate while using current MIS instruments, MIS combined with the use of robotics has been developed to help the surgeon. This technique is called "minimally invasive robotic surgery."

1.1.2 Minimally Invasive Robotic Surgery

Minimally Invasive Robotic Surgery (MIRS) has been introduced to avoid the drawbacks of manual MIS. It uses a robot to handle a surgical instrument which first occurred in the early 1970s. Then, the application of robotic manipulators in the field of laparoscopic surgery has been growing ever since, especially in the early 1990s, where steer-ability and dexterity has increased. The use of robotic systems in MIS has shown to be very helpful for surgeons in different surgical procedures [3]. The Computer Assisted System (CAS) is aimed to give the surgeon more feeling and touching by using tactile, haptic force feed-back, and motion scaling technologies. The laparoscope instrument can give the surgeon's vision when the images from the video feed are enhanced with real-time image preprocessing. This robotic surgery aims the surgeons with smaller incisions and quicker recovery times [4].

1.1.3 Digital Image Processing

An image is defined as a two-dimensional function, $f(x,y)$,where x and y are spatial coordinates and the amplitude of f at any pair of coordinates (x,y) is called intensity of the image at that point. Digital image processing (DIP) refers to processing on digital images by means of a computer algorithm [5]. A digital image composes of a finite number of elements called pixels (picture elements).Each pixel has its own location and value.

Image processing has considered in three types which consist of low, mid, and high level processes. First, low-level processes include primitive operations, such as image processing to reduce noise, contrast enhancement, and image making sharp.

This process is described by the fact that both inputs and outputs are images. Second, mid-level processing on images includes segmentation, description of objects, and classification of individual objects. This process is described by the fact that inputs generally are images, but outputs are extracted from input images. Finally, high-level processing is described the processing of recognizing the desired objects as in input image which perform the perceptive functions associated with vision. This process is used for tracking an interesting object in image [6]. Therefore, the high-level processing, which is the image segmentation, is the useful process to use in the laparoscopic surgery.

1.1.4 Digital Image Processing for Laparoscopic Surgery

Laparoscopic surgery produces enormous amounts of image sequence data. The DIP algorithm can be applied to these data to increase efficiency of laparoscopic surgery. For example, the laparoscope manipulator in the laparoscopic surgery aims at the surgical site which focuses the field of view of the surgical site. Specifically, many researchers have been working on automatic control of the laparoscope [7-11].Since the controller must have the real-time position information of the instrument tip to control the laparoscope automatically, the DIP methods become one of efficient approaches to obtain the real-time instrument tip position. The localization of the instrument tip is depending on the object tracking system.

1.1.5 The Object Tracking System for Laparoscopic Surgery

Object tracking is an important and essential topic in computer vision. The conceptual process of object tracking has three key steps consisting detection of the interesting objects, tracking of the interesting objects from frame to frame, and analysis of object tracks to recognize their behavior. The process of tracking is to locate the interesting object, which is the laparoscopic instrument tip, over a sequence of images. With object tracking, there are many issues that need to be concerned, such as the object has the information loss, noise in image, changing patterns of the target object and/or the background, non-rigid object structure, object-object and object-background occlusion, and camera motion. However, many object tracking method has been proposed solve the problems.

The object tracking system has two major components. Target Representation and Localization, a mostly a bottom-up process, are tools for locating and tracking the target object. Filtering and Data Association, mostly a top-down process, involve learning the prior information of the object, dealing with the dynamics of the tracked object, and evaluation of different hypotheses [12]. Therefore, we will use object tracking to locate the laparoscopic instrument tip in this thesis.

1.2 PROBLEM STATEMENT

One problem of MIS is that the surgeon's ability to use the surgical instrument is reduced. Because, most surgical instruments in MIS are the rigid and it takes more time for the surgeon to become skillful to use these instruments. Moreover, the surgeons may lose their feelings and visions when using the surgical instrument in MIS in a long period of time. These problems can be solved by using the da Vinci Surgical system [13]. However, the da Vinci system is a commercial system, which is extremely expensive [8]. This big system requires not only a great amount of setup times, but also many hours of training on animals which raises some ethical questions. To solve these problems in this thesis, we propose a new robot to assist holding the laparoscope which will decrease human error. In addition, this research will use the Digital Image Processing (DIP) algorithm to help controlling robot which will increase the surgeon's ability to use the laparoscope.

1.3 RESEARCH OBJECTIVES

This research consists of two main objectives. First, we will design and develop a prototype of assistant-holder robot for laparoscopic surgery. This robot proposes a new technique for holding a laparoscope which is easy to use in the operating room. Second, we will develop the object tracking algorithms to control this robot. This software will help the surgeon to control the robot. We will test the performance of this system in simulated situations.

1.4 THESIS ORGANIZATION

This thesis consists of five chapters. In Chapter 1, an introduction of MIS, MIRS, DIP, and object tracking system, as well as the scope and objective of my thesis work will be presented. Chapter 2 summarizes the literature reviews of the MIRS developments and existing object tracking algorithms for laparoscopic surgery. The MIRS section will be divided into two parts consisting of the commercial and on-going research robots, while the object tracking algorithms section will review the existing algorithms to control the laparoscope and track interesting objects. Chapter 3 will propose the hardware design which is the conceptual design of a new MIRS system. The conceptual design will explain the all parts of designing in this chapter. Chapter 4 will propose the algorithms to use in a new MIRS system. The algorithms consist of the Mean-shift algorithm and Kalman filter. In Chapter 5, the experiment results of the proposed techniques will be shown. In Chapter 6, conclusion and future work of this thesis will be provided.

CHAPTER II
LITERATURE REVIEW

This chapter reviews existing minimally invasive robotic surgery (MIRS) and the object tracking system for laparoscopic surgery. This chapter begins with the description of MIRS development which will be divided into two parts: the commercial and on-going research robots. The next section reviews features and components of object tracking system and describes the object tracking system to use in the laparoscopic surgery.

2.1 MINIMALLY INVASIVE ROBOTIC SURGERY

Many researches in the MIRS can be separated into two types consisting of the commercial and on-going research robots. Examples of the popular commercial laparoscopic robots include the AESOP (Automated Endoscope System for Optimal Positioning) by Computer Motion Inc, Goleta, CA [9], Zeus Robotic Surgical System by Computer Motion, Goleta, CA [10], and da Vinci Surgical System by Intuitive Surgical, Inc., CA [11]. Examples of the on-going research in laparoscopic robots include LER (Light Endoscope Robot) by TIMC-GMCAO Laboratory [12], KaLAR (KAIST Laparoscopic Assistant Robot) by Korea Advances Institute of Science and Technology [13], and MC^2E (compact manipulator for endoscopic surgery) by Laboratorie de Robotique de Paris [14]. These robots help the surgeons increase their performance during surgery.

2.1.1 Commercial MIRS Systems

The Zeus Surgical System

The Zeus surgical system [14] has been developed by Computer Motion, CA which is a full system for robotic surgery consisting of three robotic arms. A surgeon control is independently attached to the operating table. The left and right

arms of Zeus surgical system are used to manipulate the surgical instruments and one robotic arm is used to hold the endoscope, as shown in Figure 2.1. The surgeon console has a video console showing the video feedback from the endoscope camera. This instrument is possible to connect both 3D and 2D stereo vision from. In addition, the surgeon can control the position of this instrument by surgeon's voice command, as shown in Figure 2.2. At the console, the surgeon can control the position of the surgical instruments inside the patient's body by controlling two handles. Thus, the motion of surgeon console is scaled and tremors of the surgeon's hands are recognizing to achieve a precise micro-manipulation of the instruments inside the patient's body.

Figure 2.1 Three robotic arms of the Zeus surgical system [15]

Figure 2.2 Surgeon Console of the Zeus surgical system [15]

The AESOP System

The Automated Endoscope System for Optimal Position (AESOP) has been developed by Computer Motion, CA, USA [16]. AESOP was designed to manipulate a laparoscope which is a rigid endoscope. It has one mechanical arm which has six degrees of freedom (DOFs) and can control by foot, hand, or voice commands. The AESOP system consists of a central control unit, a robotic arm, a laparoscope holder, a hand control, and a foot control, as shown in Figure 2.3. The robotic arm of AESOP consisting of 6 joints and moving 180^{o} to $360^{o}$is used to hold the laparoscope through the incision point. The workspace of AESOP can be moved within a diameter of 30cm vertically and 57cm horizontally. Finally, AESOP has a safe function by using specialized software to control the robotic arm in each joint and to define the magnitude of translation and rotation.

Figure 2.3 The AESOP system [17]

The da Vinci Surgical System

The da Vinci surgical system has been developed by Intuitive Surgical, Inc., CA, USA [18].This system consists of a surgeon controlling console, a cart with four interactive robotic arms, an endoscopic viewing system, and EndoWrist instruments. The surgeon controlling console and a cart with four robotic arms are shown in Figure 2.4. The first robotic arm for holding the endoscope can easily change, move, zoom, and rotate the field of view through the console. The second two arms representing the left and right hands of the surgeon hold the EndoWrist instruments. The last arm is the optional arm to add the third EndoWrist instrument to perform additional tasks [13].

Figure 2.4 The da Vinci surgical system [19]

2.1.2 On-Going Research MIRS Systems

LER Robot

LER or Light Endoscope Robot was developed by TIMC-GMCAO Laboratory [20]. This robot consists of a compact camera-holder robot, which rest directly on patient's abdomen, and an electronic box which contains the electricity supply and robot controller, as shown in Figure 2.5. This robot has 3-DOFs.The first, an extension motor used to control the endoscope's insertion depth. The second, a rotation motor used to control the endoscope's rotation circle. The third, an inclination motor used to control the endoscope pan-tilt. There are three ranges of movement including60^{o} rotate around the vertical axis, 80^{o} tilt from the vertical position, and 20 cm insert the endoscope along its axis. This robot is not only small with a diameter of 110 mm and height of 75 mm, but also very lightweight, approximately about 625 g, due to its stainless steel material. Thus, the main advantages of this robot are small workspace and easy setup in the operating room.

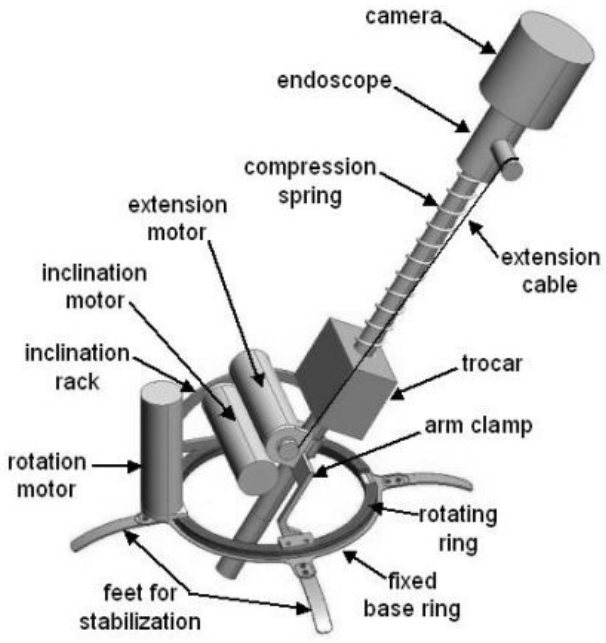

Figure 2.5 LER (Light Endoscope Robot) [20]

The KaLAR Robot

The KAIST Laparoscopic Assistant Robot or KaLAR [21] is an endoscope-holder assistant robot, which has 3-degrees of freedom (DOFs) including up/down, left/right and forward/backward movement. The KaLAR system was developed by KAIST laboratory from Korea, as shown in Figure 2.6. The end of this robot connects to a CCD camera, which can bend. The control of the KaLAR consists of 2-DOFs motions including up/down and right/left motions that are controlled by wire-driven mechanism, as shown in Figure 2.7, and 1-DOF zooming mechanism for the forward/backward movement from the linear-stage is controlled by motors, as shown in Figure 2.8. These motions are controlled by voice command via a computer. This system was designed by two main factors including safety and adaptability. For safety, they designed the robot with the optimized range of motions. The safety of this robot uses the filtering software to detect wrong commands. For adaptability, they designed the robot to have a compact size to decrease interference with the primary surgeon in the operating room. Moreover, this robot was designed to weigh less than 2 kg. This robot uses the commercial laparoscope holder for fixation to the bedside. Because the holder has multiple degrees of freedom, the robot can be positioned in various locations of the patient's abdomen. However, this system has some disadvantages. For example, it is difficult to apply to general laparoscopic surgeries due to its limited workspace.

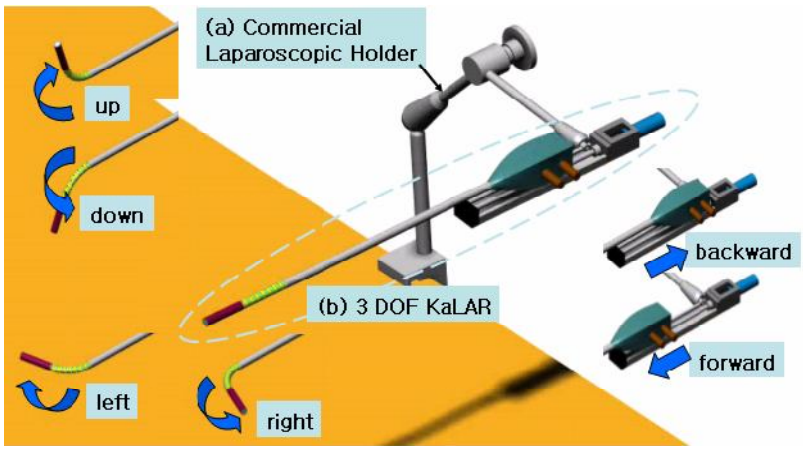

Figure 2.6 Simulation of KaLAR in the conceptual design

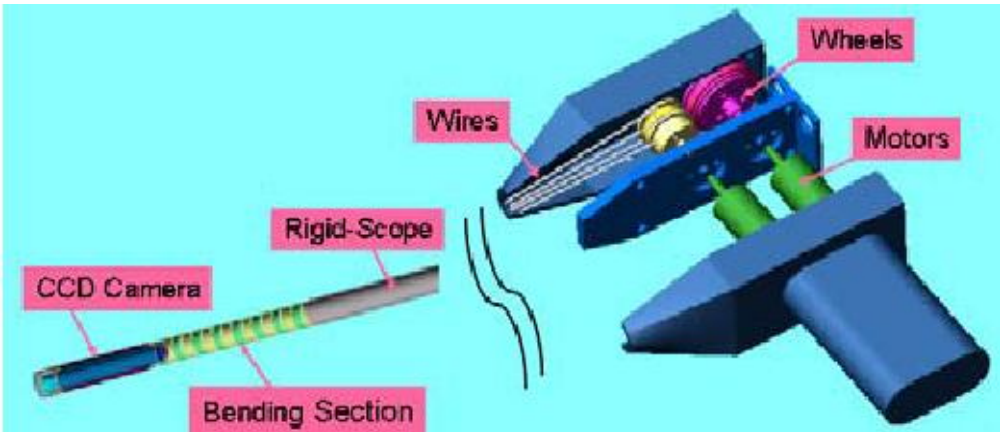

Figure 2.7 Conceptual design of bending mechanism

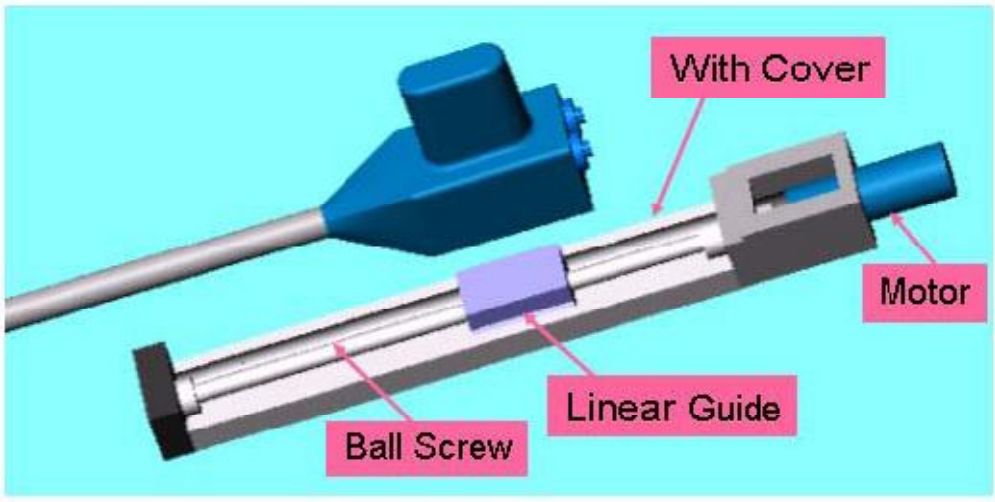

Figure 2.8 Conceptual design of zooming mechanism

The MC^{2}E Robot

The MC^{2}E robot or compact manipulator for endoscopic surgery [22] is a laparoscopy robot, which moves only the instrument. This robot consists of two parts, as shown in Figure 2.9. The lower part is a compact spherical 2-DOFs mechanism (Θ_1 and Θ_2) which has joint axes coincide with the fulcrum point providing an invariant center. The base of this part is easily installed on the patient's skin. The convenience of the installation can reduce the setup time.

The upper part of this robot is mounted on the fulcrum point. It provides the 2-DOFs for rotation about the instrument axis (Θ_3) and translation along the instrument axis (d_4). This part has translated the instrument along its penetration axis.

The rotation motion uses a motor to transmit the instrument through six soft rollers. Therefore, from the design, this robot is compact and lightweight. Because of a lightweight robot, it can be easily mounted and moved by a nurse, thus reducing the preoperative setup time and increasing safety. However, this robot has force measurement which is not necessary to use in laparoscope-holder robot because the laparoscope does not touch the surface of organs.

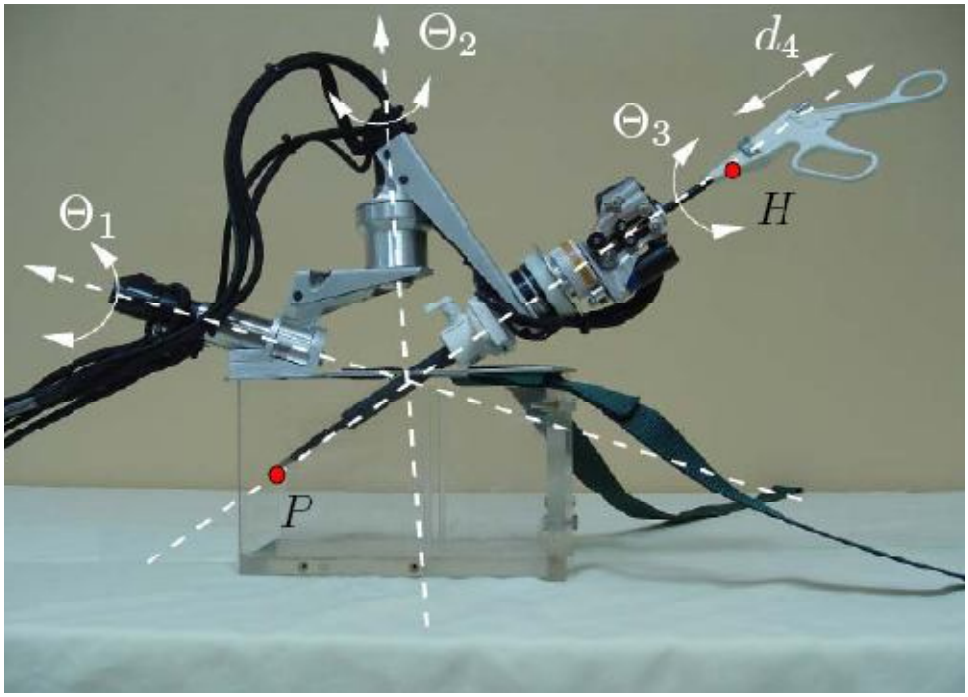

Figure 2.9 The MC^{2}E robot

2.2 OBJECT TRACKING SYSTEM FOR LAPAROSCOPIC SURGERY

In object tracking, the important parts that affect the result of tracking algorithms are object representation and the feature selection. Object representation can be represented by their shapes and appearances. The shape of object representation can be described in many types, such as points, primitive geometric shapes, object silhouette and contour, articulated shape models, and skeletal models. For points, the interest object will be represented by a point which is the center of the object. This shape is suitable for tracking a small region of the object in the frame, as shown in Figure 2.10(a), and (b). For primitive geometric shapes will be represented by rectangle, ellipse, etc. This geometric shape is suitable for simple rigid objects; however, they can be used for tracking non-rigid objects, as shown in Figure 2.10(c), and (d). In object silhouette and contour, the contour is defined the boundary of object. The silhouette of the object is the region inside the boundary. This shape is suitable for tracking complex non-rigid object, as shown in Figure 2.10(g), and (h). Articulated shape models, this shape are composed the part of body parts. The connection of the body parts are managed by the kinematic motion models. The component shapes is represented by using the cylinders or ellipses, as shown in Figure 2.10(e). Skeletal models, this skeletal shape will be extracted in the middle axis from the object contour. The skeletal representation is suitable for tracking both articulated and rigid object, as shown in Figure 2.10(f).

Feature selection is related to the object representation. It is an important part in tracking to identify uniqueness of object of interest that the object can be easily recognized in the frame. There are many features used in tracking algorithm, such as color space used in the tracking algorithm include RGB (red, green, blue) and HSV (hue, saturation, value). The primary effects have two physical factors consists of the spectral power distribution of luminance and surface reflectance properties of the object, edges are another feature to detect the object boundary. The most popular edge detection is canny edge detection. The Optical Flow feature provides a dense field of the displacement vectors which defines the translation of each pixel in the area of interest. It is usually used motion-based segmentation and tracking applications [23].

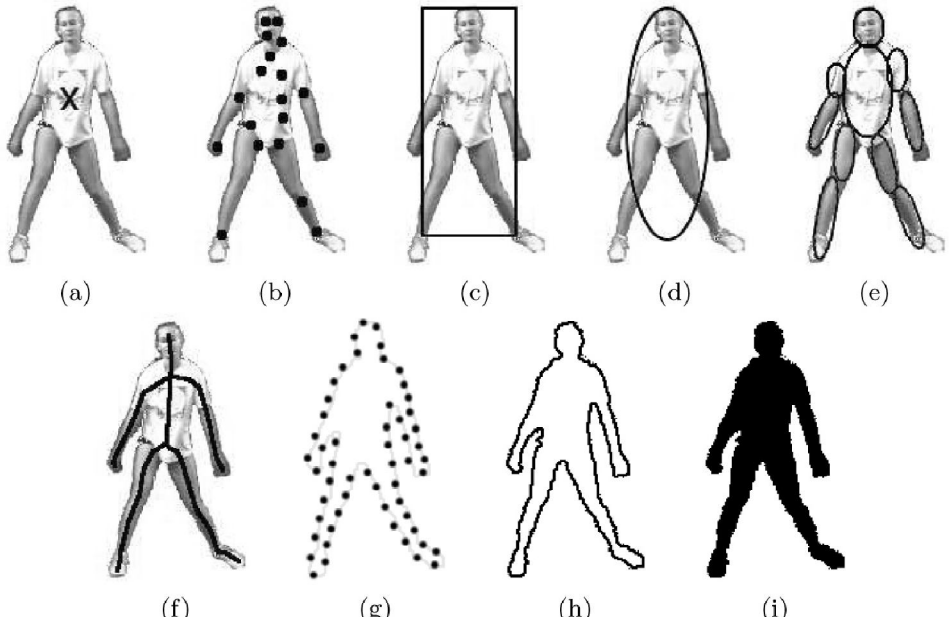

Figure 2.10 Object representations. (a) Center, (b) multiple points, (c) rectangular patch, (d) elliptical patch, (e) part-based multiple patches, (f) object skeleton, (g) complete object contour, (h) control points on object contour, (i) object silhouette[23]

The object tracking system can be divided into two major components consisting of *Target Representation and Localization*; and *Filtering and Data Association*. *Target Representation and Localization* is a mostly a bottom-up process of object tracking for locating and tracking the target object. The algorithms for locating the position of the target object can be divided into three categories. First, Point Tracking is used for detecting the points in the sequential frames. The relation of points is based on the previous points which include the position and motion of the previous result. The simple example of Point Tracking is shown in Figure 2.12(a). Many algorithms have been proposed for point tracking. For examples, the Harris detector is tracked by using points on the Mahalanobis distance based on color [24]. The Greedy Optimal Assignment (GOA) tracker uses several motion constraints to track the point of interesting on the moving object [25]. The SURF (Speeded Up Robust Features) is based on the feature motions which are proposed to depict the relationship between local feature motions and object global motion [26], as shown in Figure 2.11.

Figure 2.11 Example of SURF The training images for two objects are shown on the left. These can be recognized in a cluttered image with extensive occlusion, shown in the middle. The results of recognition are shown on the right[27].

Second, Silhouette Tracking is performed by estimating the region object in the sequential frames. These algorithms use information inside the edge of the object which is in the form of density and shape models to track the object. An example of Silhouette Tracking is shown in Figure 2.12 (c), and (d). This tracking can be classified into two subcategories consists of contour tracking, as shown in Figure 2.12 (c), and shape matching, as shown in Figure 2.12 (d). The contour tracking is the principle application to detect and track the edge of the moving object in the clustered environment. One approach to solving the tracking problem is the condensation algorithm which is a probabilistic algorithm, as shown in Figure 2.13.

Third, Kernel Tracking is the aim to track the object shape. The object shapes are represented in the forms of the rectangular or elliptical shapes and used for calculating the histogram of the object shape. This result is in the form of transformation consisting of translation, rotation, and scaling as shown in Figure 2.12 (b). These tracking algorithms are divided into two groups; template and density-based appearance model tracking and multi-view appearance models tracking.

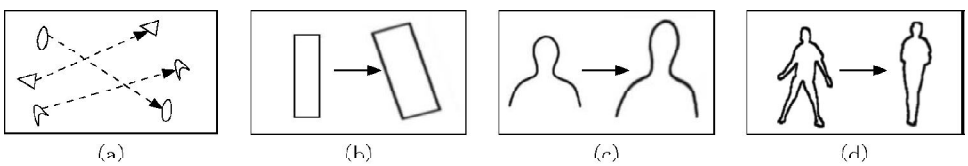

Figure 2.12 The example of Target Representation and Localization. (a) Different tracking approaches. Multipoint correspondence, (b) parametric transformation of a rectangular patch, (c, d) Two examples of contour evolution [23].

Figure 2.13 Example of Contour tracking [28]

Filtering and Data Association which is a top-down process. From result of this component involves the result of *Target Representation and Localization.* These algorithms can track the complex object which moves behind the obstructions. The main filtering algorithms have two filtering consist of Kalman Filter and Particle Filter. Although, Target Representation and Localization process is only track the object in general tracking.

In laparoscopic surgery, many researchers have proposed different DIP methods to control the laparoscope [7-11]. Omote*et al*. [7] presented a self-guided robotic laparoscope control system which was based on the color tracking method for laparoscopic surgery. This technique gave better surgical results than the human laparoscope control system. Casals *et al*. [8] used shape information of a surgical instrument as a feature for tracking a target. They used edge detection method and then verified the result with the pre-defined shape of the instrument. The disadvantage of this method is that the proposed technique controlled a laparoscopic to work only in a specific surgical situation. Lee *et al*. [9] used color and shape information to recognize the contour of the surgical instrument. Their method was easy to track the surgical instrument but did not work well in every situation. All the existing methods discussed previously are reliable under a normal situation only; however, they may not work well in all situations. For example, when some part of the instrument is blocked by some obstacles, those methods are not able to track the target features correctly. On the other hand, Wei *et al*. [10] presented a real-time visual serving

method for laparoscopic surgery. They made artificial color marks on a surgical instrument for tracking target features. Therefore, they could use a simple algorithm to track the object. However, this method required the additional task of attaching the artificial marks, which could produce many problems, such as the choice of attaching method and the sterilization of the color mark on the surgical instrument. In the real surgical situations, the main surgeon's concern is not the color mark but the surgical instrument tip, thus the tracking can fail when some of the color mark is covered by some obstacles or when it is not within the surgical image. Since most existing methods use a threshold technique to recognize the tracking target feature, they cannot successfully track the object when some feature information is lost from the scene. In addition, those existing methods have no adaptability to the changes in the illumination of the surgical environment. This is risky to apply them to real laparoscopic surgery.

Due to some limitations of previous methods, in this paper, we propose a new object tracking algorithm to track the surgical instrument called the adaptive mean-shift Kalman algorithm, which is based on the mean-shift algorithm and the Kalman filter. In this technique, the size of target candidate can be adjusted during tracking processes to increase the chance of tracking. Different scenarios of simulated videos were tested with the proposed algorithm. In addition, the proposed algorithm is intended to use for controlling our new laparoscopic-holder assistant robot [29] and tracking the tip's instrument in laparoscopic surgery.

CHAPTER III
METHODS OF HARDWARE DESIGN

In this chapter, we will explain the method of the hardware part in thesis. The hardware part proposed the conceptual design of a new robot for assistant-holding the laparoscope in laparoscopic surgery. This chapter will explain the conceptual design of the new MIRS system which consists of the passive base part, the bending laparoscope part, and external manipulator part. The last section proposed the overall of the designed robot.

3.1 CONCEPTUAL DESIGN OF THE NEW MIRS SYSTEM

The conceptual design of a new assistant-holder laparoscope robot is based on the concepts of on-going research robots. This robot will improve the working area inside and outside the surgical environment which has limited workspace. To decrease the working space in the operating room, this robot will be designed to be small and compact. From on-going research robots as described in Chapter II, the conceptual design of the proposed robot will combine the advantages of those existing robots. Therefore, the important part to design this robot will consist of three parts: a passive base part, a bending laparoscope part, and an external manipulator part.

3.1.1 The Passive Base Part

This part uses the commercial medical passive holder that can be climbed easily on the operating table. The passive base is fixed to the operating table with a clamp to adjust the robot system at the proper position as shown in Figure 3.1. There are many advantages to use this passive base part on the new laparoscope-holder robot. First, it is easily fixed to the bedside. Second, we can easily adjust the laparoscope in the proper position at the fulcrum point. Finally, it is very lightweight.

Therefore, we will use this passive base part to setup the proper position of the laparoscope-holder robot.

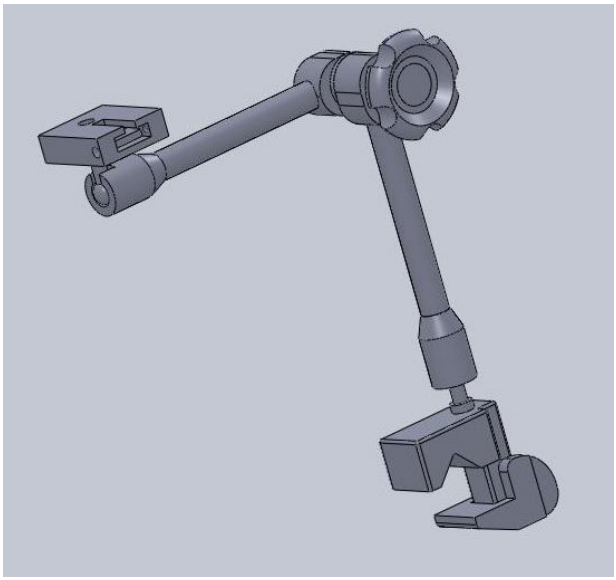

Figure 3.1 The passive base part

3.1.2 The Bending Laparoscope Part

The bending laparoscope is derived from the original KaLAR system [21], as shown in Figure 3.2. This part composes of 2-DOFs for the bending motion inside the patient's abdomen and 1-DOF for the motion outside the patient's abdomen. The bending motion driven by a wire mechanism determines the internal angle of the laparoscope. The zooming motion uses a linear guide with a ball screw to move the laparoscope. The advantage of the bending laparoscope is the flexibility to view wide areas of the internal patient's abdomen without making wide motions in the operating room. Because it can reduce motions of the robot in the operating room and increase viewing areas in the abdomen, we use this bending laparoscope mechanism to design the new laparoscope holder.

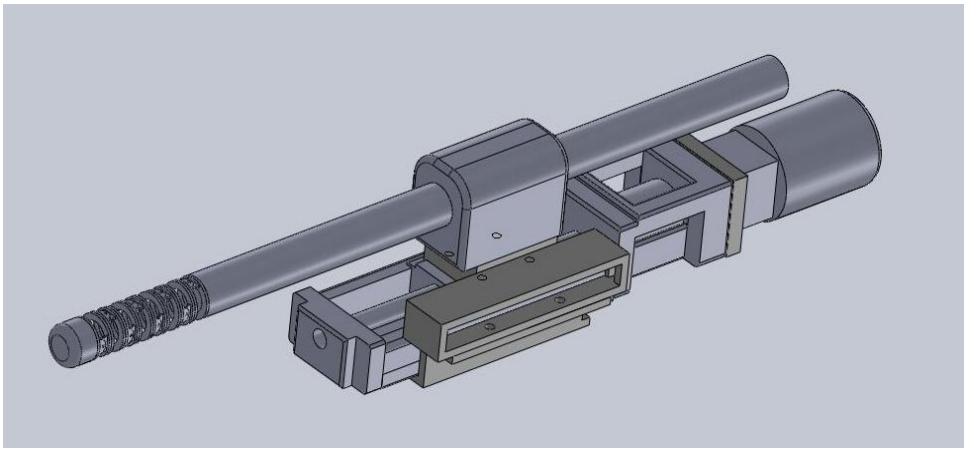

Figure 3.2 The bending laparoscope part

3.1.3 The External Manipulator Part

Since the original KaLAR system has a limited view of workspace, we develop the external manipulator is to extend the workspace of the original KaLAR system. This external manipulator uses the lower part of the MC^2E robot [22], as shown in Figure 2.9. The main advantage of the new system is a wide view of the workspace in the abdominal cavity allowing the system to apply to other laparoscopic surgeries. The external manipulator has 2-DOFs of motions which create the compact spherical motion for moving the laparoscope. Moreover, this system does not have a large rigidity problem and has a very simple structure, thus the surgeon can predict the movements of this system easily and reduce the interference in the system. Therefore, we will use this external manipulator part to increase the field of view of the workspace in the patient's abdomen, as shown in Figure 3.3.

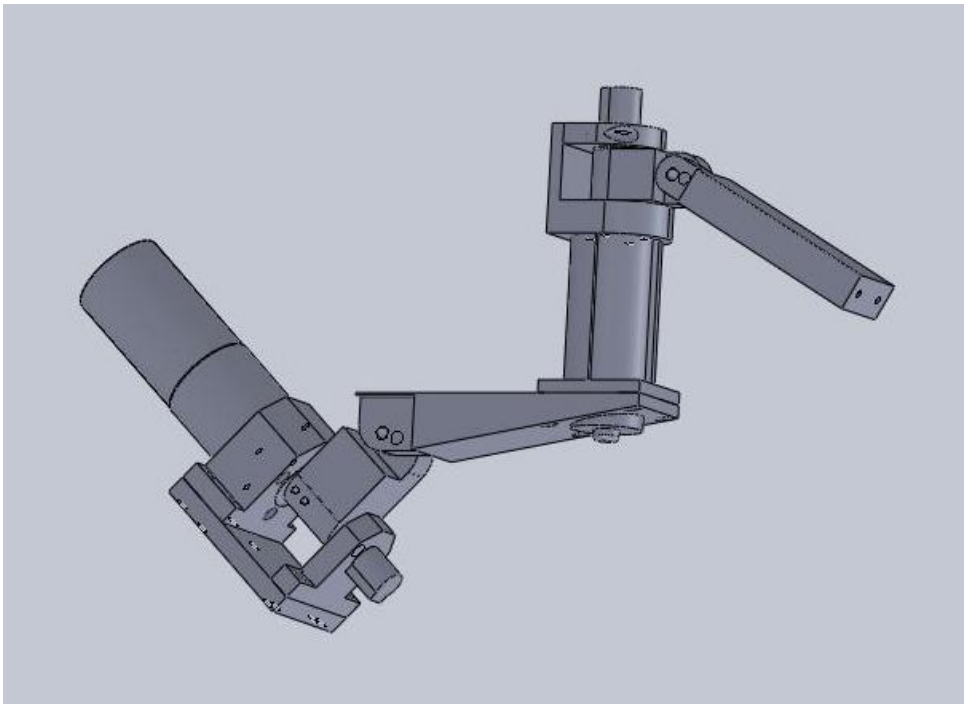

Figure 3.3 External Manipulator

3.2 THE OVERALL SYSTEM OF CONCEPTUAL ROBOT

The proposed robot is designed from two robots including the KaLAR robot and the MC^2E robot. The design separates into three parts. First, the passive base part is the commercial medical passive holder. The passive base has many DOFs for the tip position setup of the laparoscope-holder robot. Second, the bending laparoscope part is the laparoscope motions of the KaLAR robot. The bending laparoscope part has 3-DOFsof motions including 2-DOFs for bending motion in the patient's abdomen and 1-DOF for the motion outside the patient's abdomen. This part is used to reduce motions of the robot and increase viewing areas in the patient's abdomen. Finally, the external manipulator part is the lower part of the MC2E robot. The external manipulator has 2-DOFs of motions to create the compact spherical motion in the patient's abdomen. This part use to increase view area of the workspace in the patient's abdomen. Combining all different parts, the prototype of the new laparoscope-holder assistant robot is shown in Figure 3.4. In addition, the each part of the conceptual robot describe in APPENDIX which is in the Computer aided design

(CAD) of conceptual robot. The new design of the laparoscope-holder assistant robot has many advantages. First, this robot can easily be developed because it uses three motors and simple linkages. Second, this robot can easily calculate the tip of the laparoscope due to 5-DOFs of motion consisting of 2-DOFs to control the center of the fulcrum point and 3-DOFs to control the motion of the laparoscope. Third, we can easily control the laparoscope motion because this robot can be automatically controlled by computer software. Finally, the proposed robot can easily be set up in a small workspace in the surgery room without interferer the workspace of the primary surgeon because it is a small robot. The primary surgeon can control the new robot by surgeon's instruction. This new design laparoscope holder assistant robot can help holding the laparoscope in the laparoscopic surgery, thus reducing human errors and the operation time in the surgery. The required working area of laparoscopic surgery is difficult to define because of the working area varies depending on many factors such as the surgeon's preference, condition of operating room, and type of surgery. However, J. Rosen [30] measured the position of the surgical tools which creates a circular cone of working area with apex angle of 60 degrees. From this result, this conceptual robot will be able to provide a viewing area with more than that. Therefore, the overall working area will calculate in the Chapter V.

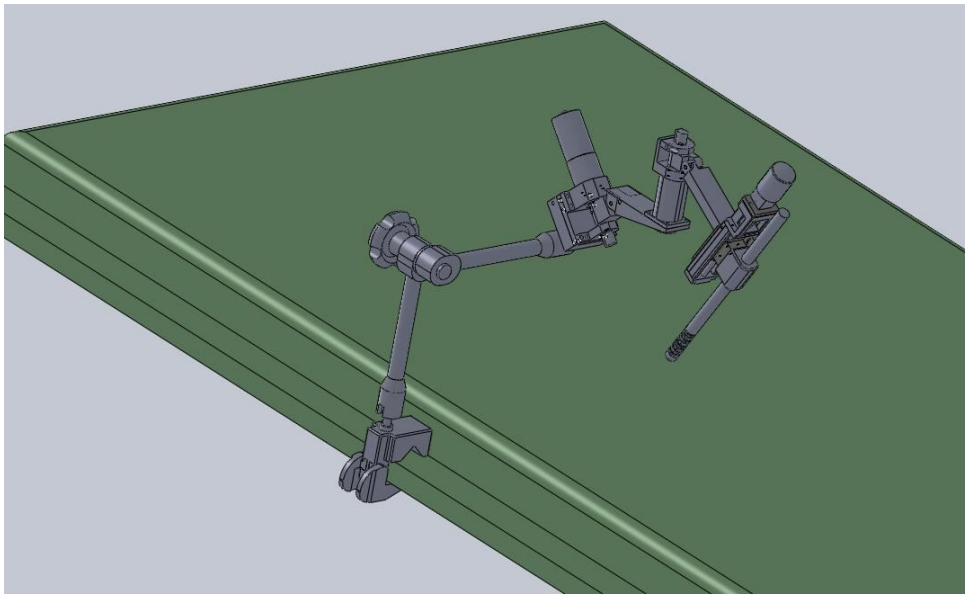

Figure 3.4 New design of the laparoscope-holder assistant robot

CHAPTER IV
METHODS OF OBJECT TRACKING

In this chapter, we explain the proposed research for the software part. Also, we propose the object tracking component. The object tracking component that we use in this thesis consist of Target Representation and Localization and Filtering and Data Association. In the Target Representation and Localization subsection, we propose the Mean-Shift algorithm. In addition, in the Filtering and Data Association subsection, we propose the Kalman filter. In this thesis, the two algorithms will be used in the object tracking system for new MIRS System.

4.1 TARGET REPRESENTATION AND LOCALIZATION

Target Representation and Localization is a main process to be used for locating and tracking of the target object. Algorithms for target Representation and Localization can be divided into three categories consist of point tracking, silhouette tracking, and kernel tracking, as described in the Chapter II. In this thesis, we focus on kernel tracking, specifically the Mean-Shift algorithm, to locate the target object. The mean-shift algorithm can be used to locate both rigid and non-rigid objects, as well as varying-size objects. Therefore, we propose the Mean-Shift algorithm for tracking the laparoscopic instrument. This algorithm will be described in the next section.

4.1.1 Mean-Shift Algorithm

A Mean-Shift algorithm [31] is an iterative process for locating the target object by maximizing the similarity function. The similarity function is the comparison between the target model, $\hat{q}$, and the target candidate, $\hat{p}(y)$. The target model and the target candidate are represented by a small elliptical or rectangular area in the frame. The pixel values in the region of interest (ROI) are used for calculating

the target model and target candidate histograms. The target histogram calculation is based on the number of an *m*-bin histogram, where *m* is an integer defining the number of quantization levels in the histogram [32]. Therefore, the target model histogram can be computed by the following equations:

$$target\ model: \quad \hat{q} = \{\hat{q}_u\}_{u=1\ldots m} = \hat{q}_1, \hat{q}_2, \ldots, \hat{q}_m \ ; \sum_{u=1}^{m} \hat{q}_u = 1 \tag{1}$$

$$\hat{q}_u = C \sum_{b(x_i)=u} k(\|x_i\|^2) \tag{2}$$

$$C = \frac{1}{\sum_{i=1}^{n} k(\|x_i\|^2)} \tag{3}$$

where $x_1, \ldots, x_n$ is the normalized pixel values at the *i*th pixel of the target model area, $b(x_i)$ is a color value at pixel x_i which depends on the *m*-bin histogram, *n* is the number of data points, $k(x)$ is the kernel function and C is a normalization factor, which can be set as a constant. Kernel function is the density estimation method. The inputs are the pixel data at in the ROI which give *n* data points $x_1, \ldots, x_n$. This equation is computed in the center point *x* as follow:

$$\hat{f}(x) = \frac{1}{n} \sum_{i=1}^{n} K(x - x_i) \tag{4}$$

$where\ K(x) = CK(\|x\|)$

The minimization of the average error between the estimate and the true density can be calculated by using the Epanechnikov kernel as follow:

$$K_E(x) = \begin{cases} C(1 - \|x\|^2) & ,if\ \|x\| \leq 1 \\ 0 & ,otherwise \end{cases} \tag{5}$$

Another kernel is the Normal kernel as follow:

$$K_N(x) = C * \exp\left[-\frac{1}{2}\|x\|^2\right] \tag{6}$$

And another kernel is the Uniform kernel as follow:

$$K_U(x) = \begin{cases} C & ,if\ \|x\| \leq 1 \\ 0 & ,otherwise \end{cases} \tag{7}$$

where C is the volume of the pixel at *x* defined as a constant.

In this case, the target model area is defined in the region of interest (ROI) where the center is the origin of the image. The target candidate histogram can be computed by the following equations:

$$target\ candidate:\ \hat{p}(y) = \{\hat{p}_u(y)\}_{u=1\ldots m} = \hat{p}_1(y), \hat{p}_2(y), \ldots, \hat{p}_m(y) \quad ; \sum_{u=1}^{m} \hat{p}_u(y) = 1 \tag{8}$$

$$\hat{p}_u(y) = C_h \sum_{b(x_i)=u} k\left[\left\|\frac{y - x_i}{h}\right\|^2\right] \tag{9}$$

$$C_h = \frac{1}{\sum_{i=1}^{n_h} k\left[\left\|\frac{y - x_i}{h}\right\|^2\right]} \tag{10}$$

where $x_1, \ldots, x_{n_h}$ is the normalized pixel locations in the target candidate which defines the center at *y* in the current frame, *y* is a 2-D coordinate of the object location which is the center of target candidate area in the current frame, $n_h = h$ is the number of data points, h is the bandwidth of the candidate area, and C_h is a normalization factor, which can be set as a constant.

To compare the difference between the target model and target candidate, the similarity function is computed between the target model histogram and the target candidate histogram. The result of the similarity function is a percentage value which will be compared among various target histograms. In this work, our the similarity function is based on the Bhattacharyya coefficient, $\rho(\hat{p}(y), \hat{q})$, which is commonly used. The Bhattacharyya coefficient measures the similarity between the histogram of the model and the candidates[12]. Therefore, the Bhattacharyya coefficient equation can be defined as follows:

$$\rho(\hat{p}(y), \hat{q}) = \sum_{u=1}^{m} \sqrt{\hat{p}_u(y)\hat{q}_u} = \sum_{u=1}^{m} \hat{p}_u(y) \sqrt{\frac{\hat{q}_u}{\hat{p}_u(y)}} \tag{11}$$

The best target candidate field is the minimum distance, according to the similarity function [33]. In addition, the minimization of the distance between the target model and target candidate can be derived as shown in below:

From the Bhattacharyya coefficient equation (11) estimates the Bhattacharyya coefficient equation using:

$$so: \rho(\hat{p}(y), \hat{q}) \approx \frac{1}{2}\sum_{u=1}^{m} \sqrt{\hat{p}_u(y_0)\hat{q}_u} + \frac{1}{2}\sum_{u=1}^{m} \hat{p}_u(y) \sqrt{\frac{\hat{q}_u}{\hat{p}_u(y_0)}} \tag{12}$$

We then substitute the following equations in to the estimation of the Bhattacharyya coefficient equation:

$$\hat{p}_u(y) = C_h \sum_{b(x_i)=u} k\left[\left\|\frac{y - x_i}{h}\right\|^2\right] \; and \; w_i = \sum_{u=1}^{m} \sqrt{\frac{\hat{q}_u}{\hat{p}_u(y_0)}} \tag{13}$$

therefore, the minimization of the Bhattacharyya coefficient equation become:

$$\therefore \; \rho(\hat{p}(y), \hat{q}) \approx \frac{1}{2}\sum_{u=1}^{m} \sqrt{\hat{p}_u(y_0)\hat{q}_u} + \frac{C_h}{2}\sum_{i=1}^{n_h} w_i k\left[\left\|\frac{y - x_i}{h}\right\|^2\right] \tag{14}$$

where $\{\hat{p}_u(y_0)\}_{u=1\ldots m}$ is the target candidate at the center location $y_0$in the current frame.

4.1.2 Mean-Shift Tracking

The main concept of the mean-shift algorithm is to locate the target object based on the maximization of the Bhattacharyya coefficient. The process to locate the target object in a single frame consists of five steps. The overall process of mean-shift tracking is shown in Figure 4.1.

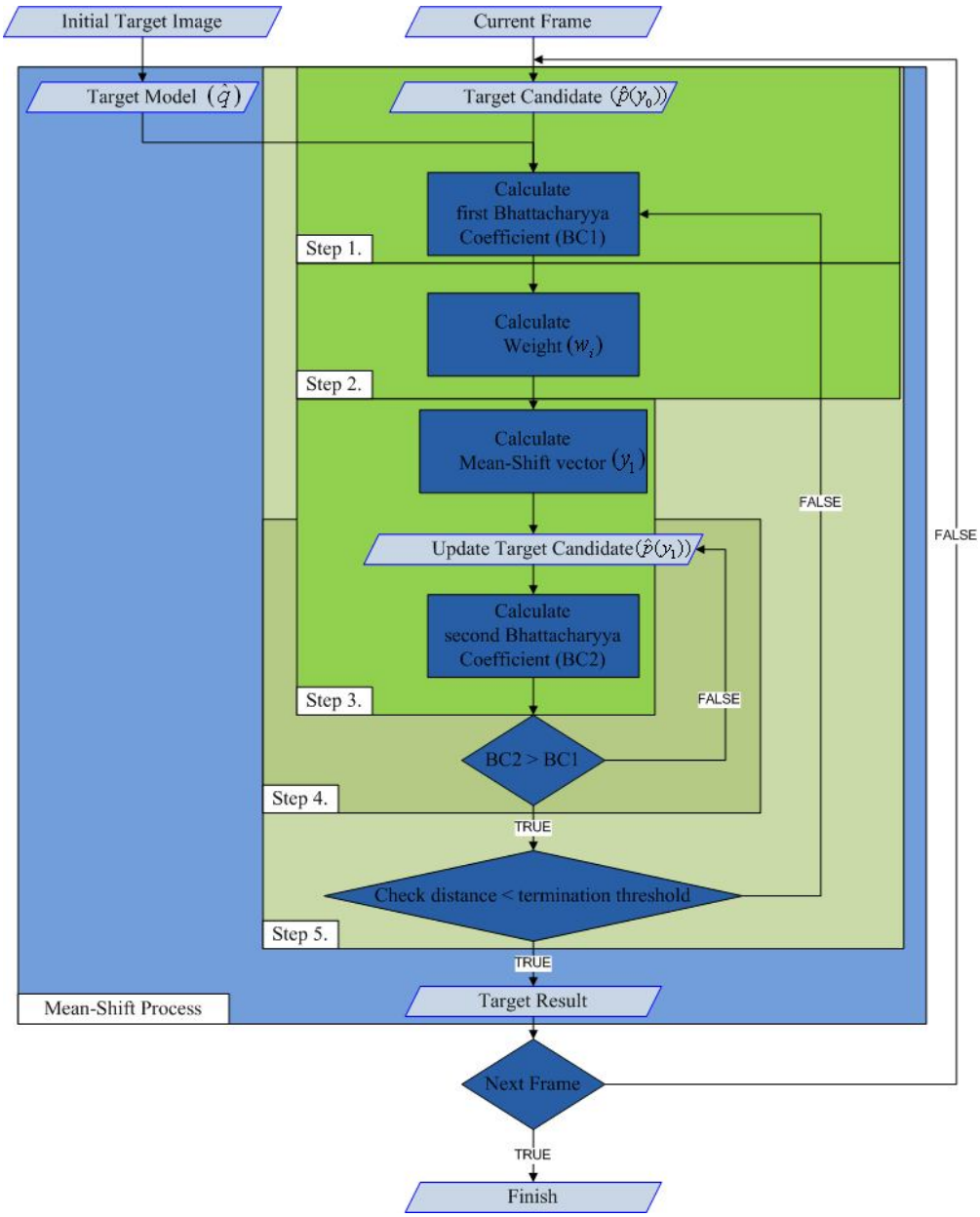

Figure 4.1 Mean-Shift Tracking Process

For the Mean-Shift tracking, we use these steps to compute each frame of video sequences. This processing locates the target object which is the target model in mean-shift algorithm. The tracking process defines the target candidate defines according to the similarity location of target model at the current frame. The tracking process uses these steps to locate the new target model in current frame. From Figure 4.1, the five steps of mean-shift tracking can be described in next sections.

In the first frame, we need to initialize $\{\hat{q}_u\}_{u=1\ldots m}$ to be the distribution of the target model and y_0 to be the center location of the target in the next frame.

Step1.

Initialize the new center location of the target in the current frame at the previous center location y_0 and compute the distribution of the target candidate at y_0:

$$\hat{p}(y_0) = \{\hat{p}_u(y_0)\}_{u=1\ldots m} \tag{15}$$

Then evaluate the first Bhattacharyya Coefficient.

$$BC1 = \rho(\hat{p}(y_0), \hat{q}) = \sum_{u=1}^{m} \sqrt{\hat{p}_u(y_0)\hat{q}_u} \tag{16}$$

Step2.

Derive the weights $\{w_i\}_{i=1\ldots n_h}$, as follows:

$$w_i = \sum_{u=1}^{m} \sqrt{\frac{\hat{q}_u}{\hat{p}_u(y_0)}} \; ; i = 1 \ldots n_h \tag{17}$$

Step3.

The mean shift vector yields the new location y_1. This result is used to calculate the minimization of the distance between target model and target candidate. This process propagates the current position y_0 to the new location y_1. Therefore, the new location of the target candidate can be written as follows:

$$y_1 = \frac{\sum_{i=1}^{n_h} x_i w_i g\left(\left\|\frac{y_0 - x_i}{h}\right\|^2\right)}{\sum_{i=1}^{n_h} w_i g\left(\left\|\frac{y_0 - x_i}{h}\right\|^2\right)} \tag{18}$$

Where $g(x) = -K'(x)$

After updating the new center target location at y_1 , the distribution of target candidate at y_1 is computed as follows:

$$\hat{p}(y_1) = \{\hat{p}_u(y_1)\}_{u=1\ldots m} \tag{19}$$

Then the second Bhattacharyya coefficient is evaluated.

$$BC2 = \rho(\hat{p}(y_1), \hat{q}) = \sum_{u=1}^{m} \sqrt{\hat{p}_u(y_1)\hat{q}_u} \tag{20}$$

Step4.

This process iterates until *BC2>BC1*; however, if *BC2 < BC1*, then the new center target y_1, will be updated, as follows:

$$\begin{aligned} &While\ \{\, BC1 < BC2 \,\} \\ &Do\ \{y_1 = \frac{1}{2}(y_0 + y_1)\} \end{aligned} \tag{21}$$

Step5.

This process checks the termination condition of the algorithm based on the predicted threshold value ϵ. The threshold value is defined as the minimum distance value between the target model and the target candidate. The condition of this step is computed as follows:

$$
\begin{aligned}
&if\ (\|y_1 - \ y_0\| < \epsilon\ ) \\
&\{\ \ Stop\ the\ process \\
&\qquad \} \\
&\qquad Else \\
&\{\ Set\ \ y_0 = y_1 \\
&\quad Go\ to\ Step\ 1 \\
&\qquad \}
\end{aligned}
\tag{22}
$$

4.2 FILTERING AND DATA ASSOCIATION

Filtering and Data Association is an adaptive process for an object tracking system. The input of this component is based on the result of *Target Representation and Localization.* These algorithms are able to locate a complex object that moves behind the obstructions. The main filtering algorithms can be divided into two types of filter: Kalman Filter and Particle Filter [23]. The kalman filter is simply an *optimal recursive data processing algorithm*. The processing estimates all actual measurement data without considering the precision. In this thesis, we focus on tracking only one target object; therefore, we use the kalman filter. The main advantage of the Kalman filter is the ability to estimate state of one target object. The main advantage of the Particle filter is the ability to track multiple objects, however it is not suitable to use in this thesis. Therefore, we propose the use of the Kalman filter to improve the result of the mean-shift algorithm, which is the main process. The measurements estimate the current value of interested variables based on the result of mean-shift algorithm. The model of kalman filter algorithm consists of (1) knowledge of the system and measurement device dynamics, (2) the statistical description of the system noise, measurement noise, errors, and uncertainty in the dynamical models, and (3) any information about initial conditions of the interested object [34]. In this section, we describe the Kalman filter in twos subtopics which consist of Kalman filter algorithm and tracking.

4.2.1 Kalman Filter Algorithm

The Kalman filter [35, 36] is based on a set of mathematical equations which implement a predictor-corrector step to estimate the result. In mathematical terms, this filter is a tool for estimating the states of a linear system. The detailed derivation of the Kalman filter is shown as follows: Appendix. The Kalman filter is a recursive filter which separates into two steps consisting of prediction and correction step. The prediction step defines the time update and the correction step defines the measurement update. Therefore, the overviews of kalman filter as shown in Figure 4.2. The time update equations and measurement update equations are presented in the next section.

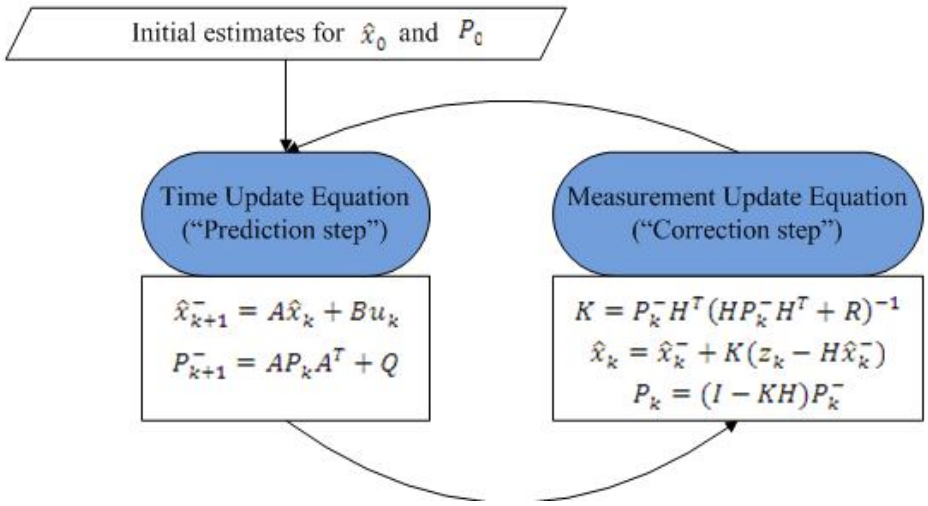

Figure 4.2 The process of Kalman filter.

This section describes the filter in the original formulation. The filter tries to estimate the state $x \in \Re^n$, where n is the number of state estimator, of a discrete-time process which control by the linear stochastic difference equation as follows:

$$x_k = Ax_{k-1} + Bu_k + w_{k-1} \tag{23}$$

where A is the $n \times n$ state transition matrix, x_{k-1} is the $n \times 1$ state matrix in the previous time(frame) step, B is the $n \times l$ optional control transition matrix, u_k is k-time optional control input which is $l \times 1$ matrix, and w_k is the process noise which is $n \times 1$

matrix or a constant. A measurement$z \in \Re^m$, where m is the number of state measurements, of a discrete-time process which control by the estimation state as follows:

$$z_k = Hx_k + v_k \tag{24}$$

where H is the $m \times n$ measurement transition matrix which relates the state x_k to measurement z_k, and v_k in the measurement noise which is $m \times 1$ matrix or a constant. The process and measurement noises are assumed to have independent, white, and normal probability distributions as follows:

$$p(w) \sim N(0, Q) \;\; ; Q = [w_k w_k^T] \tag{25}$$

$$p(v) \sim N(0, R) \;\; ; R = [v_k v_k^T] \tag{26}$$

where Q is the process noise covariance, and R is the measurement noise covariance.

A priori and a posteriori estimate errors are defined as $e_k^- \; and \; e_k$, respectively. These estimate error covariance defined in the $n \times n$ matrix form at time k. These equations can be written as:

$$e_k^- \cong x_k - \hat{x}_k^- \tag{27}$$

$$e_k \cong x_k - \hat{x}_k \tag{28}$$

where $\hat{x}_k^- \in \Re^n$ is a priori state estimate or previous estimation state in recursive process , and $\hat{x}_k \in \Re^n$ is a posteriori state estimate at step k which given a measurement z_k.

These equations can be calculated as a priori and a posteriori estimate error covariance$P_k^- \; and \; P_k$, respectively. These equations can be written as:

$$P_k^- = E[e_k^- e_k^{-T}] \tag{29}$$

$$P_k = E[e_k e_k^T] \tag{30}$$

The goal of the Kalman filter is to determine a posteriori state estimate $\hat{x}_k$which computes a linear combination of a priori state estimate $\hat{x}_k^-$and a weight difference between an actual measurement z_k and a measurement prediction $H\hat{x}_k^-$. The difference $(z_k - H\hat{x}_k^-)$ is called the measurement "innovation" or "residual". This is called "The probabilistic origins of the filter" as follows:

$$\hat{x}_k = \hat{x}_k^- + K(z_k - H\hat{x}_k^-) \tag{31}$$

where *K* is called the "Kalman gain" which is an *n x m* matrix. This matrix solution is used for the optimization problem. Thus, the Kalman gain equation can be written as follows:

$$K = P_k^- H^T (HP_k^- H^T + R)^{-1} \tag{32}$$

The Kalman gain uses minimized a posteriori estimation error covariance P_k. Therefore, the replacement of $P_k$by *K*, can be written as:

$$P_k = (I - KH)P_k^- \tag{33}$$

where *I* is a *n x n* identity matrix, P_k is the update equation for the a priori estimate error covariance with kalman gain.

The estimation state in the Kalman filter iteration is achieved by:

$$\hat{x}_{k+1}^- = A\hat{x}_k \tag{34}$$

To complete the recursive process, it is necessary to find an equation that projects the a priori estimate error covariance matrix into the next time interval, *k + 1*. Therefore, the a priori estimate error covariance at time *k+1* can be written as:

$$P_{k+1}^{-} = AP_kA^T + Q \tag{35}$$

4.2.2 Kalman Filter Tracking

The Kalman filter tracking is the iterative process of Kalman filter to be used in the video sequence. The location of target object in each frame is the estimation result of the Kalman filter. In this thesis, the iterative process of Kalman filter consists of two steps; time update and measurement update equations. The time update equations are responsible for projecting in time. These equations consist of the current state and a priori estimate error covariance for the next time step. The equations of this step consist of two processes.

1) Project the state, $\hat{x}_{k+1}^{-}$ in the next time *k+1*, as follows:

$$\hat{x}_{k+1}^{-} = A\hat{x}_k + Bu_k \tag{36}$$

2) Project the a posteriori estimation error covariance, P_{k+1}^{-} in the next time *k+1*, as follows:

$$P_{k+1}^{-} = AP_kA^T + Q \tag{37}$$

The measurement equations use the actual measurement z_k to update the state of the object. The equations of this step consist of three processes.

1) Computed the Kalman gain, *K* as follows:

$$K = P_k^{-}H^T(HP_k^{-}H^T + R)^{-1} \tag{38}$$

2) Update estimate state with actual measurement, z_k, as follows:

$$\hat{x}_k = \hat{x}_k^- + K(z_k - H\hat{x}_k^-) \tag{39}$$

3) Update the a priori estimation error covariance, P_k in the current time k, as follows:

$$P_k = (I - KH)P_k^- \tag{40}$$

From the time update equations and measurement equations, the tracking process is repeated with the previous a posteriori estimate to predict the new a priori estimate state. Therefore, the example processing of the Kalman filter tracking is a combination of the initial estimate state and a priori estimation error covariance, as shown in Figure 4.3.

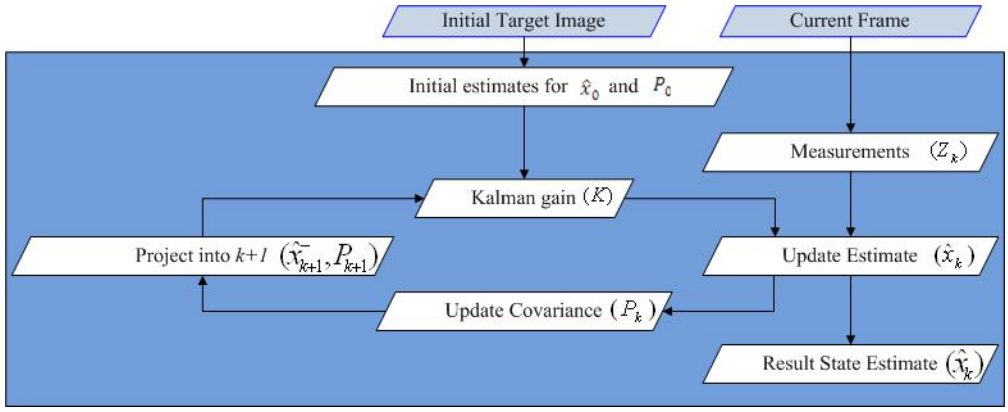

Figure 4.3 The processing of Kalman filter tracking.

4.3 OBJECT TRACKING SYSTEM FOR THE NEW MIRS SYSTEM

The object tracking system has two components which consist of *Target Representation and Localization* and *Filtering and Data Association*. In this thesis, we will propose the Mean-Shift algorithm which is an algorithm of the Target Representation and localization component, as well as the Kalman filter which is an algorithm of the Filtering and Data Association component. The main purpose of the mean-shift algorithm is to locate the interested object in the frame. This process is based on the maximum value of the similarity function which is the Bhattacharyya coefficient. Therefore, the result is the location of the target object in searching area or target candidate. The main process of the Kalman filter is based on a predictor-corrector step to estimate the result in the frame. This process is based on the previous results from the actual measurement. The results of previous frames are used to estimate the result in the current frame.

In this thesis, we propose the adaptive mean-shift Kalman tracking based on the mean-shift algorithm combined with the Kalman filter. The proposed algorithm has improved the mean-shift algorithm by its ability to adjust to different ROI sizes of the target candidate. The adaptive mean-shift Kalman algorithm is mainly used to track the object of interest. The overall process of adaptive mean-shift Kalman tracking summarized in Figure 4.4 and is explained below.

Initial step: Selection of target model

In the first frame, the user selects the target model which is the predefined ROI. From the target model, we compute the initial state of the Kalman filter.

First step: Mean-Shift algorithm process

In the next frame, the algorithm defines the target candidate which is at the same center location as the target model. However, the size of target candidate is larger than the size of the target model (the size of the region, h). The target model and the target candidate will be computed to get the second Bhattacharyya coefficient ($BC2$) in the mean-shift algorithm.

Second step: Similarity comparison from the mean-shift algorithm

Firstly, we will define the first similarity threshold value (*CT1*) to determine the tracking criteria. This value will be compared with *BC2*. If *BC2* is more than *CT1*, then we will update the Kalman filter by using the result of the mean-shift algorithm in the first step. Thus, the target result in this case will be acquired from the mean-shift algorithm, and the next sequence frame can be proceeded. However, if *BC2* is less than *CT1*, then we go to the third step.

Third step: Estimation of the Kalman filter

In this step, the estimate state of the Kalman filter is fed back to the adaptive mean-shift algorithm. If the tracking result is not in the predefined similarity threshold value, the algorithm will increase the target candidate up to twice the size of the current ROI. In addition, this target candidate will define the new location from current state of the Kalman filter. Hence, the third Bhattacharyya coefficient (*BC3*) is computed.

Fourth step: Similarity comparison between the Kalman filter and the adaptive mean-shift algorithm

We compare the second similarity threshold value (*CT2*) with the *BC3* from the third step. If *BC3* is greater than *CT2*, then we will use the result from the adaptive mean-shift algorithm. If *BC3* is smaller than *CT2*, then we will use the estimate state of the Kalman filter and go back to the third step and increase the target candidate ROI. This process is repeated until the maximum target candidate size is met. Otherwise, the target result will be acquired from the adaptive mean-shift algorithm, and the next sequence frame can be proceeded.

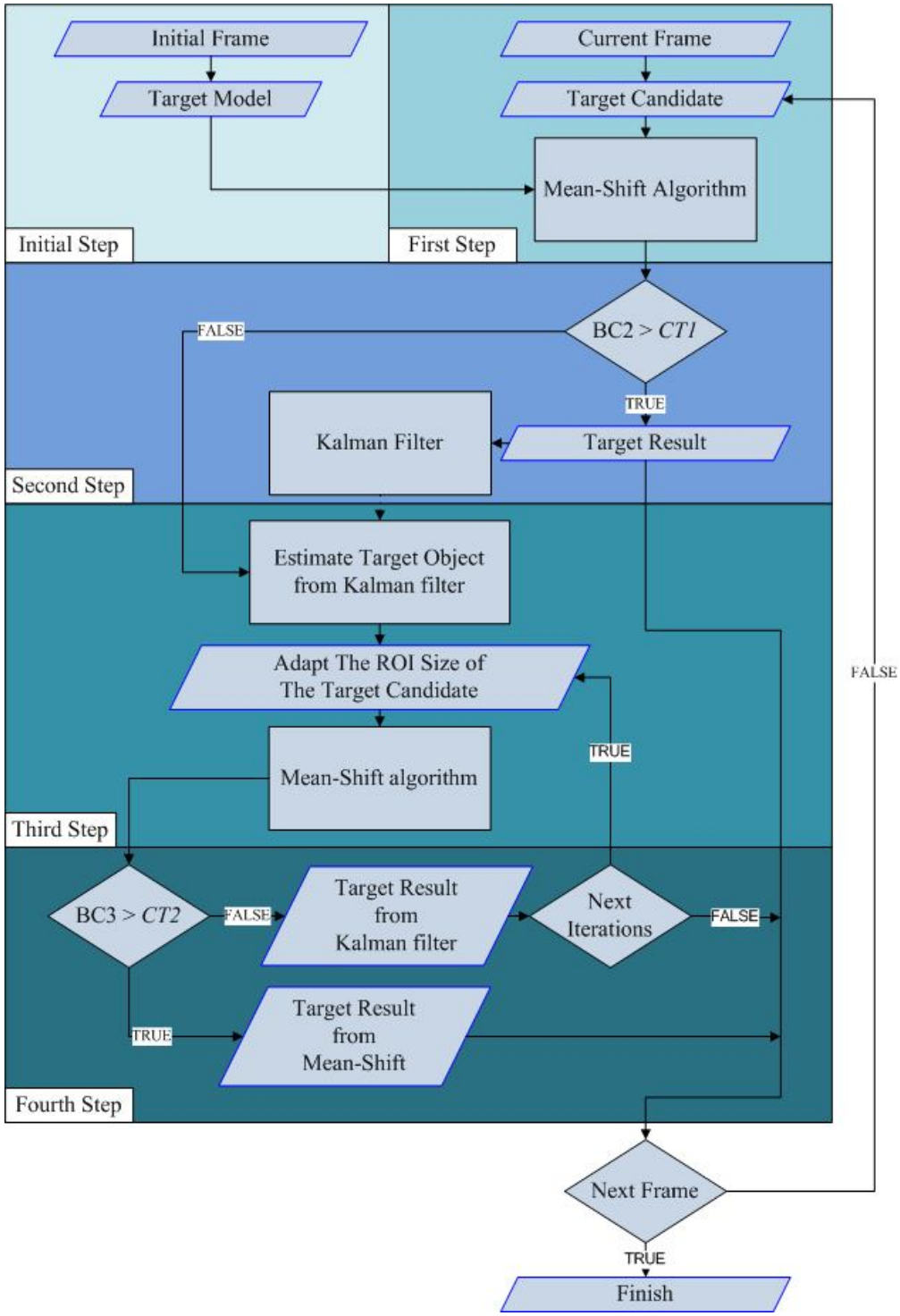

Figure 4.4 The overall of the adaptive Mean-Shift Kalman algorithm

CHAPTER V
EXPERIMWNTAL RESULTS

This chapter shows two experiment results. The first experiment represents the overall kinematics of the conceptual robot. In addition, we will compute the forward kinematics of the main motion to create the working area inside the patient's abdomen. This forward kinematics will calculate the overall workspace of the conceptual robot inside patient's abdomen. The second experiment represents the proposed object tracking algorithm which is the adaptive mean-shift kalman algorithm to track the target object. This experiment is separated three situations. First, the testing situations are five example videos to test the proposed algorithm in each problem which define as five cases. Second, the real situations are real videos in laparoscopic surgery to test the proposed algorithm in all problems. Last, the real time tracking are experiment in the phantom box.

5.1 ANALYSIS OF CONCEPTUAL ROBOT FOR THE NEW MIRS SYSTEM

From the conceptual robot design in Section 3.1 we have proposed the design of new robot with 5-DOFs. In this section, we will explain the overall kinematics of conceptual design, as well as, compute the workspace of conceptual robot which performs inside the patient's abdomen. The overall workspace is computed in terms of 3 dimensions which consist of depth, width, and height.

5.1.1 The overall kinematics of conceptual design

The conceptual design of the new MIRS system is separated into two parts: the external manipulator part and the bending laparoscope part. We have proposed 5-DOFs of motion of robot consisting of 2-DOFs to control the center of the fulcrum point and 3-DOFs to control the motion of the laparoscope. Therefore, the

kinematics of this robot will separated in two parts. In the first part, the external manipulator part has 2-DOFs which control the bending laparoscope part at the center of the fulcrum point. The 2-DOFs consist of θ_1 which is the rotation at the X axis and $\theta_2$is the rotation at the Y axis, as shown in Figure 5.1. In the second part, the bending laparoscope part has 3-DOFs which control the movement of the bending part and the end of the laparoscope. The 3-DOFs consist of $\theta_3$which is the rotation of the bending part at the X axis; $\theta_4$which is the rotation of the bending part at Y axis; and T_3which is the translation of the laparoscope at the Z axis, as shown in Figure 5.1.

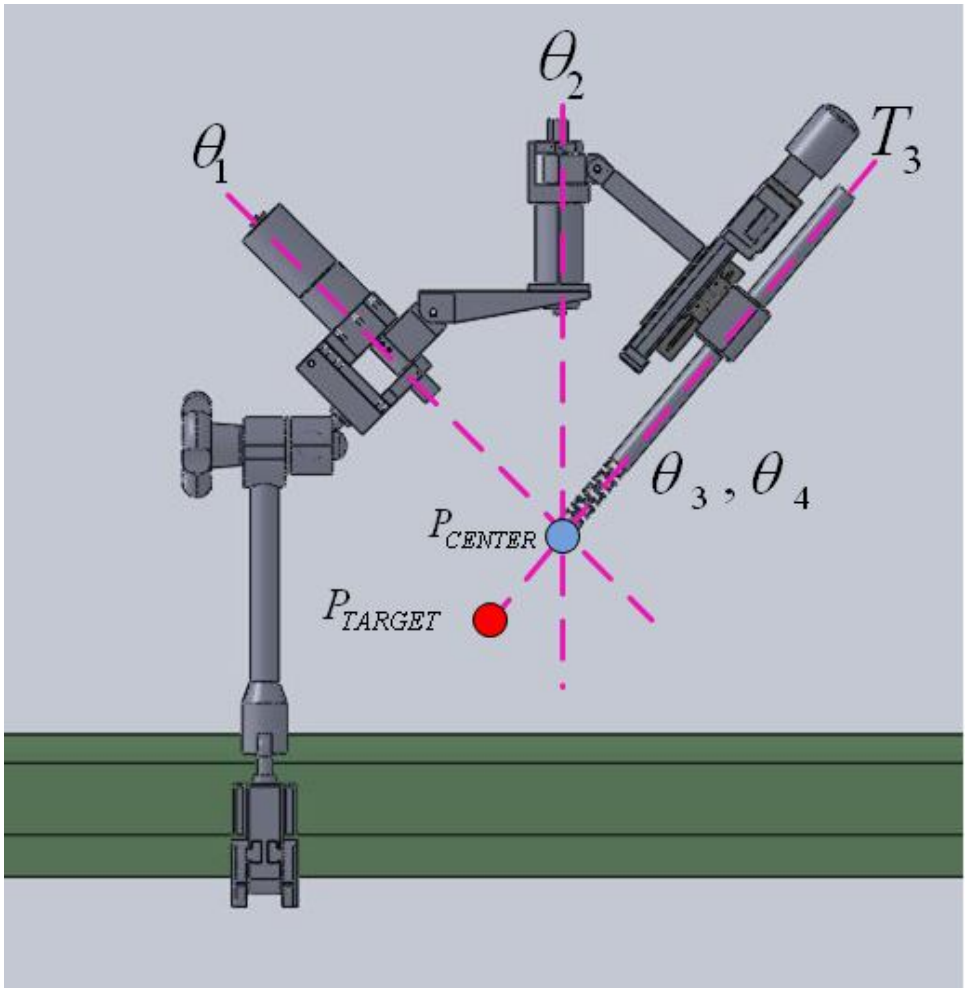

Figure 5.1 The robot kinematics

The result of the kinematics equation is the target position which is P_{Target} in Figure 5.1. The target position will depend on the fulcrum point which is P_{Center} in Figure 5.1. The P_{Center} has 2-DOFs, so the equation can be written as

$$P_{Center} = R_z(\theta_2) * R_x(\theta_1)$$

$$where;\ R_z(\theta_2) = \begin{bmatrix} \cos\theta_2 & -\sin\theta_2 & 0 & 0 \\ \sin\theta_2 & \cos\theta_2 & 0 & 0 \\ 0 & 0 & 1 & 0 \\ 0 & 0 & 0 & 1 \end{bmatrix} and\ R_x(\theta_1) = \begin{bmatrix} 1 & 0 & 0 & 0 \\ 0 & \cos\theta_1 & -\sin\theta_1 & 0 \\ 0 & \sin\theta_1 & \cos\theta_1 & 0 \\ 0 & 0 & 0 & 1 \end{bmatrix}$$

The P_{Target} has 3-DOFs whichreference from P_{Center}, thus the equation can be written as

$$P_{Target} = P_{Center} * T_z(T_3) * R_y(\theta_3) * R_x(\theta_4)$$

$$where;\ T_z(T_3) = \begin{bmatrix} 1 & 0 & 0 & 0 \\ 0 & 1 & 0 & 0 \\ 0 & 0 & 1 & T_3 \\ 0 & 0 & 0 & 1 \end{bmatrix},$$

$$R_y(\theta_3) = \begin{bmatrix} \cos\theta_2 & 0 & -\sin\theta_2 & 0 \\ 0 & 1 & 0 & 0 \\ \sin\theta_2 & 0 & \cos\theta_2 & 0 \\ 0 & 0 & 0 & 1 \end{bmatrix}, and\ R_x(\theta_4) = \begin{bmatrix} 1 & 0 & 0 & 0 \\ 0 & \cos\theta_4 & -\sin\theta_4 & 0 \\ 0 & \sin\theta_4 & \cos\theta_4 & 0 \\ 0 & 0 & 0 & 1 \end{bmatrix}$$

5.1.2 The forward kinematic modeling of the workspace robot

The overall kinematic of conceptual robot has 5-DOFs but the main motion to produce the large working area at inside the patient abdomen has 3-DOFs. Because of the motion of bending laparoscope, which has 2-DOFs consist of θ_3 and θ_4, produce very small working area inside the patient abdomen. Thus, the main motion has 3-DOFs which consist of 2-DOFs at θ_1 is the rotation at X axis and θ_2 is the rotation at Y axis and 1-DOF at T_3 is the translation of the laparoscope at Z axis, as shown in Figure 5.2. This figure sketches the graphic symbols which draw overlap the conceptual design. The symbol of main motion represents the three light blue points which represent 3-DOFs. The symbol of start point represents a dark blue

point. The symbol of length of each part represents the six blue lines which measure from the conceptual design robot. The symbol of target location laparoscope represents a red point. The value of each symbol will explain in Table 5.1.

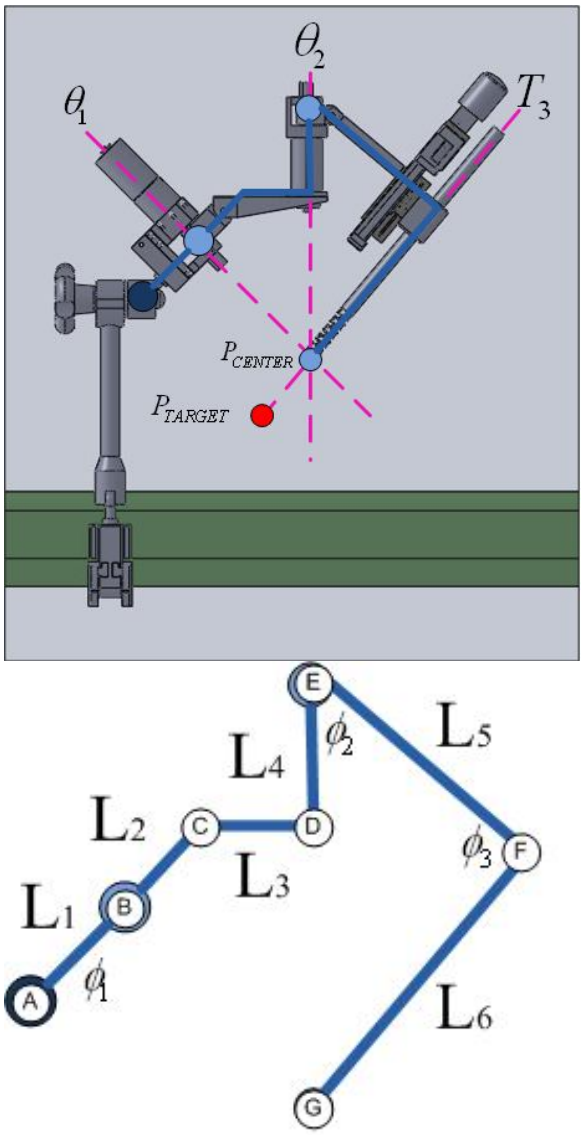

Figure 5.2 The model of conceptual robot

Table 5.1 Parameters of kinematic modeling

Parameter	Value	Unit
T_3	0 – 150	mm.
θ_2	-90 – 90	degree
θ_1	If $\theta_2 > 0$ then -70 – 20 If $\theta_2 < 0$ then -20 – 70	degree
$L_1\ (\overline{AB})$	56	mm.
$L_2\ (\overline{BC})$	60	mm.
$L_3\ (\overline{CD})$	95	mm.
$L_4\ (DE)$	86	mm.
$L_5\ (EF)$	83	mm.
$L_6\ (\overline{FG})$	100	mm.
$\emptyset_1$	45	degree
$\emptyset_2$	40	degree
$\emptyset_3$	90	degree

The model of conceptual robot will compute the working area by using the MATLAB program. This program will calculate the working area in a 3-D space. The points A – G, which show in Figure 5.2, can be written as the equation form. The start point is point A which represents at location (0, 0, 0) in a 3-D space. The equation of point A can be written as

$$P_A = [0\ 0\ 0\ 1]^T$$

The points B – E represents the rotation of θ_1. The equation of this point can be written as

$$P_B = P_A * R_x(\emptyset_1) * T_z(L_1)$$
$$P_C = P_B * R_y(\theta_1) * R_x(\emptyset_1) * T_z(L_2)$$
$$P_D = P_C * T_x(-L_3)$$
$$P_E = P_D * R_y(\theta_1) * T_z(L_4)$$

The point E represents the rotation of θ_2. The equation of this point can be written as

$$P_F = P_E * R_Z(\theta_2) * R_x(\emptyset_2) * T_x(-L_5)$$

The point G represents the translation of T_3. The equation of this point can be written as

$$P_G = P_F * R_x(\emptyset_3) * T_x(-L_6 + T_3)$$

The red point represents the position target of conceptual robot in a 3-D space. The equation of the target will equal the point G can be written as

$$P_{target} = P_G$$

These equations can create the example of kinematic model in a 3-D space as shown in Figure 5.3. This example define the input values which are $\theta_1 = 0$, $\theta_2 = 0$, and $T_3 = 0$.

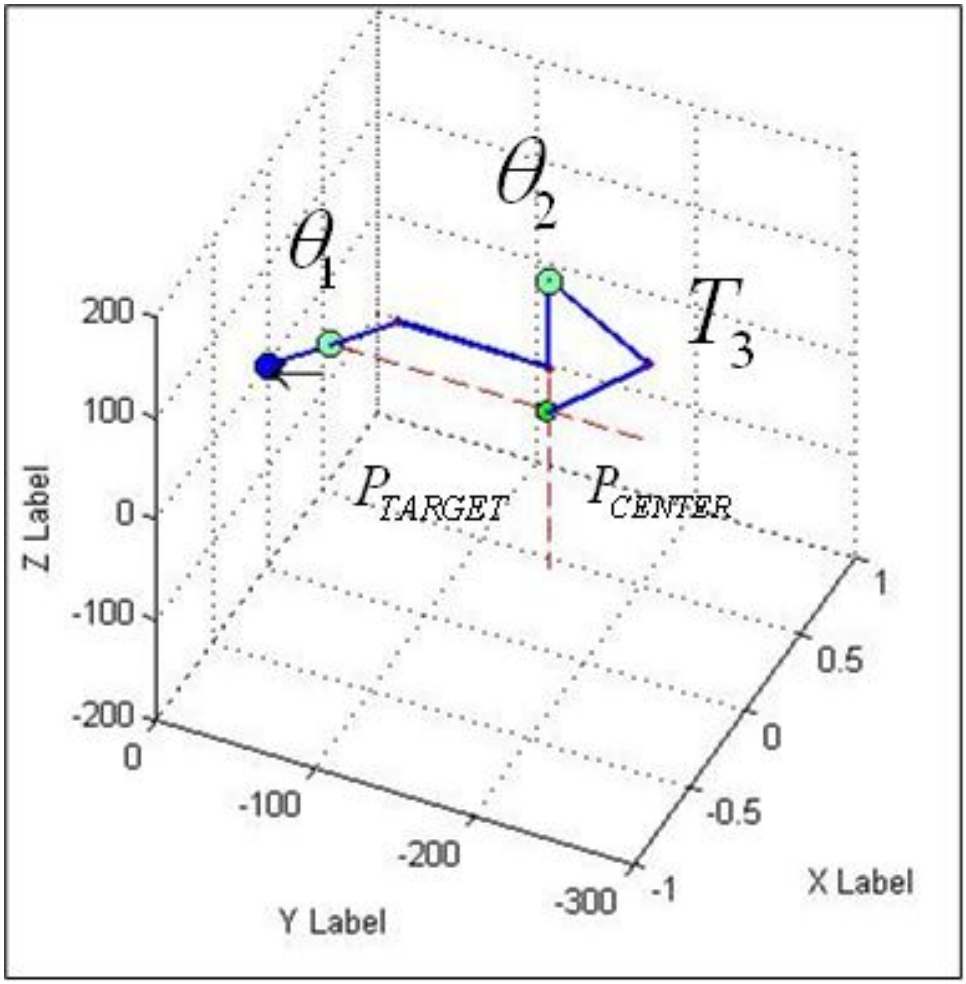

Figure 5.3 The kinematic modeling in 3-D space

5.1.3 The workspace determination of conceptual robot

From the kinematic modeling of conceptual robot, the motion limits of conceptual robot define in the Figure 5.3. We develop the MATLAB program to compute the working area inside the patient abdomen, as shown in Figure 5.6. This program will compute the working area which input the motion limits of three motions. The input data consist of rotation at θ_1, rotation at θ_2, and translation at T_3 Let the translational limits of motion at T_3 is 150 mm. In the rotational limits will separate into three groups. First group, if the rotation value of θ_1 define between -20 and 20 degrees then the rotation value of θ_2 define between -90 and 90 degrees. This group will create working area, as shown in Figure 5.4(a). Second group, if the rotation value of θ_1 define between 21 and 70 degrees then the rotation value of θ_2

define between 0 and -90 degrees. This group will create the working area, as shown in Figure 5.4(b). Third group, if the rotation value of θ_1 define between -21 and -70 degrees then the rotation value of θ_2 define between 0 and 90 degrees. This group will create the working area, as shown in Figure 5.4(c). Thus, the overall working area of conceptual robot will combine the three working area from three groups, as shown in Figure 5.4(d).

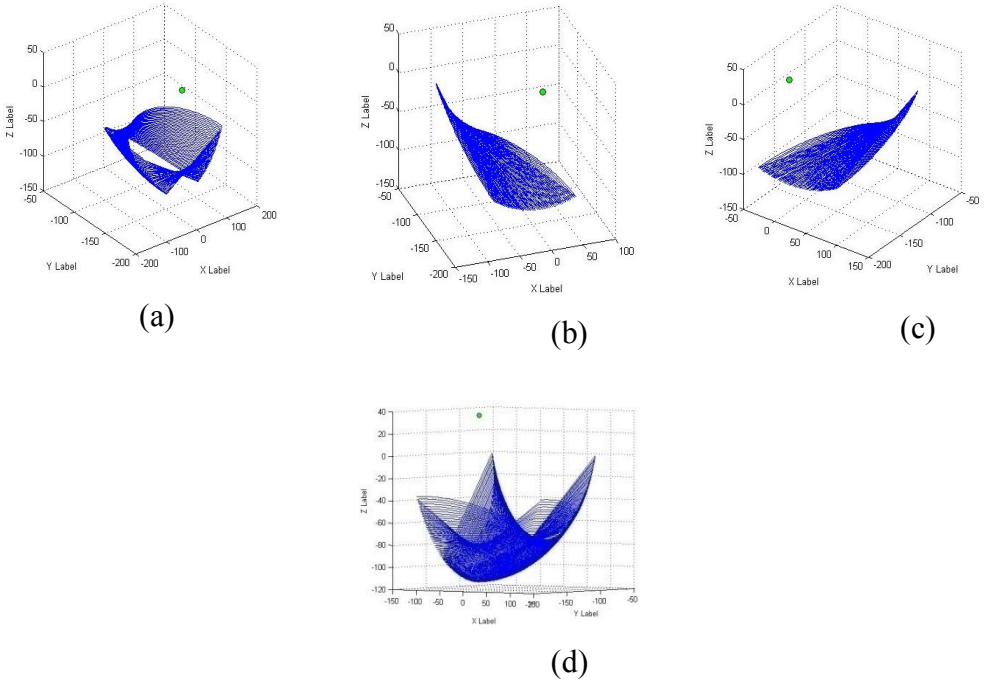

(a) (b) (c)

(d)

Figure 5.4 The working area

(a) The working area of first case (b) The working area of second case
(c) The working area of third case (d) The overall working area

From the overall working area can calculate the limitation workspace of conceptual robot which moves inside the patient abdomen. The computation of limitation workspace will separate into three parts. First part, the depth of limitation workspace will compute from the fulcrum point to the deepest point of overall working area. The depth of overall working area is 150.0926 mm, as shown in Figure 5.5(a). This figure represent the overall working area in the 2-D which is the front view consist of x-axis and z-axis. Second part, the width of limitation workspace will compute from the minimum point to maximum point in x-axis of overall working

area. The width of overall working area is 262.8 mm, as shown in Figure 5.5(b). Last part, the height of limitation workspace will compute from the minimum point to maximum point in y-axis of overall working area. The height of overall working area is 103.6215 mm, as shown in Figure 5.5(b). This figure represent the overall working area in a 2-D which is the top view consist of x-axis and y-axis. Therefore, the overall working area of conceptual robot can cover the workspace at inside the patient abdomen. In addition, this robot will create the working area in the cone shape form. From the limitation workspace of the conceptual robot, we can calculate the apex angle of 82.4 degrees which is more than the 60 degrees from [30]. Therefore, the overall working area of the conceptual robot can cover the overall workspace inside the patient abdomen.

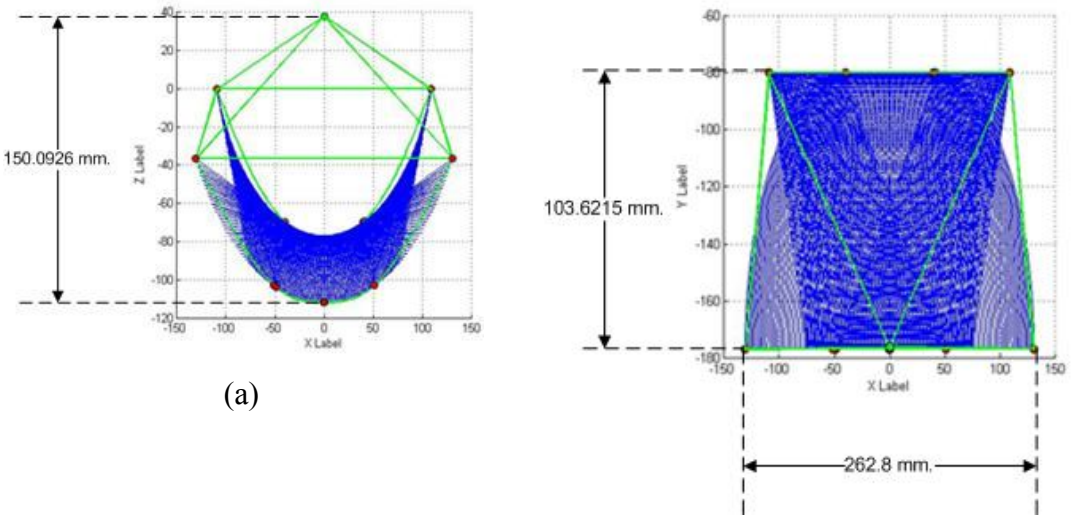

Figure 5.5 The reachable workspace of conceptual robot

(a)The working area at front-view (b) The working area at top-view

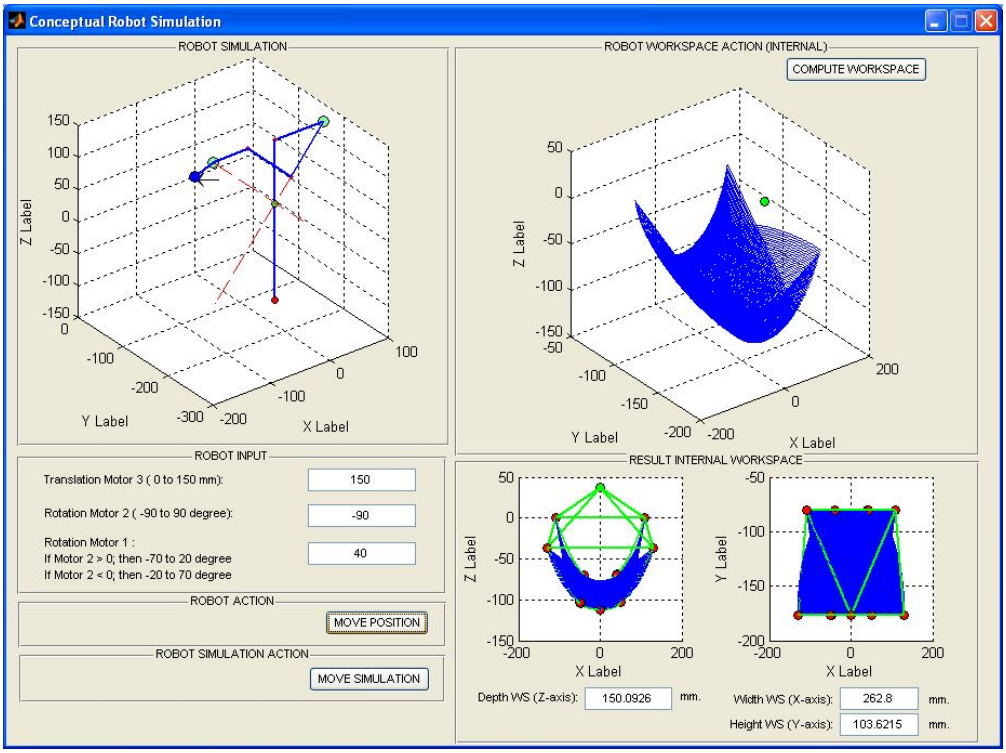

Figure 5.6 The MATLAB program to compute the working area

5.2 DEVELOP OF CONCEPTUAL ROBOT FOR THE NEW MIRS SYSTEM

The overall development of conceptual robot which consists of the passive base part, the external manipulator part and the bending laparoscope part which develop only the zooming motion to uses a linear guide with a ball screw. In the external manipulator part, we make by using the aluminum materials. In the linear guide of bending laparoscope part, we make by using the aluminum and plastic materials. In the laparoscope part, we use the webcam to connect with a rod for simulating the laparoscope. Figure 5.7 represent the comparison between the overall development of conceptual robot, as shown in Figure 5.7(a) and the overall design of conceptual robot, as shown in Figure 5.7(b). A difference between the design and the development of conceptual robot is the bending laparoscope. Therefore, this conceptual robot has 3-DOFs which consist of 2-DOFs of the external manipulator part at θ_1 is the rotation of motor 1 and θ_2 is the rotation of motor 2 and 1-DOF of

the bending laparoscope part at T_3 is the translation of a linear guide with a ball screw by motor 3, as described in Figure 5.8.

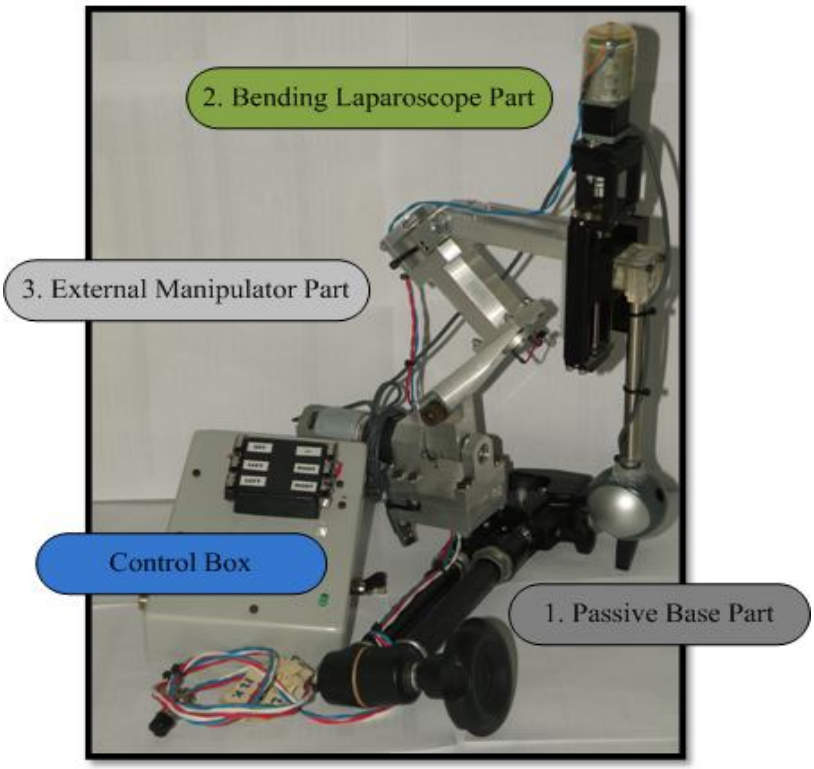

(a)

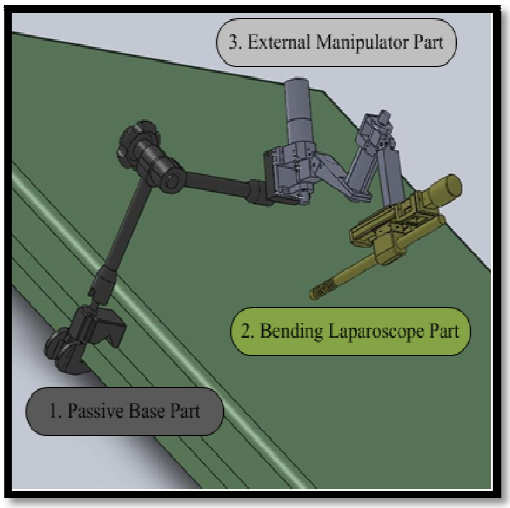

(b)

Figure 5.7 The comparison of conceptual robot

(a) The overall development of conceptual robot (b) The overall design of conceptual robot

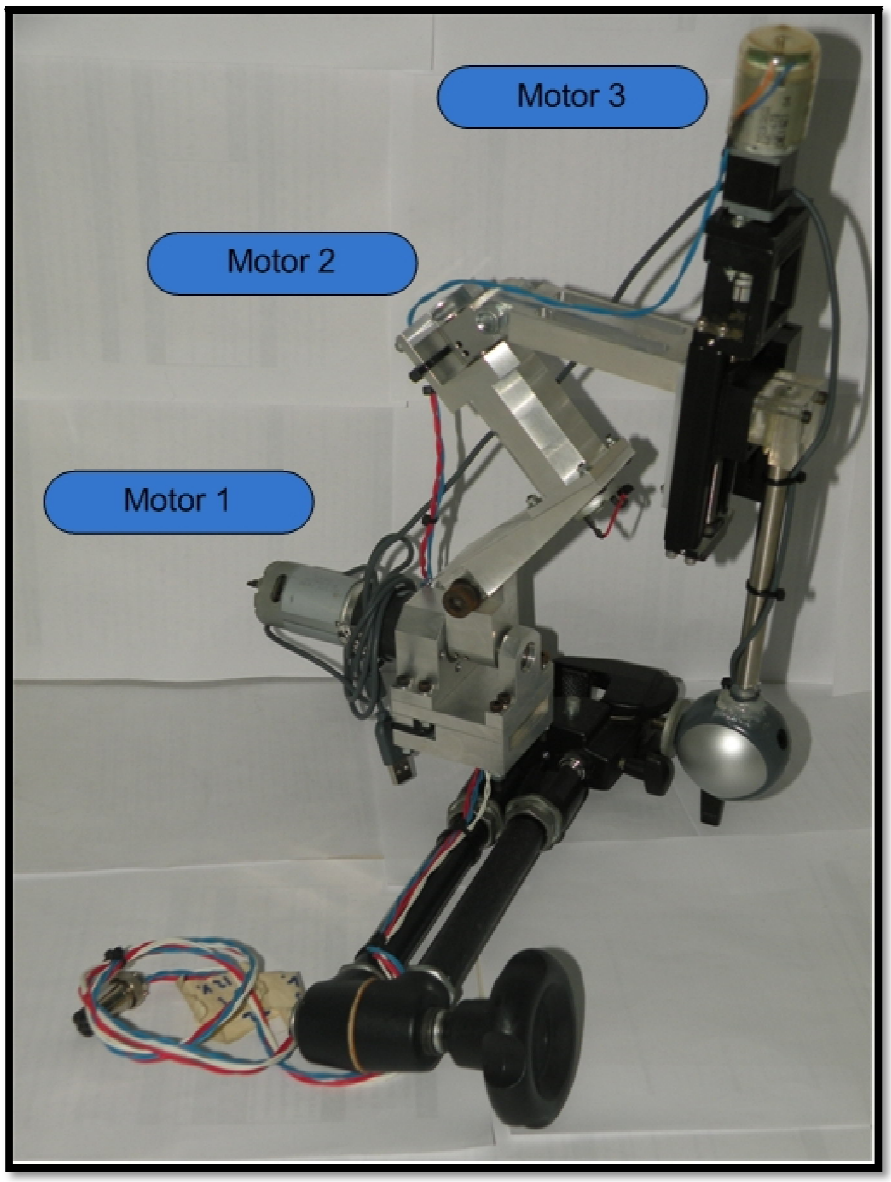

Figure 5.8 The description of the conceptual robot to develop

This robot can manually control by using the control box, as shown in Figure 5.9. This control box has six buttons which control the three motors of the conceptual robot. The motor 1 of the external manipulator part can control by down two buttons of control box. The actions of these buttons, we press the right button then the external manipulator part at motor 1 will move to the right direction, however we press the left and the right buttons then at motor 1 will move to the left direction. The motor 2 of the external manipulator part can control by center two buttons of control box. These buttons have the actions same as the down buttons. The motor 3 of

the linear guide can control by top two buttons of control box. The actions of these buttons, we press the right button then the linear guide will move forward which moves the laparoscope in the abdomen, however we press the left button then the linear guide will move backward which move the laparoscope out the abdomen.

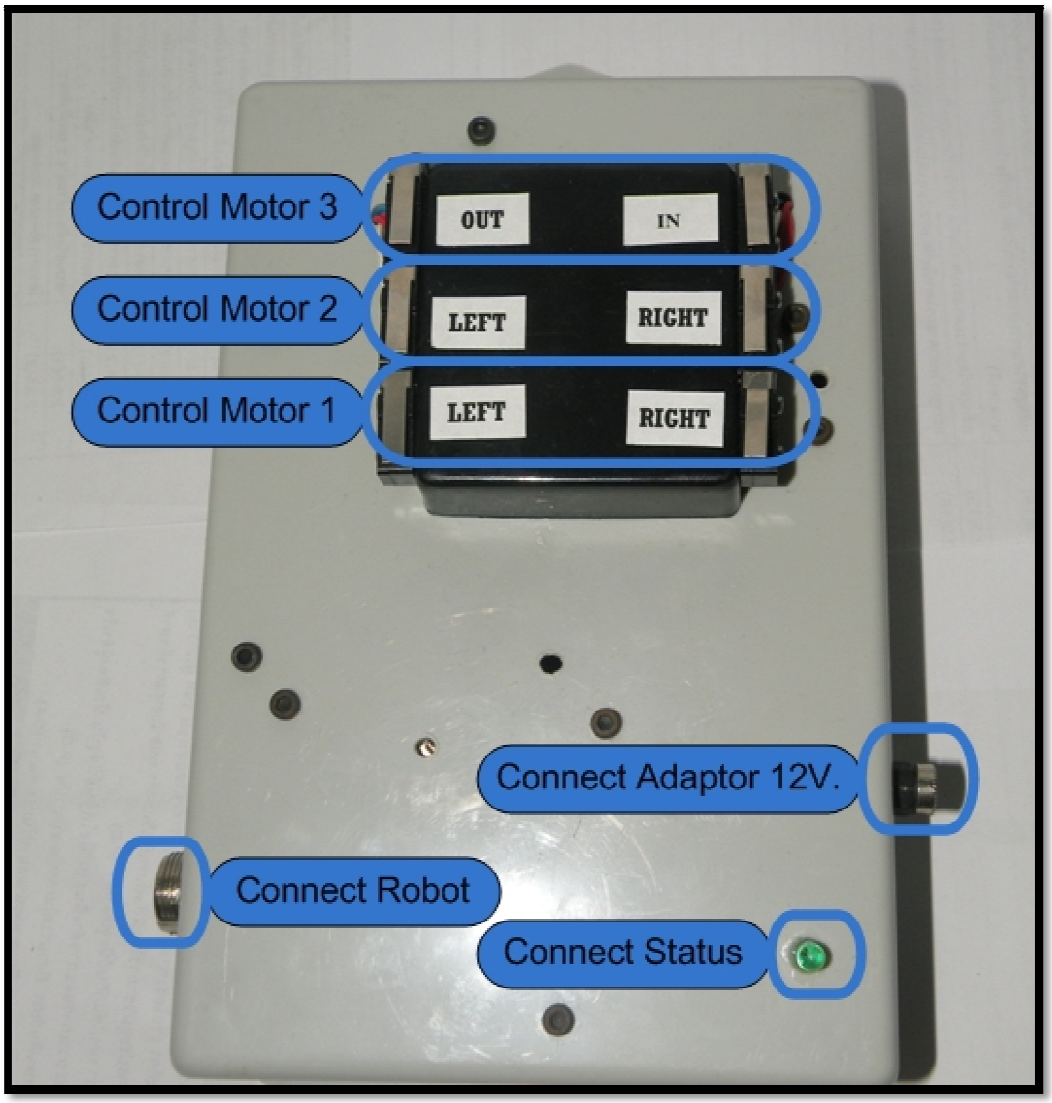

Figure 5.9 The control box of conceptual robot

5.3 ADAPTIVE MEAN-SHIFT KALMAN OBJECT TRACKING FOR THE NEW MIRS SYSTEM

From the object tracking system for the new MIRS system, we have proposed the adaptive mean-shift kalman algorithm to locate the target object which is the laparoscopic instrument. This algorithm combines the advantages of two algorithms consisting of the Mean-Shift algorithm and the Kalman filter. The overall procedure of this algorithm is shown in **Error! Reference source not found.**. To illustrate the performance of the proposed adaptive mean-shift kalman algorithm, we tested on the many situations which consist of simulated videos, real laparoscopic videos, and real time situations.

5.3.1 Simulated Video Situations

The testing situations were simulated to illustrate five scenarios. First scenario, we suddenly changed the background screen of the target object. In the second case, we changed the template of the target object. In the third case, we resized the target object by decreasing the size. In the fourth case, we combined two problem situations; resizing the target object and changing the template of target object. In the last scenario, we moved the target object behind the obstruction. In all experiments, we will compare the results between Template matching and adaptive mean-shift kalman algorithm. We initial target model as shown in Figure 5.10 was required in both algorithms. The red background in Figure 5.10 imitated the background in laparoscopic surgery, and the yellow ball represents the undesired background and the obstruction. In addition, the tip of laparoscopic instrument is represented object as the target model displayed in the white rectangle of the image.

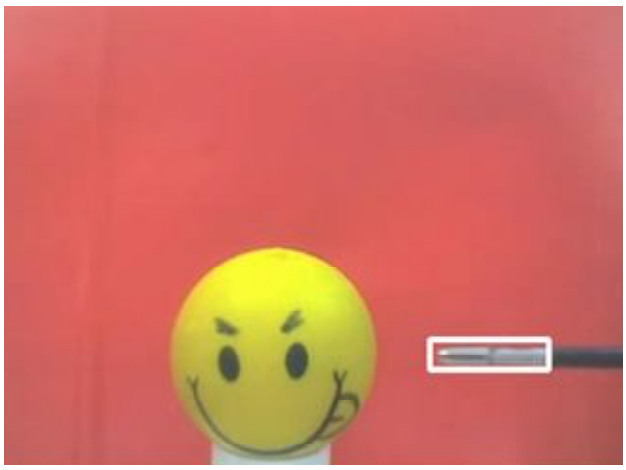

Figure 5.10 The initial target model

Case 1: changing the background screen

This case focuses on alteration of a background screen without changing the template of the target object. In this case, we compare two different algorithms: template matching (the blue rectangle in the image) and the adaptive mean-shift kalman algorithm (the green rectangle in the image). Figure 5.11 shows the overall results for six sample frames of the different times. Frame 1 is depicts the initial moving of the target object for both template matching and adaptive mean-shift kalman algorithms. Frame 7 is depicts the new location of target object which slowly moves forward the yellow ball. Then, half of target object was changed to a new background at frame 16. Both algorithms can still locate the target object. However, at frame 30, all the parts of target object fully move to the new background. Here only, the adaptive mean-shift kalman algorithm can locate the tip of the laparoscopic instrument, the template matching is not able to locate the target object. At frame 63, when half of the target object is moving back to the original background, the proposed algorithm can locate the target object better than the template matching algorithm. The last frame 101 is under the original background merely, the result of the proposed algorithm is more accurate than the result of template matching. The first scenario illustrates that the adaptive mean-shift kalman algorithm is more accurate than the template matching algorithm because the proposed algorithm can successfully locate the target object when changing background.

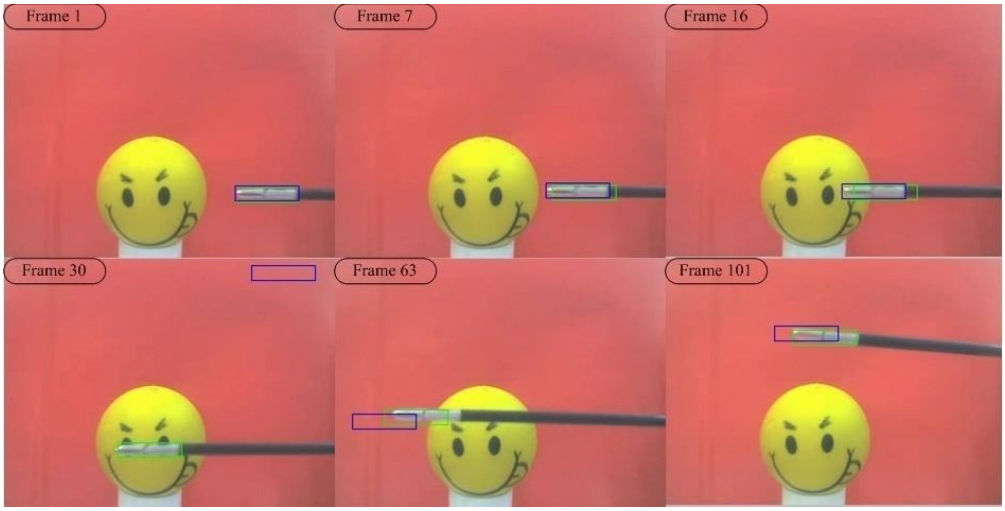

Figure 5.11 The overall results of Case 1

Case 2: changing the template of the target object

This case focuses on a non-rigid object, which is the change of the target template; i.e., the shape of the laparoscopic instrument in the image. This case compares two different algorithms: template matching (the blue rectangle in the image) and the adaptive mean-shift kalman algorithm (the green rectangle in the image) as shown in Figure 5.12. Frame 1 is depicts the initial deformation of the target object; i.e., the tip of the laparoscopic instrument like pliers is open up. At the point, both algorithms can still locate the target object but the proposed algorithm provides a more accurate location than the template matching. At frame 14, when the object is full open; i.e., its shape is totally changed. The tracking result of the proposed algorithm is more accurate than the template matching as well. Frame 59 is depicts the full deformation of the target object which slowly move. The template matching cannot locate the target object; however, the adaptive mean-shift kalman algorithm can locate the accurate target object. Frame 59 is depictes the full deformation of the target object which move near the obstruction. The only result of adaptive mean-shift kalman algorithm can locate the laparoscopic instrument. Frame 120 is depicts the full deformation of the target object which move pass the obstruction. The template matching locates the wrong location of the target object; however, the proposed algorithm can locate the correct location of laparoscopic instrument. Frame 169 shows the image when the tip of the laparoscopic instrument is

back to a normal shape. The results in this scenario show that the adaptive mean-shift kalman algorithm can correctly locate the target object when the template of the target object is changed.

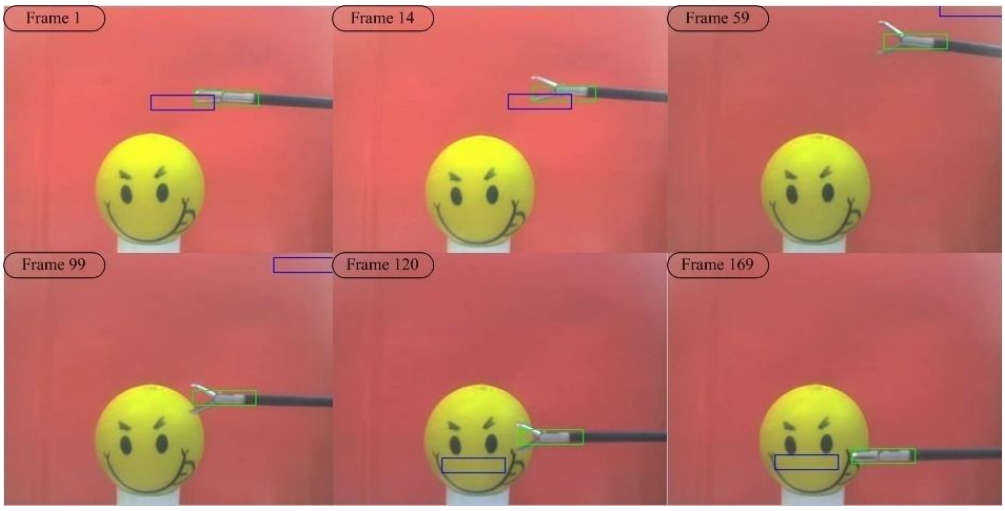

Figure 5.12 The overall results of Case 2

Case 3: resizing the target object

In this case, we resize the rigid object by zooming the target in and out. This case compares two different algorithms: template matching (the blue rectangle in the image) and the adaptive mean-shift kalman algorithm (the green rectangle in the image). The overall results are shown in Figure 5.13. This figure is depicted the two result which represent a blue rectangle and a green rectangle in the same image. This picture represents the three frames which have the different time. Frame 1 is depicts the target object which does not change the size. Frame 21 is depicts the target object changes the quarter size. The adaptive mean-shift kalman algorithm can locate the correct target and the template matching locates the wrong object. In addition, the target object changes the half size as shown in frame 90. The only proposed algorithm can locate the target object. The experiment results in this case can conclude the adaptive Mean-Shift algorithm is more accurate than the template matching. Therefore, the proposed algorithm can locate the target object which changes the size of object.

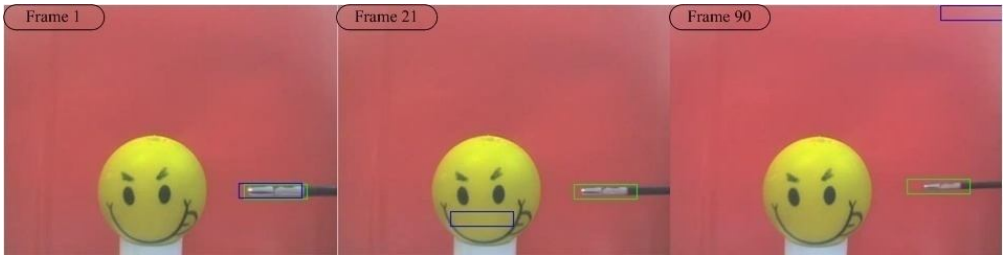

Figure 5.13 The overall results of Case 3

Case 4: resizing the target object and changing the template of target object

In this case, we change the size and the shape of the target object. This case compares two different algorithms: template matching (the blue rectangle in the image) and the adaptive mean-shift kalman algorithm (the green rectangle in the image). The overall results of this case will show in Figure 5.14. Frame 1 is depicts the initial target object which changes the half size. Frame 17, 61, and 94 are depict the target object which changes the half size and deform the template. Frame 154 and 188 are depict the target object which changes the half size but it deform backward to the initial form. The only adaptive mean-shift kalman algorithm can locate the correct target object which represents all experimental results in this case. Therefore, the adaptive mean-shift kalman algorithm can locate the target object which changes the size and deform the template object.

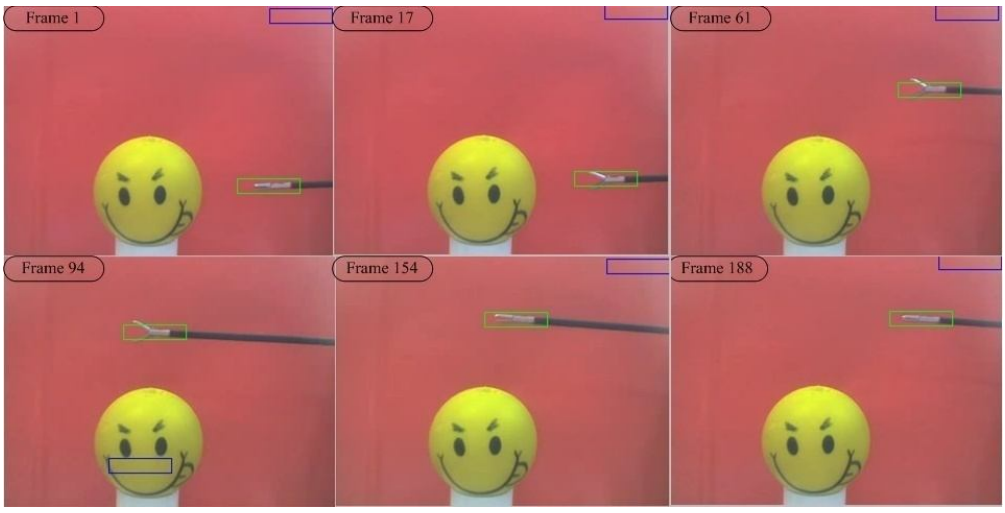

Figure 5.14 The overall results of Case 4

Case 5: the target object move behind the obstruction

In this case, we will propose the object tracking system which changes the size of target object. In addition, this case increases a difficult situation which moves the target object behind the obstruction. The first experimental result will show in Figure 5.15. This figure will show the two results: the mean-shift algorithm (the green rectangle in the image) and template matching algorithm (the blue rectangle in the image). This figure represents the six frames which have the different time. In this experiment, the template matching can't locate the all target object in sequential frame. Therefore, we will explain the only result of mean-shift algorithm. Frame 1 and 14 are depict the target object which changes the half size. These experimental results can locate the correct target object. In addition, the half target object hides behind the obstruction as shown in frame 22. This algorithm can locate the target object. However, this algorithm can't locate the target object in the next time. Because the full target object hides behind the obstruction and then the target object move across the obstruction. Therefore, the original mean-shift algorithm can't solve this problem thus we will adapt this algorithm by using the kalman filter.

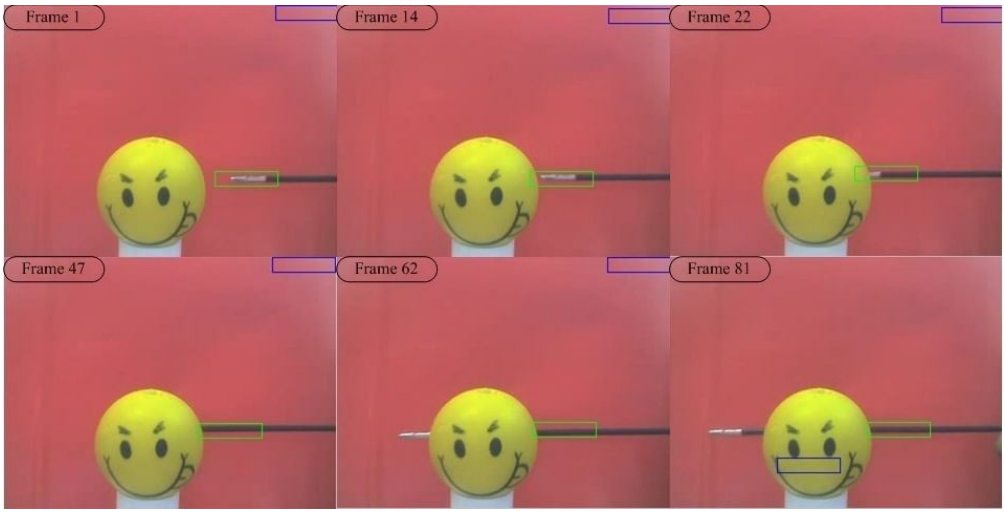

Figure 5.15 The overall results in Case 5 between mean-shift algorithm and template matching

The adaptive mean-shift kalman algorithm will show the experimental result as shown in Figure 5.16. This figure will show the three results: the mean-shift

kalman algorithm (the green rectangle in the image) and template matching algorithm (the blue rectangle in the image). The third result, the kalman filter represents the orange rectangle in the image. At frame 1, 14, and 22, the mean-shift algorithm and kalman filter can locate the correct target object. Frame 47 is depicts the full target object which hides behind the obstruction. The mean-shift algorithm locates the wrong object tracking; however the kalman filter tries to estimate the location of target object which move behind the obstruction. Frame 62 is depicts the half target object which appears behind the obstruction. The advantage of this algorithm can locate the correct target object in the image; because the result of kalman filter adapts the result of mean-shift algorithm to locate the target object. This procedure called adaptive mean-shift kalman algorithm. Frame 81 is depicts the full target object after across the obstruction. The adaptive mean-shift kalman algorithm can locate the correct target object. The adaptive mean-shift kalman algorithm will estimate the location of target object when it hides behind the obstruction. Therefore, the adaptive mean-shift kalman algorithm can locate the target object which hides behind the obstruction.

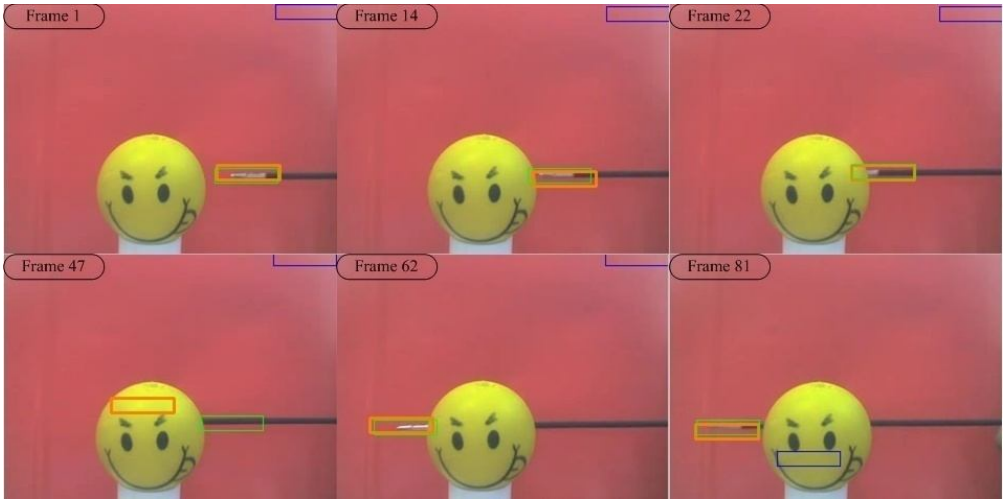

Figure 5.16 The overall results in Case 5 between adaptive mean-shift kalman algorithm and Template matching

5.3.2 Real Video Situations

The real situation videos are derived from the real laparoscopic surgery in the operating room [37]. Real laparoscopic surgery is more complicated than the

previous simulated situations, because it combines different situations at the same time.

Real Laparoscopic Surgery Case1

This experiment compares the results between template matching and adaptive mean-shift kalman algorithms in the real video of laparoscopic surgery. This video represents a sub-process of appendectomy [37] to cut a cord by serrated scissors. In the first frame, we initial the target model for two algorithms, as shown in Figure 5.17. The tip of laparoscopic instrument represents the target model which is shown in the blue rectangle in this image.

Figure 5.17 Initial target model in real situation case 1

True object tracking algorithms are compared in this experiment: the template matching algorithm (the blue rectangle in the image) and the adaptive mean-shift kalman algorithm (the orange rectangle in the image). The overall results are show in Figure 5.18 and Figure 5.19. This picture represents the nine sample frames at the different times. At frame 35, the two algorithms can correctly locate the target object. However, the target object changes the quarter size and change the object template as shown in frame 65-72. The adaptive mean-shift kalman algorithm can locate the correct target and the template matching locates the wrong object. Frame 86-90 represent the changing view of background which happens by moving of the laparoscope. The two algorithms can locate the target object. Frame 105-112

represent the tip of laparoscopic instrument which is the target object to hide behind another laparoscopic instrument. This problem is the difficult situation to locate the target object. However, the only adaptive mean-shift kalman algorithm can locate the correctly target object. Frame 122-126 represent the target object which is increase size and change the template. The only adaptive mean-shift kalman algorithm can locate the correctly target object which is in this situation. The experiment results in this case can conclude the adaptive Mean-Shift algorithm is more accurate than the template matching. Therefore, the proposed algorithm can locate the tip of laparoscopic instrument which is in real laparoscopic surgery.

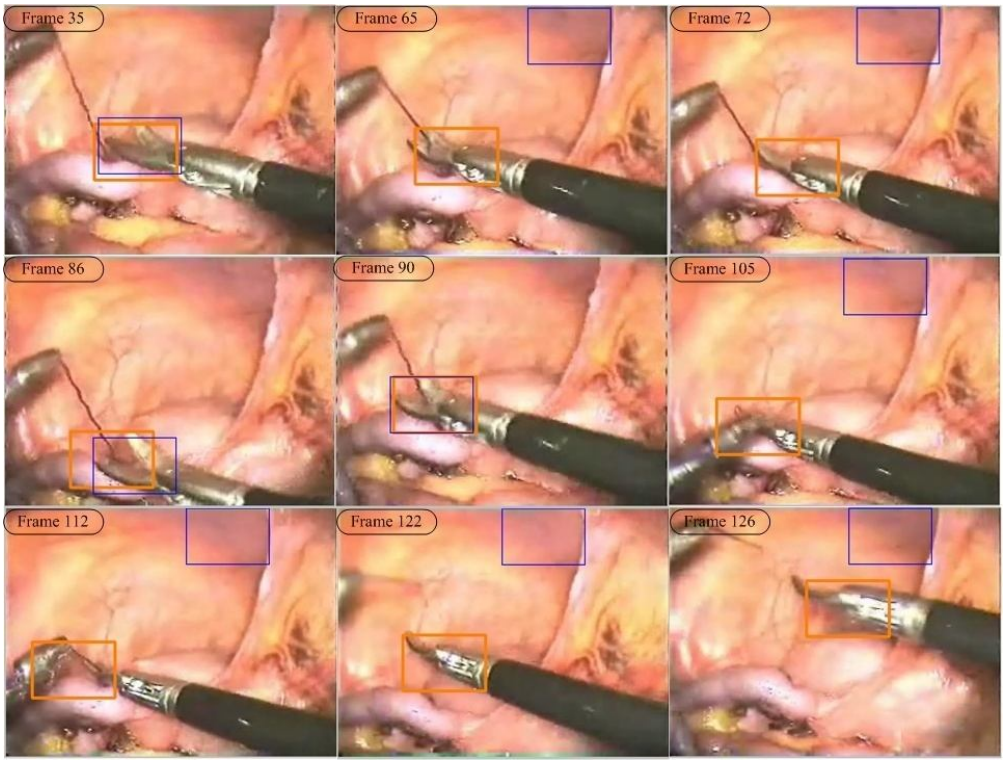

Figure 5.18 The sample results in the real situation case 1 between adaptive Mean-Shift algorithm and template matching algorithm

Figure 5.19 The overall results in real situation case 1

Real Laparoscopic Surgery Case 2

In this experiment, we used the real video that coagulates a tissue by electrode instrument [37]. At the first frame, we initialized the target model for two algorithms, as shown in Figure 5.20.

Figure 5.20 Initial target model in real situation case 2

The results of this case will show in Figure 5.21 and Figure 5.22. This figure is depicted the two result which represent a blue rectangle and a green rectangle in the same image. This picture represents the six frames which have the different time. At frame 32, the two algorithms can correctly locate the target object. At frame 35, the changed background has occurred from the moving of laparoscope. The result of two algorithms can correctly locate the target object. At frame 59, the initial smoke has occurred from the electrode instrument. The adaptive mean-shift kalman algorithm can locate the correct target and the template matching locates the wrong object. At frame 77, the little smoke has covered an image. The result of two algorithms can nearly locate the target object. At frame 79, the many smoke has covered an image. The adaptive mean-shift kalman algorithm can locate the correct target and the template matching locates the wrong object. At frame 91, the many smoke has covered an image and hide the target object. The only adaptive mean-shift kalman algorithm can locate the correctly target object which is in this situation. The experiment results in this case can conclude the adaptive Mean-Shift algorithm is more accurate than the template matching. Therefore, the proposed algorithm can locate the tip of laparoscopic instrument which is in this situation.

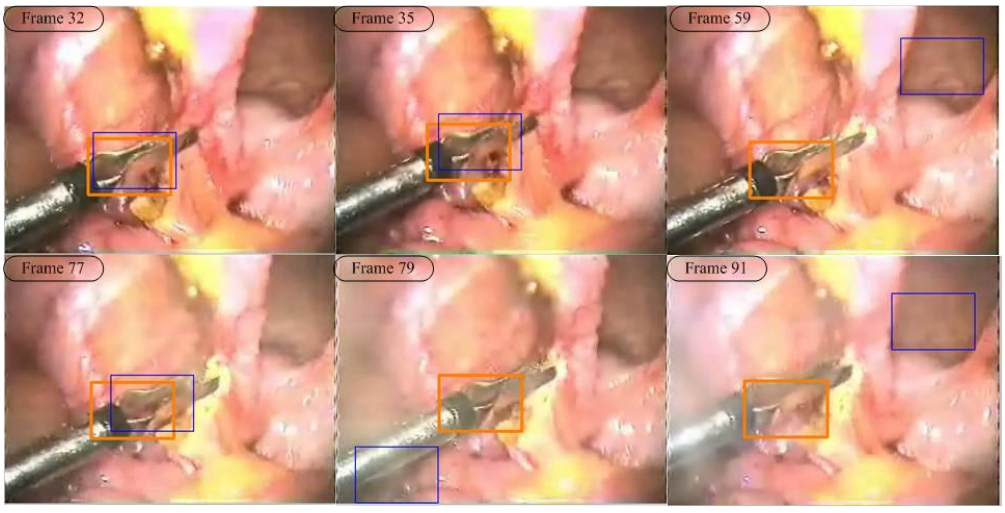

Figure 5.21 The sample results in the real situation case 2 between adaptive Mean-Shift algorithm and template matching algorithm

Figure 5.22 The overall results in real situation case 2

5.4 PERFORMANCE OF THE NEW MIRS SYSTEM

In this research, we make a phantom box which simulates the working area inside abdomen to test our proposed new MIRS system, as shown in Figure 5.23. Inside the box, the red color background mimics the same color inside abdomen. At the top of the box, it has three holes to simulate the ports for inserting the laparoscopic instruments and the laparoscope, as shown in Figure 5.24. The center hole is used for inserting the camera of the conceptual robot. The left and right holes are used for inserting the laparoscopic instruments. In addition, we simulate the light source in the working area which is opened by pressing the red switch at the top of the box.

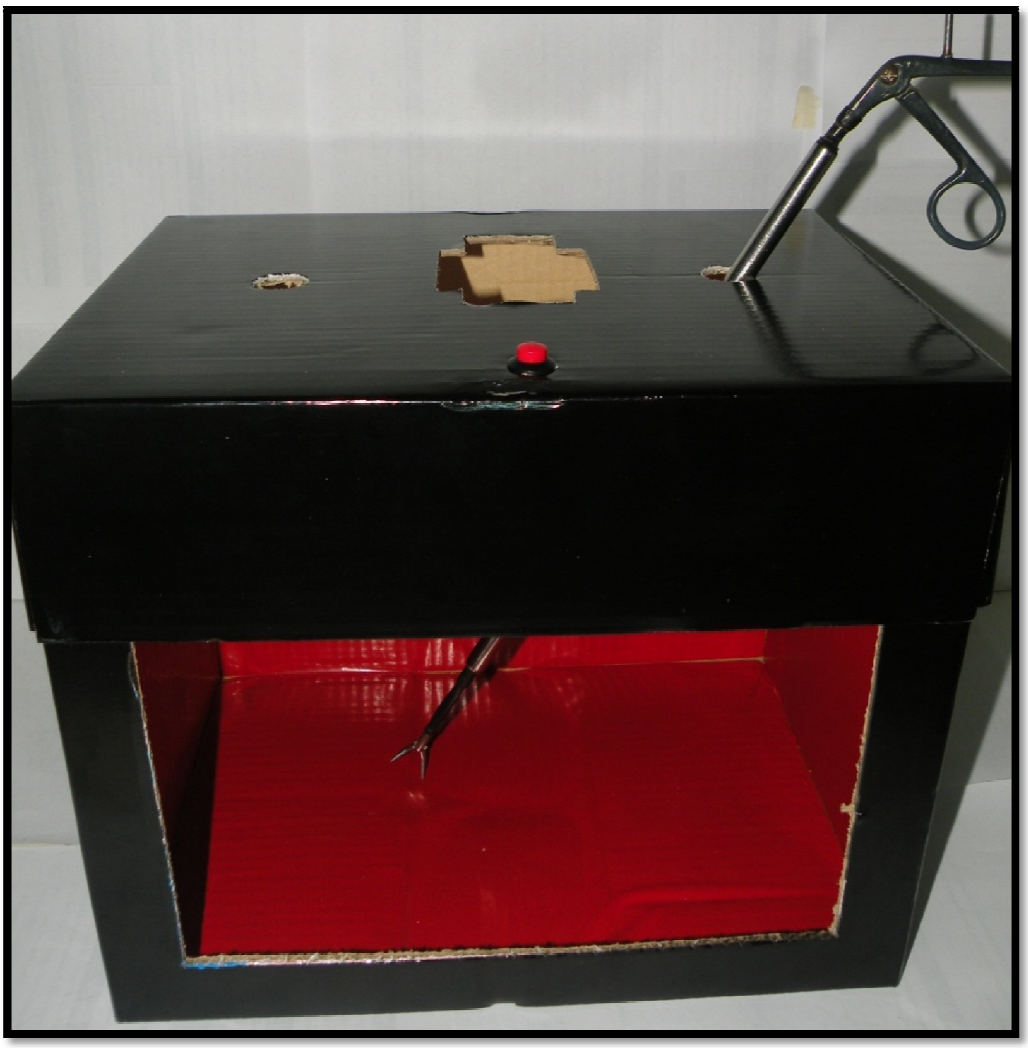

Figure 5.23 The overall phantom box

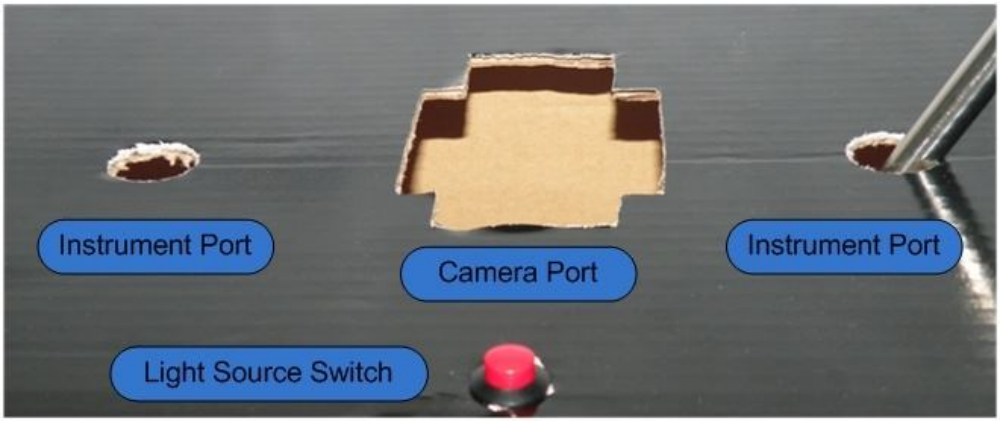

Figure 5.24 The top of the phantom box

The new MIRS system combines the conceptual robot with the proposed adaptive mean-shift kalman algorithm to track a laparoscopic instrument. The overall experiment setup is shown in Figure 5.25. This study is too demonstrate the performance of the new MIRS system in the real-time using the phantom box.

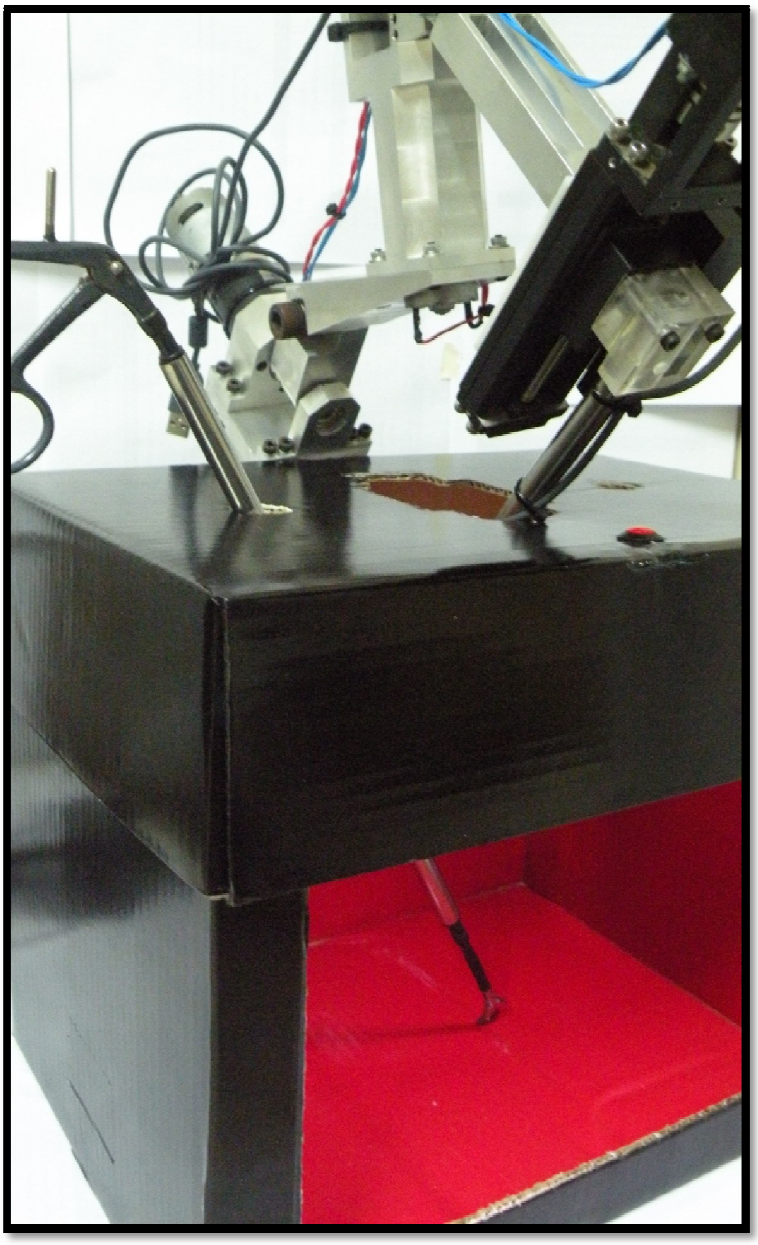

Figure 5.25 The overall experiment setup

5.4.1 Real Time Tracking with Manually Controlling the Robot

The process of tracking in software consists of five steps. First, we press the "connection" button for connecting the camera. Second, the software will show the real image from the camera on the screen of software. Third, we select the target object on the real image which in shown on the screen. The selected area of target object will be represented in the pink rectangle on the image. Fourth, the selected of the target object will be shown as a small image on the software. If one wants to change the target object, he can just press the "Delete Target" button and then select the new target object. Last, we press the "Real Time Tracking All" button on the program. This button is to start the tracking process which is the adaptive mean-shift kalman tracking algorithm. The result of the proposed algorithm represents by the orange rectangle on the real image. The overall process of tracking software is shown in Figure 5.26.

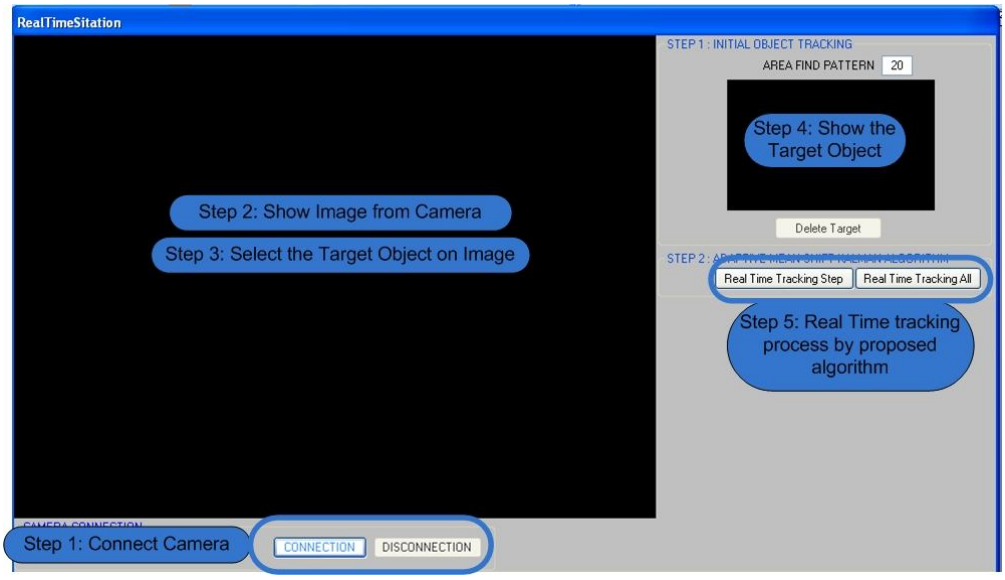

Figure 5.26 The overall process of tracking software to manually control the robot

The real time experiment will process in the real images which are received from the camera of the conceptual robot. This experiment demonstrates many situations, such as changing the target object template, and changing the size of target object. In addition, this experiment increase situations which are actions of the conceptual robot consist of move left, move right, camera zoom in, and camera zoom

out. The process of this experiment consists of 4 steps. The first step is to set up the work station of the real-time experiment as in Figure 5.25. The second step is to connect the camera with the real time tracking software, as shown in Figure 5.27 (a). The real time image from the camera will be shown on the screen of the software. The third step is to select the ROI of the target object which is the real image on the software, as shown in Figure 5.27 (b). The ROI is displayed in the white rectangle on the screen. Forth step is to select the "Real Time Tracking All" button on the software for tracking the target object, as shown in Figure 5.27 (c). The result of the tracking algorithm is displayed in the orange rectangle on the screen of software, as shown in Figure 5.27 (d). The overall result of real time experiment is shown in Figure 5.28. From the overall result, we can track the target object in the correct position. Since, this proposed algorithm can be performed in the real-time; the new MIRS System can be used in real surgery.

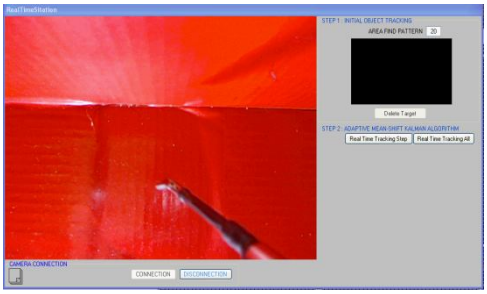

(a) Connect camera with software

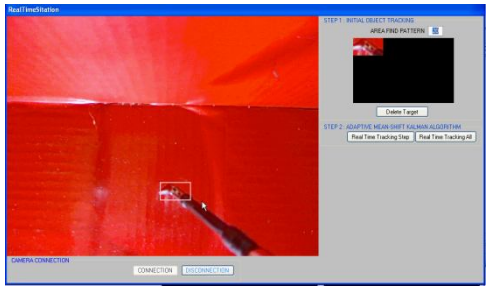

(b) Select the ROI of target object

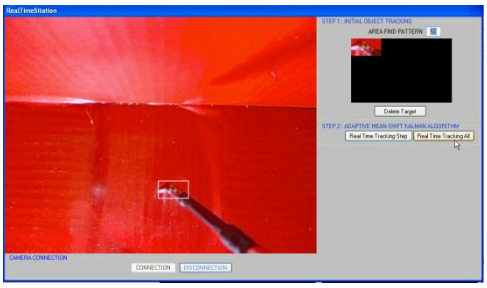

(c) Start the tracking process

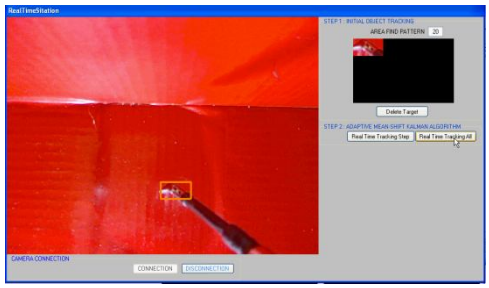

(d) Result of the proposed algorithm

Figure 5.27 Four steps for the real time tracking setup

Figure 5.28 The overall result in real time experiment

5.4.2 Real Time Tracking with Automatically Control the Robot

The process of the tracking software consists of seventh steps. The five steps have same the previous experiment, as describe in section 5.4.3. In this experiment, the program connects with the robot to automatically control the robot by using the proposed algorithm. The sixth step, we press the “automatic control” button for changing the control of robot to automatically control. The last step, we press the “Real Time Tracking All” button on the program. This button is the start of tracking process which is the adaptive mean-shift kalman tracking algorithm. The result of the proposed algorithm represents by the orange rectangle on the real image. The overall process of automatic tracking software shows in Figure 5.29.

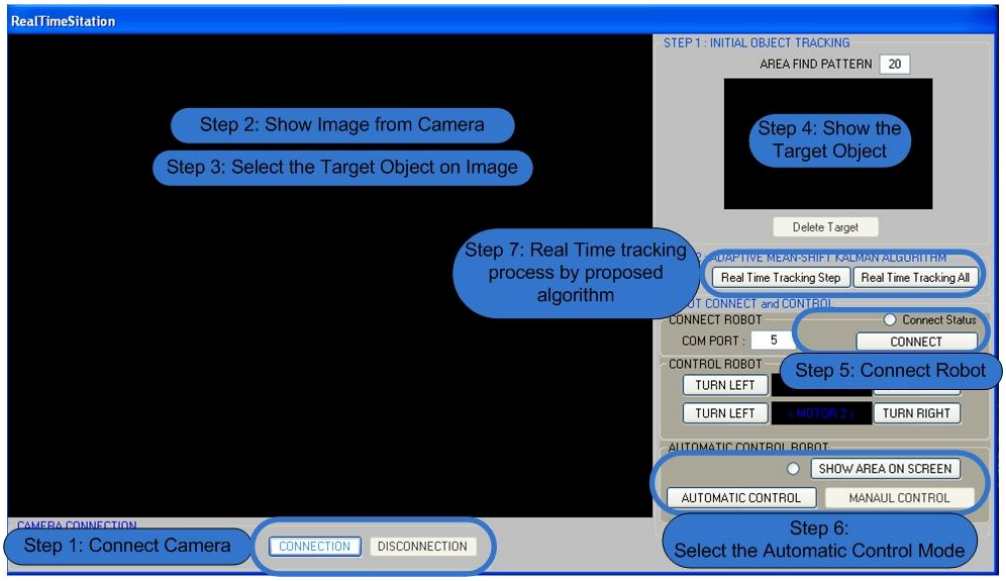

Figure 5.29 The tracking software for automatically controlling the robot

The area of interest is located at the center of the image which is about 3/5 of image size. There are four conditions to automatically control the conceptual robot. First, the robot moves to the left when the position of the target object in the x-axis is smaller than the initial position in the x-axis of the area of interest. Then, the program instructs the conceptual robot to moves the motor 1 to rotate counterclockwise. Second, the robot moves to the right when the position of the target object is greater than the maximum position in the x-axis of the interesting area. Then, the program instructs the conceptual robot to moves the motor 1 to rotate clockwise. Third, the robot moves up ward when the position of the target object in the y-axis is less than the minimum position in the y-axis of the area of interest and more than half of the position in the x-axis. The position of the target object is more than the maximum position in y-axis of the interesting area and is less than the half position in x-axis of the interesting area. Then, the program instructs the conceptual robot to moves motor 2 to counterclockwise. In the last condition, the robot will move down when the position of the target object in the y-axis is less than the minimum position in the y-axis of the interesting area and is less than the half position in the x-axis of the interesting area, or the position of the target object is more than the maximum position in the y-axis of the interesting area and is more than the half position in the x-axis of the interesting area. Then, the program instructs the conceptual robot will

move motor 2 to clockwise. The overall conditions use to automatically control the robot, as shown in Figure 5.30.

Figure 5.30 The overall functions of automatic controlling

The aim of the real-time experiment is to track the tip of the laparoscopic instrument in the real image. In addition, the result of the proposed algorithm is used for automatically controlling the conceptual robot. The initial setup of the system is shown in Figure 5.31. From the experiment result, the target object move to left which more than the focusing area. The conceptual robot will move to left for tracking the target object, as shown in Figure 5.32. In other case, the target object move to right which more than the focusing area. The conceptual robot moves to right for tracking the target object, as shown in Figure 5.33. The overall experiment results are the automatically control of conceptual robot which control by the proposed algorithm, as shown in Figure 5.34.

Figure 5.31 The initial to automatic controlling system

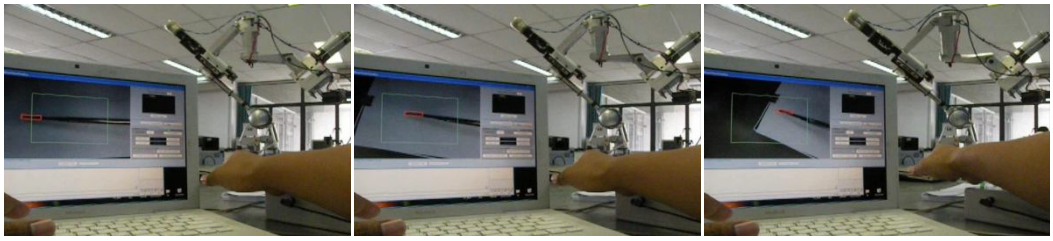

Figure 5.32 The actions of the conceptual robot move in the left

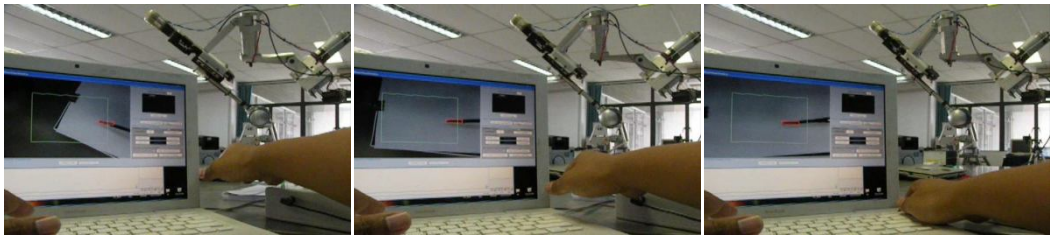

Figure 5.33 The actions of the conceptual robot move in the right

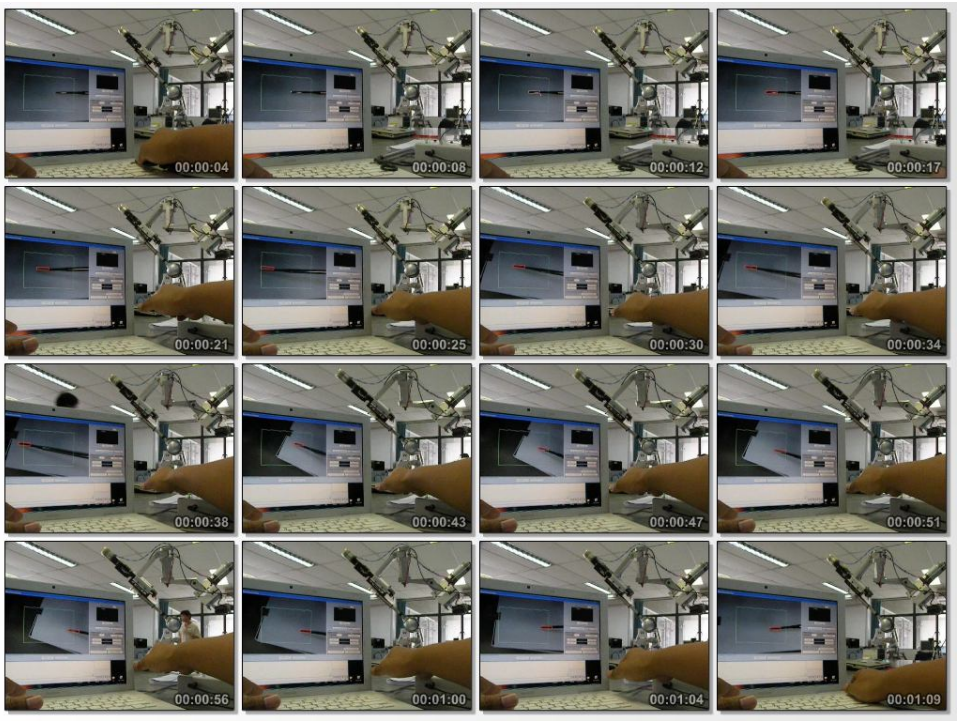

Figure 5.34 The overall result for automatic controlling of the MIRS system

CHAPTER VI
CONCLUSION AND FUTURE WORK

In this thesis, we proposed both hardware design and software tracking algorithm of the new MIRS system. In the first part, we proposed the design and analysis of the conceptual robot to hold the endoscope in the laparoscopic surgery. The conceptual robot has 5-DOFs of motion consisting of 2-DOFs to control the center of the fulcrum point and 3-DOFs to control the motion of the laparoscope. This robot has many advantages. First, it can easily be developed because it uses only three motors and simple linkages. Second, this robot can easily calculate the tip of the laparoscope. Third, we can easily control the laparoscope motion. Fourth, the proposed robot can easily be set up in a small workspace in a surgery room without interfering the workspace of the primary surgeon due to a small robot. The primary surgeon can control the new robot by the surgeon's instruction. Finally, it will reduce the human errors and the operation time in the surgery. In this study, we also computed the overall working area of the conceptual robot by calculating the forward kinematics of the main motion. The overall working area of the conceptual robot has the cone shape with the height of 103.6 mm and the apex angle of 82.4 degrees which is wisher than the required apex angle. Therefore, this conceptual robot can cover the overall workspace inside the patient's abdomen. In the second part, we proposed the new object tracking algorithm naming is the adaptive mean-shift kalman algorithm. This algorithm combined two algorithms consisting of mean-shift algorithm and kalman filter. From the experimental results, the proposed algorithm can locate the target object correctly when changing the background, template of object, and the size of object. Moreover, the algorithm can locate the target object even when it is hidden behind the obstruction and real-time tracking is also possible. Therefore, this algorithm is suitable for tracking a tip of the laparoscopic instrument inside the patient's abdomen in the real surgery.

For future work, the camera of the conceptual robot should be changed to the real laparoscope in laparoscopic surgery. The electric circuit for controlling the

conceptual robot should be changed to the commercial circuit to yield high precision. In addition, the motors of the prototype robot should be changed to reduce the back lash of the robot. The proposed algorithm should be increase the times to track the tip of laparoscopic instrument in the real time.

REFERENCES

1. *The Laparoscopic Gallbladder Surgery Procedure*, in *Available at (http://www.laparoscopicsurgeryinfo.com/procedure.html)*.
2. *Surgical Update Creating Pneumoperitoneum Safely in Patients with Previous Surgical Scars*, in *Available at (http://www.indmedica.com/journals.php?journalid=&issueid=125&articleid=1669&action=article)*.
3. Taylor, R.H., et al., *An overview of computer-integrated surgery at the IBM Thomas J. Watson Research Center.* IBM Journal of Research and Development, 1996. Volume 40 (Issue 2): p. 163 - 183
4. Way, L.W., S. Bhoyrul, and T. Mori, *Learning laparoscopic surgery*, in *Fundamentals of laparoscopic surgery*, L.W. Way, Editor. 1995, Churchill-Livingstone: London, UK.
5. aka, F.P., *An Introduction To Digital Image Processing* 2003: France.
6. Gonzalez, R.C., *Digital Image Processing*. second ed. 2002: Prentice Hall.
7. Omote, K., Feussner, H., Ungeheuer, A., Arbter, K., Guo-Qing Wei, *Self-guided robotic camera control for laparoscopic surgery compared with human camera control.* The American journal of surgery, 1999. Volume 177: p. 21-24.
8. Casals, A., Amat, J., Laporte, E., *Automatic guidance of an assistant robot in laparoscopic surgery.* International Conf. on Robotics and Automation, 1996. Vol. 1: p. 895-900.
9. Cheolwhan Lee, Y.-F.W., Uecker, D.R., Yulun Wang, *Image analysis for automated tracking in robot-assisted endoscopic surgery.* Proceedings of the 12th IAPR International Conference, 1994. Vol. 1: p. 88-92.
10. Guo-Qing Wei, A., K., Hirzinger, G., *Real-time visual servoing for laparoscopic surgery, "Controlling robot motion with color image segmentation".* IEEE Engineering in Medicine and Biology, 1997. Vol. 16(Issue 1): p. 40-45.

11. Kim, M.-S., J.-S. Heo, and J.-J. Lee, *Real-time Visual Tracking for Laparoscopic Surgery*. Fuzzy Systems and Knowledge Discovery, 2005: p. 44-51.
12. Tsung-Kang Chiang, J.-J.L., and Cheng-Shian Lin. *An Improved Mean Shift Algorithm Based Tracking System for Soccer Game Analysis*. in *An Improved Mean Shift Algorithm Based Tracking System for Soccer Game Analysis*. October 4-7, 2009. Sapporo, Japan.
13. Bodnera, J., et al., *The da Vinci robotic system for general surgical applications: a critical interim appraisal*. Swiss Medical Weekly, 2005.
14. Hollands, C.M. and L.N. Dixey, *Robotic-Assisted Esophagoesophagostomy*. Journal of Pediatric Surgery, 2002. 7: p. 983-985.
15. *Robotic Surgery: The Future Is Now, Business Strategies Medical Technology Executives (MX)*. [cited; Available from: http://en.wikipedia.org/wiki/Robotic_Surgery.
16. Ashok, K.H. and K. Rajeev, *Laparoscopy in Urology*. Journal of Minimal Access Surgery, 2005.
17. Chatzilias, P., et al., *Robotic control in hand-assisted laparoscopic nephrectomy in humans - a pilot study.*, in *IEEE Eng Med Biol Soc*. 2004.
18. Bentas, W., et al., *Da Vinci robot assisted Anderson-Hynes dismembered pyeloplasty*. Springer-Verlag, 2003.
19. *Intuitive Surgical, Product Image Library*.[cited; Available from: http://www.intuitivesurgical.com/corporate/newsroom/mediakit/product_images.aspx.
20. Jean-Alexandre, L., et al., *Development of the Miniaturised Endoscope Holder LER (Light Endoscope Robot) for Laparoscopic Surgery*. Journal of Endourology, 2006(August 2007, 21): p. 911-914.
21. Lee, Y.-J., et al., *Design of a Compact Laparoscopic Assistant Robot : KaLAR*. Proc. of the International Conference on Control, Automation and Systems, 2003: p. 2648-2653.
22. Zemiti, N., et al., *Mechatronic Design of a New Robot for Force Control in Minimally Invasive Surgery*. IEEE/ASME TRANSACTIONS ON MECHATRONICS, APRIL 2007: p. 143-153.

23. Alper Yilmaz, O.J., and Mubarak Shah, *Object Tracking: A Survey*. ACM Computing Surveys, 2006. 38(4): p. 1 - 45.

24. P. Gabriel, J.-B.H., J. Piater, and J. Verly. *Object Tracking using Color Interest Points*. in *Advanced Video and Signal Based Surveillance, 2005. AVSS 2005. IEEE Conference on* 2005.

25. Veenman, C.J.R., M.J.T.; Backer, E., *Resolving motion correspondence for densely moving points.* Pattern Analysis and Machine Intelligence, IEEE Transactions on 2001. 23(1): p. 54 - 72

26. Wei He ; Yamashita, T.H.L.S.L. *SURF Tracking*. in *Computer Vision, 2009 IEEE 12th International Conference on* 2009.

27. Lowe, D.G., *Distinctive Image Features from Scale-Invariant Keypoints.* International Journal of Computer Vision, 2004. 60(2).

28. Peihua Li, T.Z., and E.C. Pece, *Visual contour tracking based on particle filters* Image and Vision Computing, 2003. 21(1): p. 111-123

29. Sa-Ing, V., et al. *Design of A New Laparoscopic-Holder Assistant Robot*. in *The 3rd International Symposium on Biomedical Engineering (ISBME 2008)*. 2008. Bangkok, Thailand.

30. Rosen, J., et al. *The BlueDRAGON - A System for Measuring the Kinematics and the Dynamics of Minimally Invasive Surgical Tools In-Vivo*. in *lntemational Conference on Robotics 8 Automation*. 2002. Washington, DC.

31. Dorin Comaniciu , P.M., Senior Member *Mean shift: A robust approach toward feature space analysis.* IEEE Transactions on Pattern Analysis and Machine Intelligence 2002. 25(5): p. 603 - 619

32. Dong Xu , Y.W., Jinwen An *Applying a New Spatial Color Histogram in Mean-Shift Based Tracking Algorithm*, in *image & vision computing*. 2005.

33. Comaniciu, D.R., V.; Meer, P., *Real-time tracking of non-rigid objects using mean shift*, in *Computer Vision and Pattern Recognition, 2000. Proceedings. IEEE Conference on* 2000: Hilton Head Island, SC , USA p. 142 - 149.

34. Bishop, G.W.a.G., *An Introduction to the Kalman Filter*. 2001, University of North Carolina at Chapel Hill Chapel Hill, NC, USA.

35. Masreliez, C. and R. Martin, *Robust bayesian estimation for the linear model and robustifying the Kalman filter*. Automatic Control, IEEE Transactions on 2003. 22(3): p. 361 - 371

36. Yan Wang, T.L., Ming Li. *Object Tracking with Appearance-based Kalman Particle Filter in Presence of Occlusions*. in *Global Congress on Intelligent Systems*. 2009.

37. Mishra, R.K., *Free Surgical Laparoscopic Videos*, in *http://www.laparoscopyhospital.com/DOWNLOADS.HTM*, lap_appendectomy.wmv, Editor. 2008.

APPENDIX

COMPUTER AIDED DESIGN (CAD) OF THE CONCEPTUAL ROBOT

The overall parts of conceptual robot

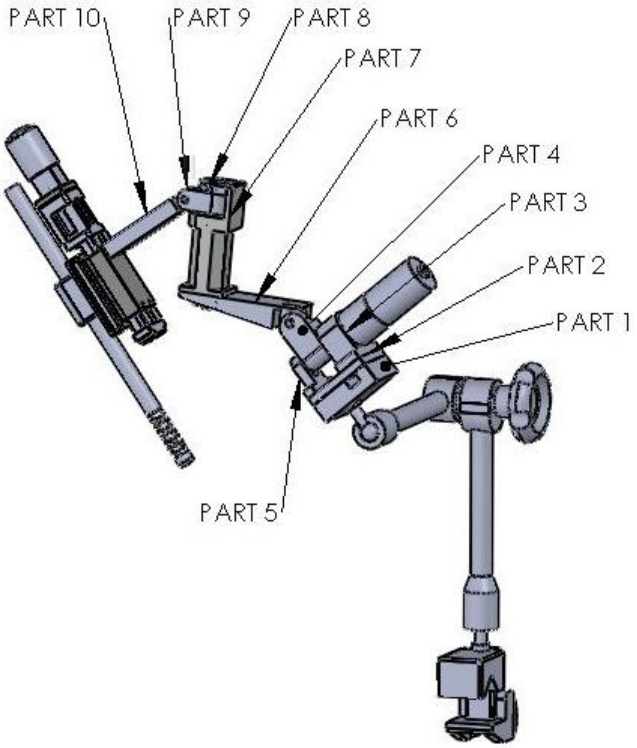

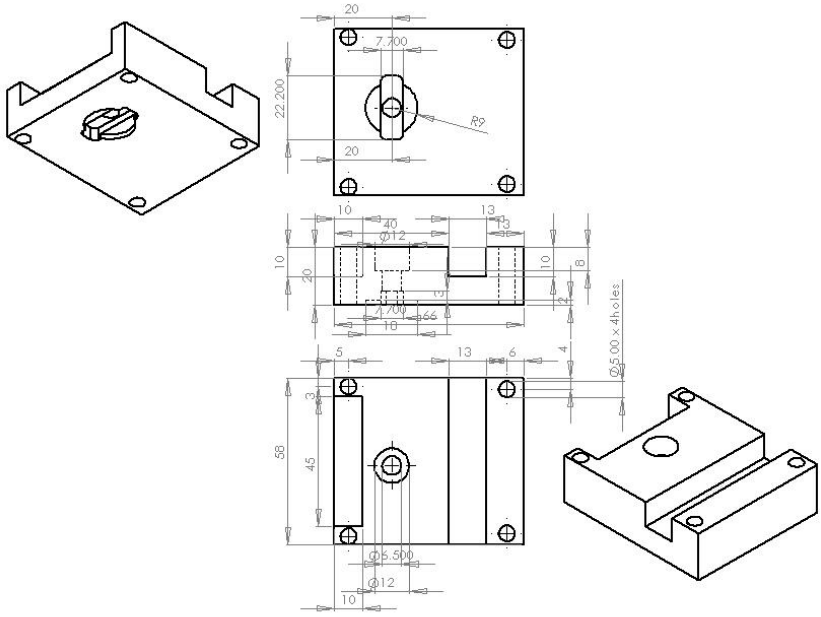

Part 1 The connection between the passive base part and the manipulator part

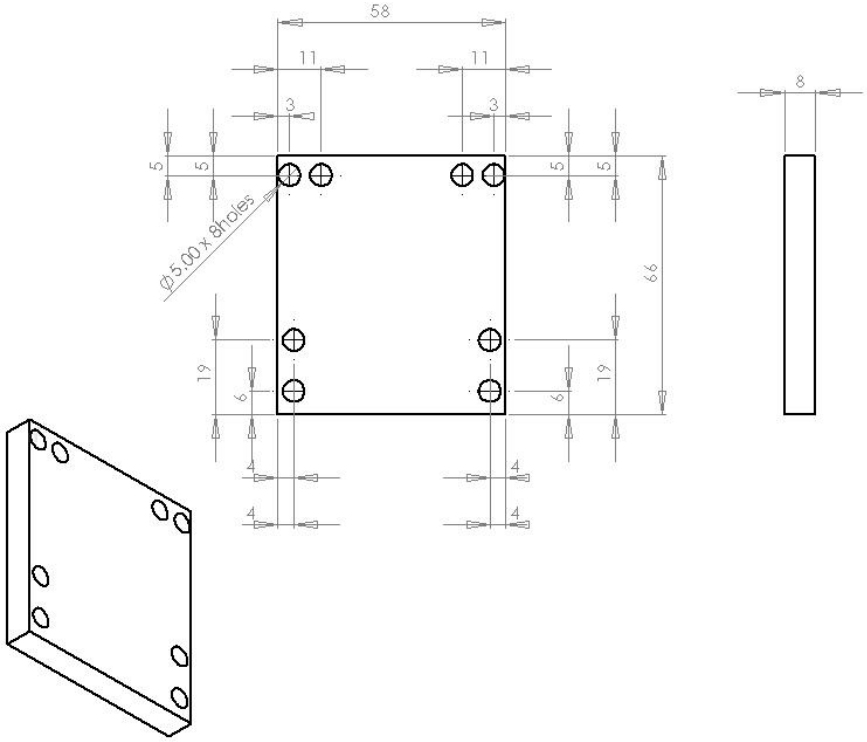

Part 2 The base of Joint 1

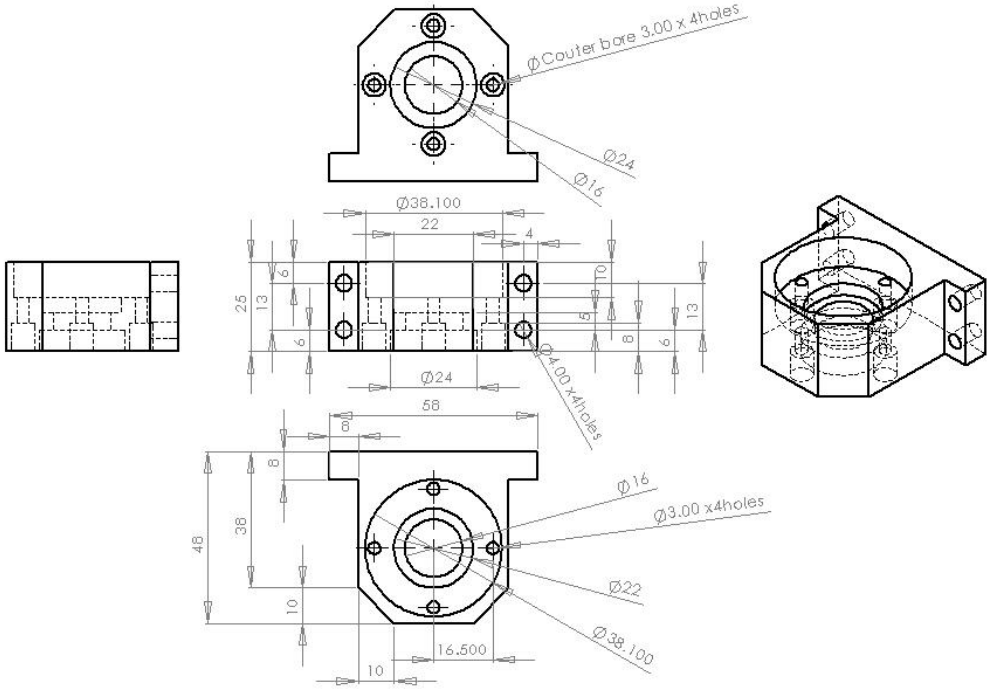

Part 3 The connector of motor 1

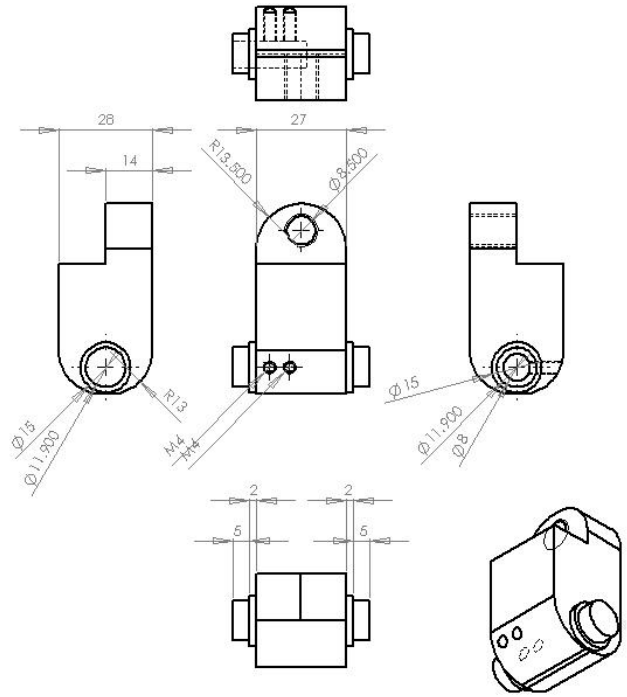

Part 4 The motion Joint 1

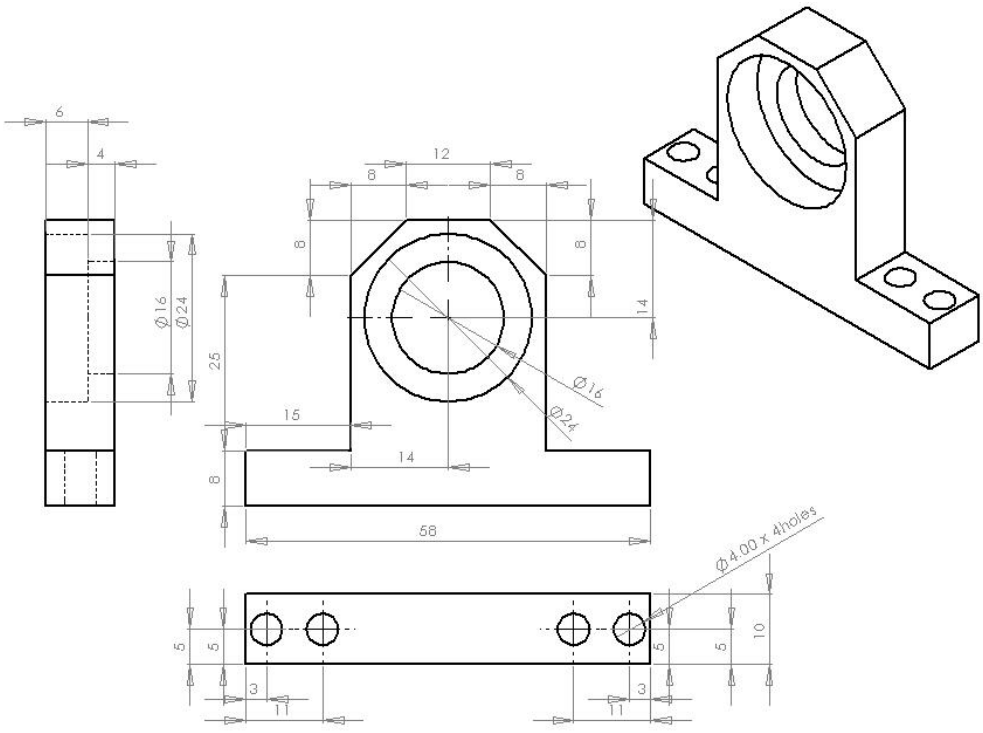

Part 5 The lock of motion Joint 1

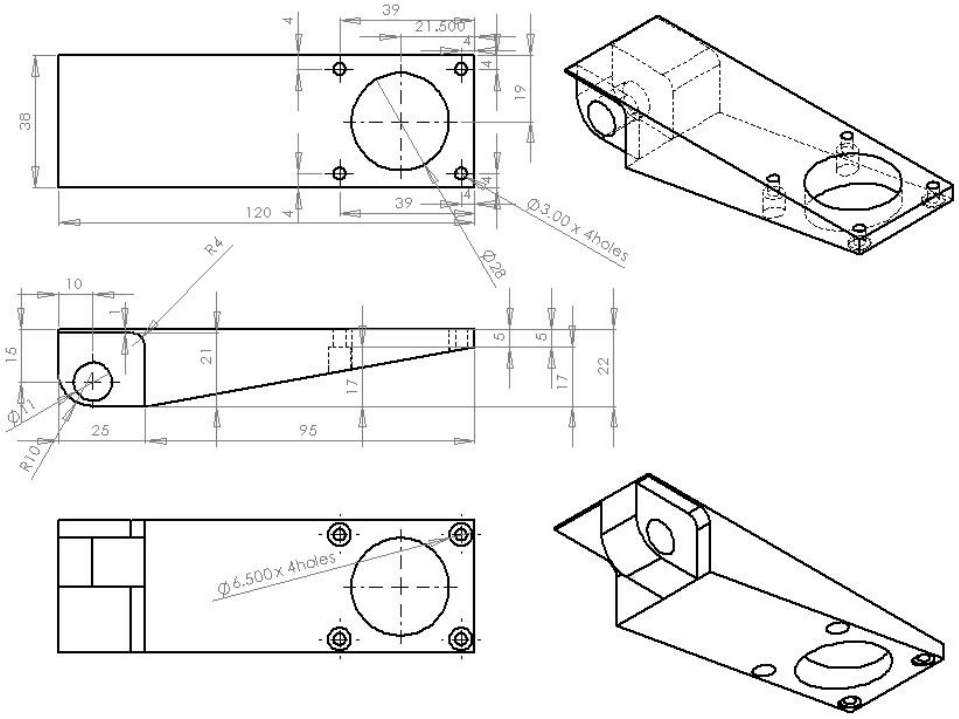

Part 6 The base of Joint 2

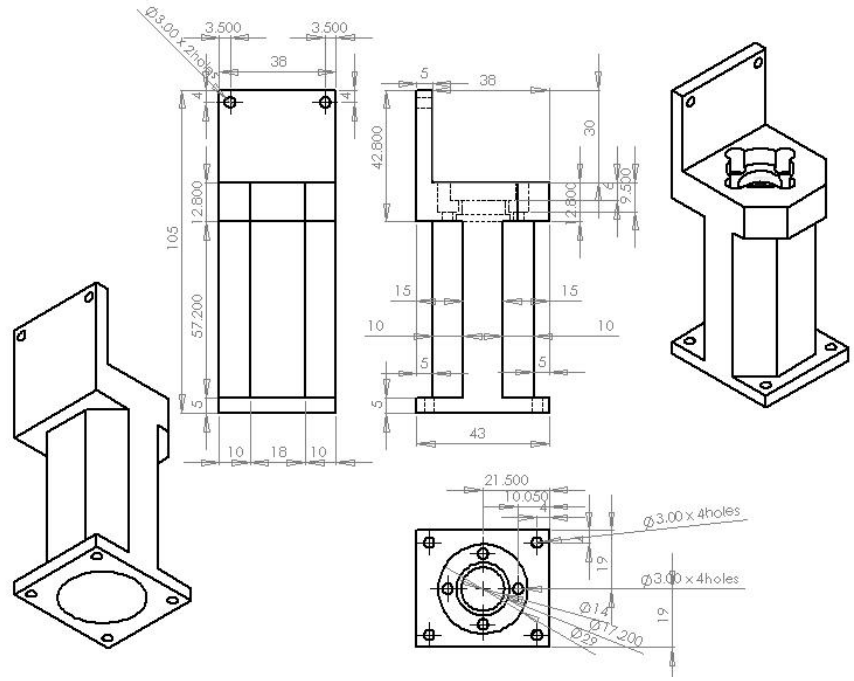

Part 7 The connector of motor 2

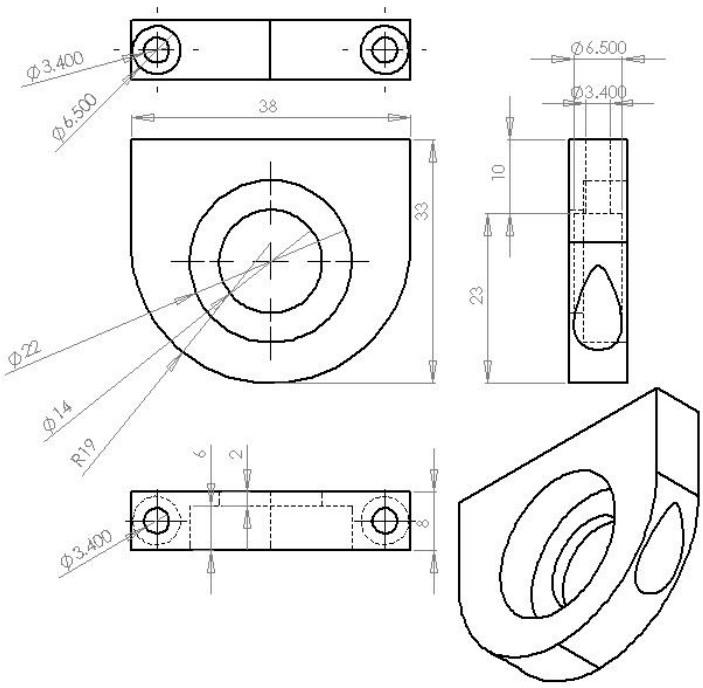

Part 8 The lock of motion Joint 2

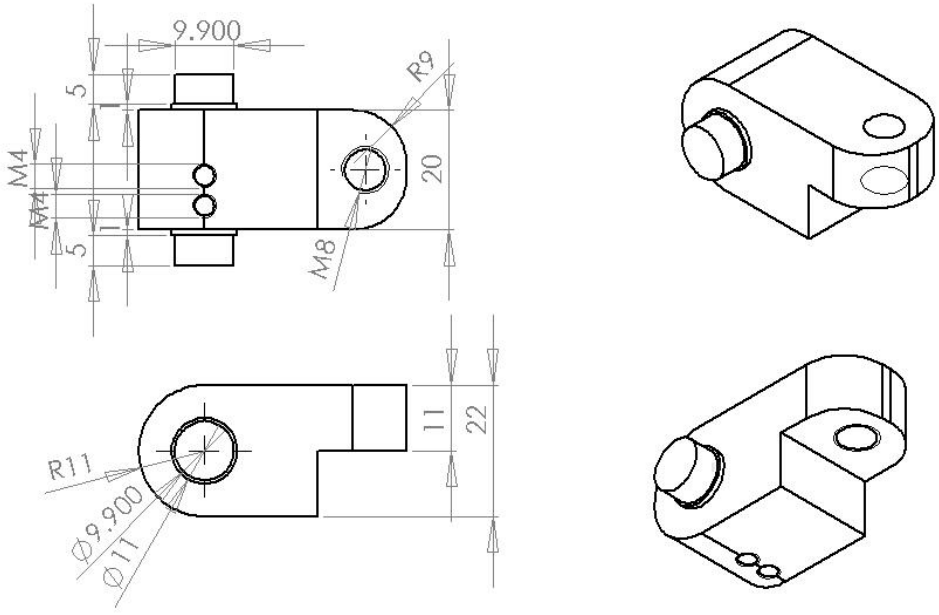

Part 9 The motion Joint 2

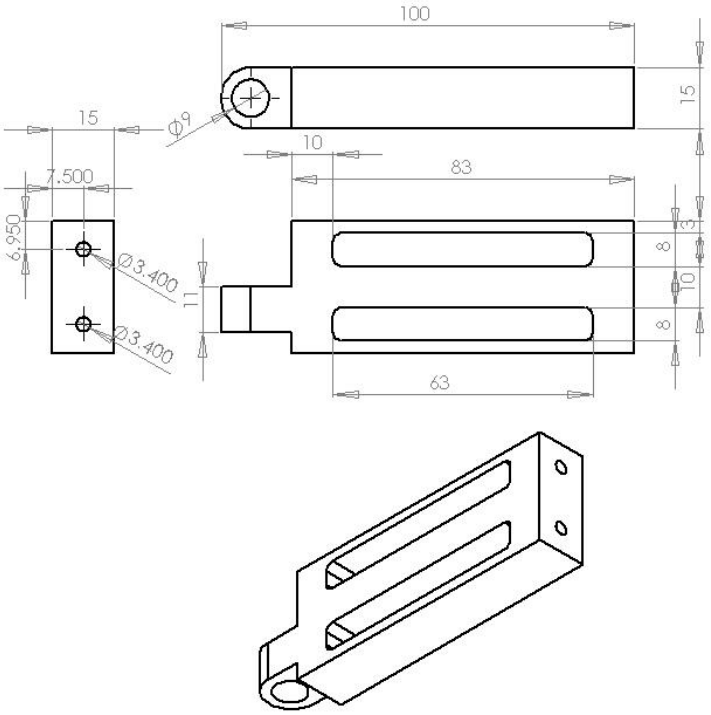

Part 10 The connector of linear part

THE DERIVATION OF KALMAN FILTER

The Kalman filter is a tool which can estimate the states of a linear system. The estimation of the state *x* will be defined an equation as follow:

$$x_k = Ax_{k-1} + Bu_k + w_{k-1}$$

where the state measurement as follow:

$$z_k = Hx_k + v_k$$

and the random variables are w_k and v_k which represent the process and measurement noise, respectively. The equations can be written as:

$$p(w) \sim N(0, Q) \quad ; Q = [w_k w_k^T]$$

$$p(v) \sim N(0, R) \; ; R = [v_k v_k^T]$$

where *A* is the state transition matrix *(n * n)*, x_{k-1} is the state matrix *(n * 1)* in previous time step *k-1* to estimate the state at the current step *k*, *B* is the optional control transition matrix *(n * l)*, u_k is the optional control input $u \in \Re^l$ to the state *x*, *H* is the measurement transition matrix *(m * n)* which relate the state x_k to measurementz_k, *Q* is the process noise covariance, and *R* is the measurement noise covariance.

A priori and posteriori estimate error define $e_k^- \; and \; e_k$, respectively. These estimate error covariance defined in the matrix *(n * n)* form at time k. These equations can be written as:

$$e_k^- \cong x_k - \hat{x}_k^-$$
$$e_k \cong x_k - \hat{x}_k$$

where $\hat{x}_k^-$ is a priori state estimate, and $\hat{x}_k$ is a posteriori state estimate at step k which given a measurement z_k.

These equations can be calculated a priori and posteriori estimate error covariance$P_k^- \; and \; P_k$, respectively. These equations can be written as:

$$P_k^- = E[e_k^- e_k^{-T}]$$

$$P_k = E[e_k e_k^T]$$

In the deriving the equations, the goal of the Kalman filter is to determine a posteriori state estimate $\hat{x}_k$ as follows:

$$\hat{x}_k = \hat{x}_k^- + K(z_k - H\hat{x}_k^-)$$

Therefore, the deriving of the a posteriori estimate error covariance P_k as follows:

$$P_k = E[e_k e_k^T]$$
$$P_k = E[(x_k - \hat{x}_k)(x_k - \hat{x}_k)^T] \quad ; \; e_k = \; x_k - \hat{x}_k$$

From:$\hat{x}_k = \hat{x}_k^- + K(z_k - H\hat{x}_k^-)$

$$\hat{x}_k = \hat{x}_k^- + K(Hx_k + v_k - H\hat{x}_k^-) \quad ; \; z_k = Hx_k + v_k$$
$$\hat{x}_k = \hat{x}_k^- + KHx_k + Kv_k - KH\hat{x}_k^-$$

So: $x_k - \hat{x}_k = \; x_k - [\hat{x}_k^- + KHx_k + Kv_k - KH\hat{x}_k^-]$

$$x_k - \hat{x}_k = \; x_k - \hat{x}_k^- - KHx_k - Kv_k + KH\hat{x}_k^-$$
$$x_k - \hat{x}_k = (I - KH)(x_k - \hat{x}_k^-) - Kv_k; (I - KH)(x_k - \hat{x}_k^-)$$
$$= x_k - \hat{x}_k^- - KHx_k + KH\hat{x}_k^-$$

Therefore: $P_k = E\left[\left((I-KH)(x_k-\hat{x}_k^-)-Kv_k\right)\left((I-KH)(x_k-\hat{x}_k^-)-Kv_k\right)^T\right]$

$$P_k = (I-KH)E[(x_k-\hat{x}_k^-)(x_k-\hat{x}_k^-)^T](I-KH)^T + KE[v_k{v_k}^T]K^T$$
$$P_k = (I-KH)P_k^-(I-KH)^T + KRK^T$$
$$if: P_k^- = E[(x_k-\hat{x}_k^-)(x_k-\hat{x}_k^-)^T], and\ R = E[v_k{v_k}^T]$$
$$P_k = P_k^- - KHP_k^- - P_k^-H^TK^T + KHP_k^-H^TK^T + KRK^T$$
$$P_k = P_k^- - KHP_k^- - P_k^-H^TK^T + K(HP_k^-H^T + R)K^T$$

The trace, which is the sum of the diagonal elements of the matrix, of P_k is the sum of mean squared error. Therefore, this is first differential with respect to K and the result set to zero in order to find the condition of the minimum, this equation will be computed as follow:

$$T[P_k] = T[P_k^-] - T[KHP_k^-] - T[P_k^-H^TK^T] + T[K(HP_k^-H^T + R)K^T]$$
$$T[P_k] = T[P_k^-] - 2T[KHP_k^-] + T[K(HP_k^-H^T + R)K^T]$$
$$\frac{dT[P_k]}{dK} = -2(HP_k^-)^T + 2K(HP_k^-H^T + R)$$
$$2(HP_k^-)^T = 2K(HP_k^-H^T + R)$$
$$P_k^-H^T = K(HP_k^-H^T + R)$$
$$\therefore K = P_k^-H^T(HP_k^-H^T + R)^{-1}$$

where K is the Kalman gain which is matrix *(n * m)*.

The Kalman gain use minimized a posteriori estimation error covariance P_k. Therefore, the replacement $P_k$by K, can be written as:

$$P_k = P_k^- - P_k^-H^T(HP_k^-H^T + R)^{-1}HP_k^- - P_k^-H^TK^T$$
$$+P_k^-H^T(HP_k^-H^T + R)^{-1}(HP_k^-H^T + R)K^T$$
$$P_k = P_k^- - P_k^-H^T(HP_k^-H^T + R)^{-1}HP_k^- - P_k^-H^TK^T + P_k^-H^TK^T$$
$$P_k = P_k^- - P_k^-H^T(HP_k^-H^T + R)^{-1}HP_k^-$$
$$P_k = P_k^- - KHP_k^- \quad ; K = P_k^-H^T(HP_k^-H^T + R)^{-1}$$
$$\therefore P_k = (I-KH)P_k^-$$

where *I* is the identity matrix*(n * n)*, P_k is the update equation for the priori estimate error covariance with kalman gain.

The state projection is achieving as:

$$\hat{x}_{k+1}^{-} = A\hat{x}_k$$

To complete the recursive process, it is necessary to find an equation which projects the priori estimate error covariance matrix into the next time interval, *k + 1*. This equation can be written as:

$$P_{k+1}^{-} = E[e_{k+1}^{-} {e_{k+1}^{-}}^{T}]$$

$if:\ e_{k+1}^{-} = x_{k+1} - \hat{x}_{k+1}^{-}$

$e_{k+1}^{-} = (Ax_k - w_k) - A\hat{x}_k$

$where:\ x_{k+1} = Ax_k - w_k$

$and: \hat{x}_{k+1}^{-} = A\hat{x}_k$

$so: e_{k+1}^{-} = A(x_k - \hat{x}_k) + w_k$

$e_{k+1}^{-} = Ae_k + w_k \quad ;\ e_k = x_k - \hat{x}_k$

where e_k and w_k have cross-correlation because the process noise w_k actually accumulates between time *k* and *k+1*.

Therefore, the priori estimate error covariance at time *k+1* can be written as:

$$P_{k+1}^{-} = E[(Ae_k + w_k)(Ae_k + w_k)^T]$$
$$P_{k+1}^{-} = E[(Ae_k)(Ae_k)^T] + E[w_k w_k^T]$$
$$P_{k+1}^{-} = AE[e_k e_k^T]A^T + Q \quad ; Q = E[w_k w_k^T]$$
$$\therefore P_{k+1}^{-} = AP_kA^T + Q \quad ;\ P_k = E[e_k e_k^T]$$

DESIGN OF A NEW LAPAROSCOPIC-HOLDER ASSISTING ROBOT

Vera Saing[1, 2] , Saowapak Sotthivirat, Ph.D. [3], Prof. Chumpon Vilasrusmee R.N. [4],
Asst. Prof. Jackrit Suthakorn, Ph.D.[1,2,*]

[1]Center for Biomedical and Robotics Technology, Faculty of Engineering, Mahidol University, THAILAND

[2]Department of Biomedical Engineering, Faculty of Engineering, Mahidol University, THAILAND

[3]National Electronics and Computer Technology Center, THAILAND

[4]Department of Surgery, Faculty of Medicine Ramadhibodi Hospital, Mahidol University, THAILAND

[*]Corresponding Author: egjst@mahidol.ac.th

Abstract

The minimally invasive surgery (MIS) is new technology of surgery. There are many advantages to patient to use this technology. The laparoscopic surgery, a type of MIS, is performed with several laparoscopic tools and with a laparoscope. In this paper, design of a new laparoscopic-holder assisting robot is developed to help the primary surgeon. The system is 5 degrees of freedom robotic system to hold and control laparoscope. The design is improved from well-known laparoscopic robots, the KaLAR robot and the MC^{2}E robot, to reduce some disadvantages from our analysis. The robot base is enhanced from the lower part of the MC^{2}E robot and the holder is adjusted from the laparoscope-holder of the KaLAR robot while other parts are developed by our own. In conclusion, the study presented in this paper is a consequence sub-project of the development of robot-assisted laparoscopic surgical system project.

Introduction

The development of surgery is moving toward minimization or elimination of incision. The minimization of incision is known as minimally invasive surgery (MIS) [1]. Patients can receive many benefits from the MIS. For example, blood loss can be reduced, thus reducing the risk of blood transfusion; smaller incision reduces pain and shortens recovery time; less pain leads to less pain medication needed; and exposure of internal organs to possible external contaminants decreases the risk of acquiring infections.

Laparoscopic surgery, a type of MIS, is performed with several endowrist instruments and a laparoscope which is a telescopic rod lens system connecting to a CCD camera. A fiber optic cable system is used to connect a light source to illuminate the operative field. These tools insert through the trocar (a hollow cylinder with sharply tip) three to five openings, which are called ports in the abdomen. The surgical site is viewed through a laparoscope equipped with a CCD camera.

An operating room for laparoscopy has a limited space and may require a lot of surgeons depending on surgical complexity and surgeon's techniques, as shown in Figure 1 [2]. The camera operator stands beside the primary surgeon and the first assistant is on the opposite side of the primary surgeon. The primary surgeon mainly operates and the first assistant surgeon supports the primary surgeon.

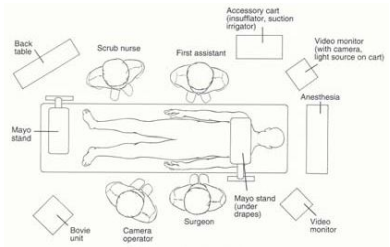

Figure 1. Operation room configuration

Due to the small space in the operation room, sometimes the camera operator needs to manipulate the laparoscope through a very small space, such as the primary surgeon's underarm. The position of the laparoscope is changed by the instruction from the primary surgeon, as shown in Figure 2.

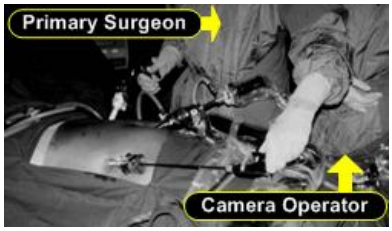

Figure 2. The complexity in the real operation room between the primary surgeon and the camera operator

Instead of using the camera operator by a man which may encounter human errors, in this paper, we propose a new robotic approach to avoid those errors and improve the outcome of the surgery. We designed the new laparoscope-holder assistant robot by combining the advantages of two uncommercial laparoscope-holder robots including the KaLAR robot and MC^{2}E robot. This robot is used to hold the laparoscope in laparoscopic surgery which can increase the workspace in the operating room, and decrease the problem of human errors.

Existing Laparoscopy

The development of laparoscope-holder assistant robot can be separated into two types consisting of the commercial and uncommercial laparoscope-holder robots. Examples of the commercial laparoscope-holder robots include the AESOP (the automated endoscope system for optimal positioning) by Computer Motion Inc, Goleta, CA [3], EndoAssist by Armstrong Healthcare, High Wycombe, Bucks, UK [4], and LapMan by MEDSYS, Gembloux, Belgium [5]. Examples of uncommercial laparoscope-holder robot includes LER (Light Endoscope Robot) by TIMC-GMCAO Laboratory [6], KaLAR (KAIST Laparoscopic Assistant Robot) by Korea Advanced Institute of Science and Technology [7], and MC^{2}E (compact manipulator for endoscopic surgery) by Laboratorie de Robotique de Paris [8]. In this paper we develop a new laparoscope-holder robot by combining the advantages of two uncommercial laparoscope-holder robots including the KaLAR robot and MC^{2}E robot.

The KaLAR Robot

The KaLAR robot [7] is an endoscope-holder assistant robot, which has 3-degrees of freedom (DOFs) including up/down, left/right and forward/backward movement, as shown in Figure 3. The end of this robot connects to a CCD camera, which can bend. The control of the KaLAR consists of 2-DOFs motions including up/down and right/left motions that are controlled by wire-driven mechanism, and 1-DOF zooming mechanism for the forward/backward movement from the linear-stage, which controlled by motors. These motions are controlled by voice command via a computer.

This system is designed by two major including safety and adaptability. For safety, they designed the robot with the optimized range of motions. The motions are controlled by voice command. This robot has the safety by using the software to detect wrong commands. This software has a filtering system to oppose the wrong commands. For adaptability, they designed the robot to have a compact size to decrease interference with the primary surgeon in the operating room. They designed the robot to weight less than 2 kg. This robot used the commercial laparoscope holder for fixation to the bedside. Therefore, the robot can be positioned in various locations of the patient's abdomen because the holder has multiple degrees of freedom. However, this system has some disadvantages. For example, it is difficult to apply to general laparoscopic surgeries due to its limited workspace.

The MC^{2}E Robot

The MC^{2}E robot [8] is a laparoscopy robot, which moves only the instrument. This robot consists of two parts, as shown in Figure 4. The lower part is a compact spherical 2-DOFs mechanism (Θ_1 and Θ_2) which joint axes coincide with the fulcrum point providing an invariant center. The base of this part is easily installed on the patient's skin. The convenient of the installation can reduce the setup time. The upper part of this robot is mounted on the fulcrum point. It provides the 2-DOFs for rotation about the instrument axis (Θ_3) and translation along the instrument axis (d_4). This part has translated the instrument along its penetration axis. The rotation motion used a motor to transmit the instrument through six soft rollers. Therefore, from the design, this robot is compact and lightweight. However, this robot has force measurement to unnecessary to laparoscope-holder robot because laparoscope does not touch the surface of organ.

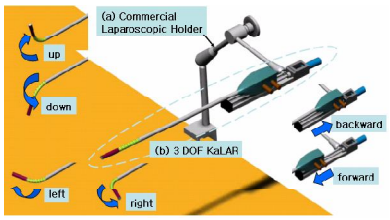

Figure 3. Simulation of KaLAR in the conceptual design

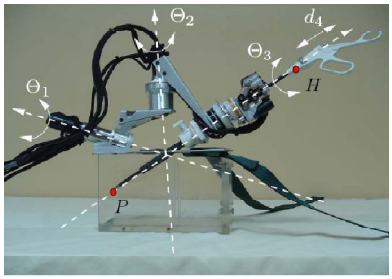

Figure 4. The MC^{2}E robot

CONCEPTUAL DESIGN ROBOT

To combine the advantages of existing robots, we design a new laparoscope-holder assistant robot. This entire system consists of three parts: a passive base part, a bending laparoscope part, and an external manipulator part. The proposed robot system can be used in the surgical environments which has limited workspaces.

The Passive Base Part

This part uses the commercial medical passive holder that can be climbed easily on the operating table. The passive base is fixed to the operating table with a clamp and the system at the proper position. This part is shown in Figure 5. There are many advantages to use this passive base part on the new laparoscope-holder robot. First, this part is easily fixed to the bedside. Second, we can easily adjust the laparoscope in the proper position at the fulcrum point. Finally, it is very lightweight. Therefore, we will use this passive base part to setup the proper position of the laparoscope-holder robot.

Figure 5. A passive base

Bending Laparoscope Part

The bending laparoscope is derived from the original KaLAR system [7], as shown in Figure 6. This part composes of 2-DOFs for the bending motion inside the patient's abdomen and 1-DOF for the motion outside the patient's abdomen. The bending motion driven by a wire mechanism determines the internal angle of the laparoscope. The zooming motion uses a linear guide with a ball screw to move the laparoscope. The advantage of the bending laparoscope is the flexibility to view wide areas of the internal patient's abdomen without making wide motions in the operating room. Because it can reduce motions of the robot in the operating room and increase viewing areas in the abdomen, we use this bending laparoscope mechanism to design the new laparoscope-holder in this paper.

Figure 6. Bending laparoscope
External Manipulator Part

Since the original KaLAR system has a limited view of workspace, we develop the external manipulator is to extend the workspace of the original KaLAR system. This external manipulator uses the lower part of the MC^2E robot [8], as shown in Figure 4. The advantages of the new system are a wide view of the workspace in the abdominal cavity allowing the system to apply to other laparoscopic surgeries. The external manipulator has 2-DOFs of motions which create the compact spherical motion for moving the laparoscope. Moreover this system does not have a large rigidity problem and has a very simple structure, thus the surgeon can predict the movements of this system easily and reduced the interference in the system. Therefore, we will use this external manipulator part to increase view of the workspace in the patient's abdomen, as shown in Figure 7.

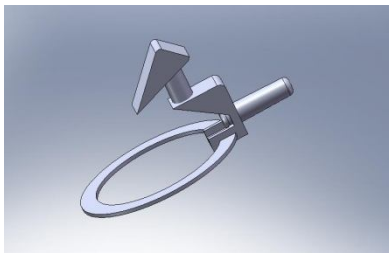

Figure 7. External manipulator

The Prototype of the Overall Proposed System

The proposed robot is designed from two robots including the KaLAR robot and the MC^2E robot. The design separates into three parts. First, the passive base part is the commercial medical passive holder. The passive base has many DOFs for setup the tip position of the laparoscope-holder robot. Second, the bending laparoscope part is the laparoscope motions of the KaLAR robot. The bending laparoscope part has 3-DOFs of motions include 2-DOFs for bending motion in the patient's abdomen and 1-DOF for the motion outside the patient's abdomen. This part is used to reduce motions of the robot and increase viewing areas in the patient's abdomen. Finally, the external manipulator part is the lower part of the lower part of the MC^2E robot. The external manipulator has 2-DOFs of motions to create the compact spherical motion in the patient's abdomen. This part use to increase view area of the workspace in the patient's abdomen. From these parts, the prototype of the new laparoscope-holder assistant robot is shown in Figure 8. The new design of the laparoscope-holder assistant robot has many advantages. First, this robot can easily be developed because it uses three motors and simple linkages. Second, this robot can easily calculate the tip of the laparoscope due to 5-

DOFs of motion consisting of 2-DOFs to control the center of the fulcrum point and 3DOF to control the motion of the laparoscope. Third, we can easily control the laparoscope motion because this robot can control by voice command of the surgeon. Finally, the proposed robot can easily be set up in a small workspace in the surgery room without interfering the workspace of the primary surgeon because it is a small robot. The primary surgeon can control the new robot by surgeon's instruction. This new design laparoscope-holder assistant robot can help holding the laparoscope in the laparoscopic surgery, thus reducing human errors and the operation time in the surgery.

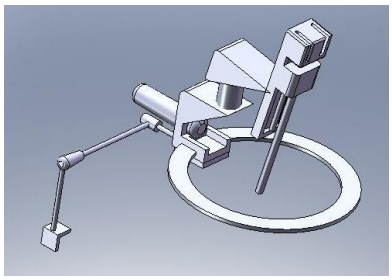

Figure 8. New design of the laparoscope-holder assistant robot.

CONCLUSION

In this paper, we have reviewed many robots, such as commercial laparoscope-holder system (AESOP, EndoAssist, LapMan) and uncommercial laparoscope-holder system (LER, KaLAR, and MC^2E). The advantages and disadvantages of these robots are discussed to design a new laparoscope-holder robot. The design of the new robot combines two structure robots, the KaLAR and MC^2E robot. This new robot is divided into three parts: the passive base part, the bending laparoscope part, and the external manipulator part. The first part, the passive base part, uses the commercial medical passive holder. The bending laparoscope part is designed from the laparoscope-holder of the KaLAR robot. This part has 3-DOFs mechanism composing of 2-DOFs for bending motion in the patient's abdomen and 1-DOF for in and out motions of the laparoscope outside the patient's abdomen. The external manipulator part is designed from the lower part of the MC^2E robot. This part has 2-DOFs mechanism for controlling the invariant center at the fulcrum point. With the proposed design, the robot can easily be developed and simply control the laparoscope motion. Due to a small-sized robot, the new design of the laparoscope-holder assistant robot is used to hold the laparoscope in the laparoscopic surgery which has limited workspaces.

Acknowledgment

The authors would like to thank Thailand Graduate Institute of Science and Technology (TGIST) for their financial support.

References

[1] R. H. Taylor, J. Funda, L. Joskowicz, A. D. Kalvin, S. H. Gomory, A. P. Gueziec, and L. M. G. Brown, "An overview of computer-integrated surgery at the IBM Thomas J. Watson Research Center," *IBM J. Research and Development*, vol. 40, pp. 163-183, 1996.

[2] B. V. Jr. MacFadyen and J. L. Ponsky, *Operative Laparoscopy and Thoracoscopy*. Lippincott-Raven, Philadelphia, 1996.

[3] P.Chatzilias, Z.Kamarianakis, S. Golemati and M. Christodoulou, "Robotic control in hand-assisted laparoscopic nephrectomy in humans– a pilot study", *Proc in IEEE Engineering in Medicine and Biology Society*, vol. 4, pp.2742-2745, 2004.

[4] Sashi S. Kommu , "Initial experience with the EndoAssist camera-holding robot in laparoscopic urological surgery", *J Robotic Surgical*, vol. 1, no. 2, pp. 133-137, July 2007.

[5] R. Polet and J. Donnez , "Gynecologic Laparoscopic Surgery with a Palm-Controlled Laparoscope Holder", *Journal of the American Association of Gynecologic Laparoscopists*, vol. 11, no. 1, pp. 73-78, 2004.

[6] J.-A. LONG, P. Cinquin, J. Troccaz, S. Voros, J.-L. Descotes, P. Berkelman, C. Letoublon, and J.-J. Rambeaud, "Development of the Miniaturised Endoscope Holder LER (Light Endoscope Robot) for Laparoscopic Surgery", *TIMC-GMCAO Laboratories (UMR CNRS 5525) Grenoble,* France, 2006.

[7] L. Yun-Ju, K. Jonathan, K. Seong-Young, L. Woo-Jung, K. Dong-Soo, "Design of a Compact Laparoscopic Assistant Robot : KaLAR ", *ICCA*, 2003.

[8] Z. Nabil, M. Guillaume, O. Tobias, B. Nicolas, "Mechatronic Design of a New Robot for Force Control in Minimally Invasive Surgery", *IEEE/ASME Transactions on Mechatronics*, France, 2007.

ADAPTIVE MEAN-SHIFT KALMAN TRACKING FOR LAPAROSCOPIC SURGERY

Vera Sa-Ing, Jackrit Suthakorn
Department of Biomedical Engineering
Mahidol University
Nakornpathom, THAILAND
jack_rotor@hotmail.com

Saowapak S. Thongvigitmanee
Image Technology Lab
National Electronics and Computer Technology Center
Pathumthani, THAILAN

Chumpon Wilasrusmee
Department of Surgery Ramathibodi Hospital
Bangkok, THAILAND

Abstract—In this paper, we propose the adaptive mean-shift Kalman tracking based on the mean-shift algorithm combined with the Kalman filter for tracking the laparoscopic instrument in laparoscopic surgery. With an iterative increment update of the target candidate in the mean-shift process, the proposed algorithm has improved the performance over a typical mean-shift algorithm. In addition, the Kalman filter is employed to enhance the chance of tracking accuracy, especially when the object disappears from the scene. We tested the tracking performance of our proposed algorithm by using different situations from simulated videos. From all experimental results, the proposed algorithm can locate the target object correctly even when the size and the shape of the target have been changed. Moreover, in the difficult situation when the target is hiding behind an obstacle, this algorithm can still track the target object correctly after it comes out. Therefore, this proposed algorithm can be used for locating the tip of the laparoscopic instrument in real laparoscopic surgery.

Keywords-mean-shift algorithm; Kalman filter; object tracking; laparoscopic surgery; minimally invasive surgery

I INTRODUCTION

The development of surgery is moving toward minimization or elimination of incision, which is known as minimally invasive surgery (MIS) [1]. Patients can receive many benefits from MIS. For example, blood loss can be reduced (reducing the risk of blood transfusion); small incision results in reducing pain and shortens recovery time; and exposure of internal organs to possible external contaminants decreases the risk of acquiring infections. Laparoscopic surgery, a type of MIS, is performed with several laparoscopic instruments and a laparoscope which is a telescopic rod lens system connecting to a CCD camera. A fiber optic cable system is used to connect a light source to illuminate the operative field. The surgical site is viewed through a laparoscope which represents a 2D image. The position of the laparoscope is changed by the instruction from primary surgeon. In addition, laparoscopic surgery requires a lot of surgeon's skill to operate the instrument.

Many researchers have proposed different methods to track the laparoscopic instrument. Omote *et al*. [2] presented the color tracking algorithm to control a robotic laparoscope instead of using human; however, this method cannot track many types of instruments. Casals *et al*. [3] introduced feature tracking algorithm based on shape information of a surgical instrument; however, it works only with a specific surgical instrument. Lee *et al*. [4] proposed a color and shape tracking algorithm by using the contour of the surgical instrument. This algorithm worked well in the normal situation, but not when the instrument is blocked by some obstacles. Wei *et al*. [5] presented a simple algorithm for tracking target features. However, this algorithm is based on the artificial color marks attached to a surgical instrument, but there are many disadvantages, such as sterilization of the mark on the surgical instrument and its convenience in the real practice.

Due to some limitations of previous methods, in this paper, we propose a new object tracking algorithm to track the surgical instrument called the adaptive mean-shift Kalman algorithm, which is based on the mean-shift algorithm [6] and the Kalman filter [7]. In this technique, the size of target candidate can be adjusted during tracking processes to increase the chance of tracking. Different scenarios of simulated videos were tested with the proposed algorithm. In addition, the proposed algorithm is intended to use for controlling our new laparoscopic-holder assistant robot [8] and tracking the tip's instrument in laparoscopic surgery.

II OBJECT TRACKING SYSTEM

In general, object tracking can be divided into two parts: *Target Representation and Localization* and *Filtering and Data Association* [9]. *Target Representation and Localization* is the

main part for locating and tracking the target object, which consists of three different techniques: point tracking, silhouette tracking, and kernel tracking. In this study, we will focus on kernel tracking, specifically the Mean-Shift algorithm, to locate the target object. The mean-shift algorithm can locate both rigid and non-rigid objects, as well as varying-size objects. *Filtering and Data Association* is a supplementary process to improve object tracking capability to overcome some difficult tasks, such as a case when the object is blocked by some obstacles. This process utilizes the result of *Target Representation and Localization.* Examples of filtering algorithms are Kalman Filters and Particle Filters. In this part, we will use the Kalman filter because we focus on tracking only one target object and the Kalman filter is the suitable estimation state of one target object

.

Mean-Shift Algorithm

A Mean-Shift algorithm [6] is an iterative process to locate the target object by maximizing the similarity function. The similarity function will be compared between the target model, $\hat{q}$, and the target candidate, $\hat{p}(y)$. The target model and the target candidate are represented by a small elliptical or rectangular area in the frame. The pixel values in the region of interest (ROI) are used for calculating the target model and target candidate histograms. This algorithm consist five steps when computing each frame of video sequences. The result of processing in the current frame is the target object which is the target model in the mean-shift algorithm. The five steps are performed as described below.

In the first frame, we need to initialize $\{\hat{q}_u\}_{u=1\ldots m}$ to be the distribution of the target model and y_0 to be the center location of the target in the current frame. The target model can be computed by the following equation:

$$\hat{q}_u = C\sum_{b(x_i)=u} k(\|x_i\|^2) \quad (1)$$

where x_i is the normalized pixel value at the *i*th pixel of the target model area, $b(x_i)$ is a color value at pixel x_i which depends on the *m*-bin histogram, C is a normalization factor, which can be set as a constant, $k(x)$ is a kernel function, such as a Normal kernel as follows:

$$k_N(x)\ C * \exp\left[-\frac{1}{2}\|x\|^2\right] \quad (2)$$

Step 1: Initialize the new center location of the target in the current frame at the previous center location y_0 and compute the distribution of the target candidate at y_0:

$$\hat{p}(y_0) = \{\hat{p}_u(y_0)\}_{u=1\ldots m} \quad (3)$$

$$\hat{p}_u(y_0) = C_h\sum_{b(x_i')=u} k\left[\left\|\frac{y_0 - x_i'}{h}\right\|^2\right] \quad (4)$$

where x_i' is the normalized pixel locations in the target candidate which is defined to have the center at y_0 in the current frame, y_0 is a 2-D coordinate of the object location which is the center of the target candidate area in the current frame, h is the bandwidth of the candidate area, and C_h is a normalization factor, which can be set as a constant.

To compare between the target model and the target candidate, the similarity function, $\rho(\hat{p}(y), \hat{q})$, is based on the Bhattacharyya Coefficient as follows:

$$BC1 = \rho(\hat{p}(y_0), \hat{q}_u) = \sum_{u=1}^{m}\sqrt{\hat{p}_u(y_0)\hat{q}_u}$$
$$= \sum_{u=1}^{m}\hat{p}_u(y_0)\sqrt{\frac{\hat{q}_u}{\hat{p}_u(y_0)}} \quad (5)$$

Step2: Derive the weights $\{w_i\}_{i=1\ldots n_h}$, as follows:

$$w_i = \sum_{u=1}^{m}\sqrt{\frac{\hat{q}_u}{\hat{p}_u(y_0)}}\ ; i = 1\ldots n_h \quad (6)$$

Step3: The mean shift vector computes the new location y_1, by calculating the minimum distance between the target model and the target candidate. The current position y_0 will be moved to the new location y_1. Therefore, the new location of the target candidate can be derived as follows:

$$y_1 = \frac{\sum_{i=1}^{n_h} x_i' w_i g\left(\left\|\frac{y_0 - x_i'}{h}\right\|^2\right)}{\sum_{i=1}^{n_h} w_i g\left(\left\|\frac{y_0 - x_i'}{h}\right\|^2\right)} \quad (7)$$

where $g(x) = -k(x)$

After updating the new center target location at y_1, the distribution of target candidate at y_1 is computed as follows:

$$(y_1) = \{\hat{p}_u(y_1)\}_{u=1\ldots m} \quad (8)$$

Then the second Bhattacharyya coefficient or the similarity function between the target model and the target candidate of the new location is evaluated.

$$BC2 = \rho(\hat{p}(y_1), \hat{q}_u) = \sum_{u=1}^{m}\sqrt{\hat{p}_u(y_1)\hat{q}_u}$$

(9)

Step4: This process will iterate until BC2>BC1; however, if BC2 < BC1, then the new center target y_1 will be updated as follows:

$$While\{\ \ BC1 < BC2\ \ \}$$
$$Do\left\{\ \ y_1 = \frac{1}{2}(y_0 + y_1)\ \ \right\}$$

Step5: This process will check the condition to terminate the algorithm based on the predicted threshold value ϵ. The threshold value is defined to be the minimum distance value between the target model and the target candidate. The condition of this step will be computed as follows:

$$if\ (\|y_1 - y_0\| < \epsilon\ )$$
$$Stop\ the\ process$$
$$Else$$
$$Set\ y_0 = y_1$$

Go *to Step* 1

The Kalman Filter Algorithm

The Kalman filter [7] is based on a set of mathematical equations which implements a predictor-corrector step to estimate the result. This filter is a tool for estimating the states of a linear system. The Kalman filter is a recursive process which is separated into two steps consisting of prediction and correction steps. The prediction step defines the time update equations and the correction step defines the measurement equations. The goal of the Kalman filter is to determine a posteriori state estimate $\hat{x}_k$.

The time update equations, responsible for projecting in time, consist of the current state and the priori estimate error covariance for the next time step as follows:

Project the state, $\hat{x}_{k+1}^-$, in the next time, k+1, as follows:

$$\hat{x}_{k+1}^- = A\hat{x}_k + Bu_k + w_k \qquad (10)$$

where *A* is an *n x n* state transition matrix, $\hat{x}_k$ is an *n x 1* state matrix in the previous time (frame) step, *n* is number of estimate values, *B* is an *n x l* optional control transition matrix, *l* is the number of the control values, u_k is a *k*-time optional control input which is an *l x 1* matrix, and w_k is the process noise which is an *n x 1* matrix or a constant.

Project the posteriori estimation error covariance, P_{k+1}^-, in the next time, k+1, as follows:

$$P_{k+1}^- = AP_kA^T + Q \qquad (11)$$

where $Q = [w_k w_k^T]$ is the process noise covariance which is an *n x n* matrix, and P_k is the update equation for the priori estimate error covariance.

The measurement equations use the actual measurement z_k to update the state object consisting three processes as follows:

Computed the Kalman gain, K as follows:

$$K = P_k^- H^T (HP_k^- H^T + R)^{-1} \qquad (12)$$

where *K* is called the "Kalman gain" which is an *n x m* matrix, P_k^- is a priori estimate error covariance, *H* is an *m x n* measurement transition matrix, $R = [v_k v_k^T]$ is an *n x n* measurement noise covariance matrix.

Update estimate state with actual measurement, z_k, as follows:

$$\hat{x}_k = \hat{x}_k^- + K(z_k - H\hat{x}_k^-) \qquad (13)$$

where $\hat{x}_k^-$ is an *n x 1* priori state estimate matrix, z_k is an *m x 1* actual measurement matrix, which can be written as follows:

$$z_k = Hx_k + v_k \qquad (14)$$

where v_k in the measurement noise which is an *m x 1* matrix or a constant, x_k is the result of the Target Representation and Localization part which is an *m x 1* matrix.

Update the priori estimation error covariance, P_k in the current time k, as follows:

$$P_k = (I - KH)P_k^- \qquad (15)$$

III ADAPTIVE MEAN-SHIFT KALMAN TRACKING

In this research, we propose the adaptive mean-shift Kalman tracking based on the mean-shift algorithm combined with the Kalman filter. The proposed algorithm has improved the mean-shift algorithm by its ability to adjust different ROI sizes of the target candidate. The adaptive mean-shift Kalman algorithm mainly uses to track the object of interest. The overall process of adaptive mean-shift Kalman tracking summarized in Fig1 is explained below.

Initial step: Selection of target model

In the first frame, the user selects the target model which is the predefined ROI. From the target model, we will compute the initial state of the Kalman filter.

First step: Mean-Shift algorithm process

In the next frame, the algorithm defines the target candidate which is at the same center location as the target model. However, the size of target candidate is larger than the size of target model (the size of the region, *h*). The target model and target candidate will be computed to get the second Bhattacharyya coefficient (*BC2*) in the mean-shift algorithm.

Second step: Similarity comparison from the mean-shift algorithm

First, we will define the first similarity threshold value (*CT1*) to determine the tracking criteria. This value will be compared with *BC2*. If *BC2* is more than *CT1*, then we will update the Kalman filter by using the result of the mean-shift algorithm in the first step. Thus, the target result in this case will be acquired from the mean-shift algorithm, and the next sequence frame can be proceeded. However, if *BC2* is less than *CT1*, then go to the third step.

Third step: Estimation of the Kalman filter

In this step, the estimate state of the Kalman filter will feed back to the adaptive mean-shift algorithm. If the tracking result is not in the predefined similarity threshold value, the algorithm will increase the target candidate up to twice the size of the current ROI. In addition, this target candidate will define the new location from current state of Kalman filter. Hence, the third Bhattacharyya coefficient (*BC3*) is computed.

Fourth step: Similarity comparison between the Kalman filter and the adaptive mean-shift algorithm

We compare the second similarity threshold value (*CT2*) with the *BC3* from the third step. If *BC3* is greater than *CT2*, then we will use the result from the adaptive mean-shift algorithm. If *BC3* is smaller than *CT2*, then we will use the

estimate state of the Kalman filter and go back to the third step and increase the target candidate ROI. This process is repeated until the maximum target candidate size is met. Otherwise the target result will be acquired from the adaptive mean-shift algorithm, and the next sequence frame can be proceeded.

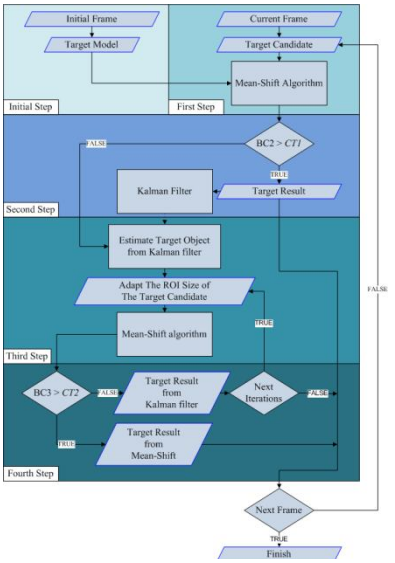

Fig1. The overall process of the adaptive Mean-Shift Kalman tracking

IV EXPERIMENTAL RESULTS

To test the proposed algorithm, we used the simulated videos for different situations. From the simulated videos in Fig2, the red background represents the color of the internal body in laparoscopic surgery. The yellow ball represents an obstacle. The tip of the real laparoscopic instrument represents the target object, which is shown in the white rectangle. The green rectangle in the tracking process is the result of the tracking algorithm. In the first frame, we need to initialize the target model for the proposed algorithm as shown in Fig2.

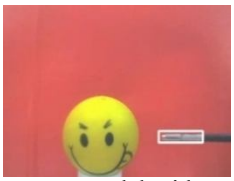

Fig2. The target model with an initial value in the white rectangle

Experiment 1: Change the shape of the target model and move in front of the obstacle

The goal of this experiment is to track the target object when changing the shape of the target and moving the target in front of the obstacle. This experiment was computed on a video with 196 frames covering about 20 seconds. Thus, the average of frame rate is 9.8 frames per second. Fig3 shows fifteen sample frames at different times. This experiment shows that the proposed algorithm can track the target object with the correct locations.

Experiment 2: Resize and change the shape of the target

The goal of this experiment is to track the target object when changing the size as well as the shape of the target. This experiment was computed on a video with 240 frames covering about 25 seconds. The tracking results in some frames are shown in Fig4. The proposed algorithm can track the target object in all frames.

Experiment 3: Move behind the obstacle

The goal of this experiment is to track the target object when the object moves behind the obstacle. This experiment was computed on a video with 140 frames covering about 14 seconds. Some tracking results are shown in Fig5. From 4-12 seconds, the whole target object was hiding behind the obstacle. After that, the target appeared in the scene again and the tracking process can track the target correctly. This is due to the estimation process in the Kalman filter to improve tracking performance. Without the Kalman filter, we were not able to track the target object correctly after it disappeared from the scene.

V CONCLUSION

In this paper, we have proposed the adaptive mean-shift Kalman tracking based on the mean-shift algorithm combined with the Kalman filter. The ROI size of the target candidate at each frame can be adjusted to increase the chance of tracking. All experimental results show that the proposed algorithm can locate the target object correctly even when the size and the shape of the target have been changed. In addition, when the target is hiding behind some obstacles, this algorithm can still track the target object after it comes out. Thus, this proposed algorithm will be suitable for locating the tip of the laparoscopic instrument, as well as, guiding the path of our conceptual robot in real laparoscopic surgery.

ACKNOWLEDGMENT

The authors would like to thank Thailand Graduate Institute of Science and Technology (TGIST) for their financial support.

REFERENCES

[1] R. H. Taylor, J. Funda, L. Joskowicz, A. D. Kalvin, S. H. Gomory, A. P. Gueziec, and L. M. G. Brown, “An overview of computer-integrated surgery at the IBM Thomas J. Watson Research Center,” *IBM J. Research and Development*, vol. 40, pp. 163-183, 1996.

[2] K. Omote, H. Feussner, A. Ungeheuer, K. Arbter, A. Guo-Qing Wei, "Self-guided robotic camera control for laparoscopic surgery compared with human camera

control," *The American Journal of Surgery,* vol. 177, pp. 21-24, 1999.

[3] A. Casals, J. Amat, E. Laporte, "Automatic guidance of an assistant robot in laparoscopic surgery," *International Conf. on Robotics and Automation,* vol. 1, pp. 895-900, 1996.

[4] C. Lee, Y. F. Wang, Uecker, Y. Wang, "Image analysis for automated tracking in robot-assisted endoscopic surgery," *Proceedings of the 12th IAPR International Conference,* vol. 1, pp. 88-92, 1994.

[5] A. Guo-Qing Wei, G. Hirzinger, "Real-time visual servoing for laparoscopic surgery. Controlling robot motion with color image segmentation," *IEEE Engineering in Medicine and Biology,* vol. 16, pp. 40-45, 1997.

.

[6] D. Comaniciu, P. Meer, "Mean shift: A robust approach toward feature space analysis," *IEEE Transactions on Pattern Analysis and Machine Intelligence* vol. 25, pp. 603 – 619, 2002.

[7] C. Masreliez, and R. Martin, "Robust bayesian estimation for the linear model and robustifying the Kalman filter," *IEEE Transactions on Automatic Control,* vol. 22, pp. 361 – 371, 2003.

[8] V. Sa-Ing, S. Sotthivirat, C. Wilasrussamee, J. Suthakorn, "Design of A New Laparoscopic-Holder Assistant Robot," in *The 3rd International Symposium on Biomedical Engineering (ISBME 2008)*, Bangkok, Thailand, pp. 278 – 281, 2008.

[9] A. Yilmaz, O. Javed and M. Shah, "Object Tracking: A Survey," *ACM Computing Surveys,* vol. 38, pp. 1 - 45, 2006

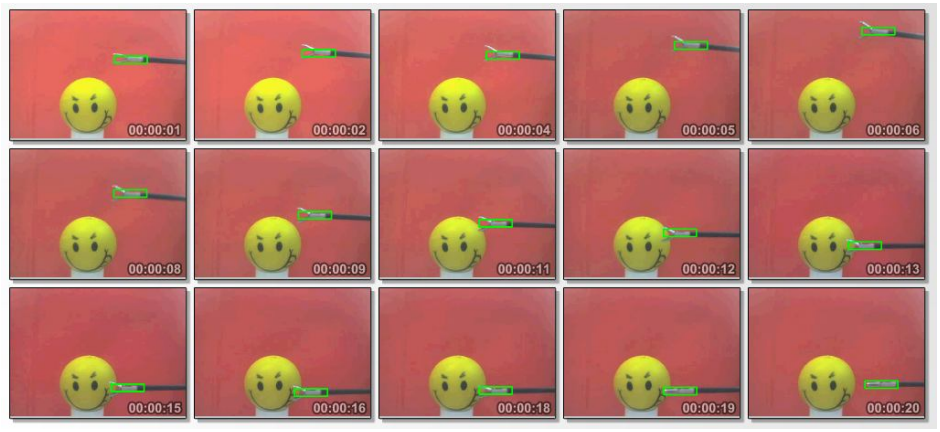

Fig3. Sample results in Experiment 1 using the proposed algorithm

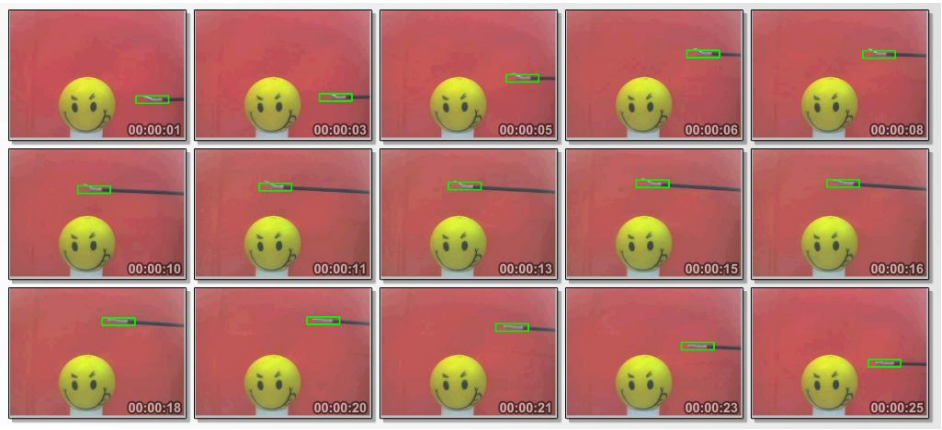

Fig4. Sample results in Experiment 2 using the proposed algorithm

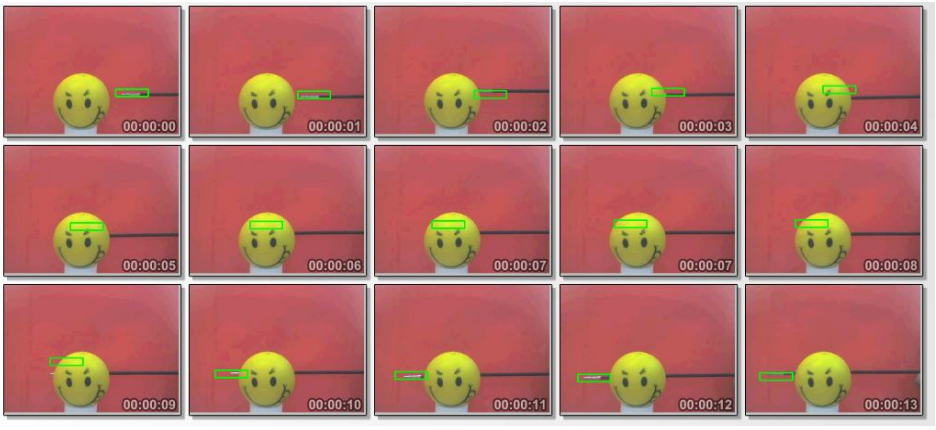

Fig5. Sample results in Experiment 3 using the proposed algorithm

BIOGRAPHY

NAME	Vera Sa-ing
DATE OF BIRTH	September 30, 1983
PLACE OF BIRTH	Trat, Thailand
INSTITUTUTIONS ATTENDED	Suranaree University of Technology (2002 – 2005) Bachelor of Engineering (Computer Engineering) Mahidol University (2007 – 2011) Master of Engineering (Biomedical Engineering)
HOME ADDRESS	194/16 Moo 1, Chonprathan Rd, Maung, Trat, Thailand, 23000 Tel: +66(0)81-946-9217 E-mail: jack_rotor@hotmail.com

WORK EXPERINCE

1. Assistant Researcher, Image Technology Lab
   (Previously Medical Instrument Section),
   (2005 - 2007) National Electronics and Computer Technology Center (NECTEC),
   National Science and Technology Development Agency (NSTDA)

PUBLICATION

1. Vera Saing, Saowapak Sotthivirat, Chumpon Vilasrusmee, and Jackrit Suthakorn, "Design of a New Laparoscopic-Holder Assisting Robot," *Proc. of the 3rd International Symposium on Biomedical Engineering (ISBME 2008)*, Nov 10-11, 2008, pp. 278-281.

2. Vera Saing, Saowapak Sotthivirat, Chumpon Vilasrusmee, and Jackrit Suthakorn, "Adaptive Mean-Shift Kalman Tracking for Laparoscopic Surgery," *the 4th IEEE International Conference on Computer Science and Information Technology (ICCSIT 2011)*, June 10-12, 2011

AWARD

2008 The Best Autonomous of Thailand Rescue Robot Championship (THAILAND)

2009 The Second Prize and of Robocup Japan Open (JAPAN)

2009 The SICE Award of Robocup Japan Open (JAPAN)

2009 The Best Autonomous of Thailand Rescue Robot Championship (THAILAND)

2009 The First Prize of Thailand Rescue Robot Championship (THAILAND)

2010 The First Prize of Robocup Japan Open (JAPAN)

2010 The Second Prize of World Robocup (SINGAPORE)